The response of planktonic and aggregated bacterial cells in aqueous media to photodisinfection techniques

A thesis submitted to Dublin City University in fulfilment of the requirements for the award of the degree of Doctor of Philosophy

By

Ana Carolina Maganha de Almeida, B.Sc., Lic., M.Sc.

School Of Biotechnology,

Dublin City University

Dublin 9,

Ireland

Research Supervisor: Dr. Bríd Quilty

July 2013

I hereby certify that this material, which I now submit for assessment on the programme of study leading to the award of PhD is entirely my own work, that I have exercised reasonable care to ensure that the work is original, and does not to the best of my knowledge breach any law of copyright, and has not been taken from the work of others save and to the extent that such work has been cited and acknowledged within the text of my work.

Signed: _____ (Candidate) ID No.: _____

Date: _____

It was fair, it was honourable, and it was worthy.

Dedicated to the lovely memory of

Elvira Lunardelli Maganha

and

Lídia Tumollo de Almeida

ACKNOWLEDGMENTS

I would like to thank the Environmental Protection Agency (EPA) of Ireland for providing the scholarship and the financial support to carry out this research.

I would like to offer my gratitude to my supervisor Dr. Bríd Quilty, School of Biotechnology, Dublin City University. Her patience, encouragement and valuable guidance were crucial to the accomplishment of this research.

I would like to acknowledge the support of all the members of the School of Biotechnology. Particular thanks to Dr. Ciarán Fagán, Head of School, Dr. Michael Parkinson for guidance with statistical analysis, Dr. Enrico Marsili for reading my work and adding valuable discussion about the biofilms and photocatalysis sections and the technical staff for their constant presence.

I am indebted to the collaborators on this project, Prof. Michael Oelgemöller and Dr. Kevin McGuigan. In particular Prof. Oelgemöller, James Cook University, Australia and formerly School of Chemical Sciences, Dublin City University, for his time and attention during the selective process which resulted in my enrollement as a PhD student in Dublin City University and for his guidance in photochemistry.

I am very grateful for the help of Dr. Mary Pryce, School of Chemical Sciences, Dublin City University, for manufacturing the LED reactor. Also to Dr. Kieran Nolan and Dr. Alexander Yavorsky, School of Chemical Science, Dublin City University, for the discussion regarding fluence-rate measurements. I kindly thank Dr. Sharon Murphy and Dr. Oksanna Shvydkiv for their time and help with the UV reactors. Thanks to Kieran Joyce for the discussions about photosensitisers, and to Ciprian and Brendan for helping me with the light measurements.

I would like to offer my sincere gratitude to my friends Prof. Dr. Sandra Mara Martins Franchetti, for the discussions about Chemistry and Photochemistry and

to the kind support of my previous supervisor of my MSc. thesis, Dr. Carlos Renato Corso.

I would like to express my love and gratitude to my family for all their faith on my work and choices. To my parents, Regina and Jorge, I express my gratitude for all their encouragement and the love to handle we had to be apart from each other. They are the best parents, good-tempered, full of peace and so kind to me and to the others. I wish I could become as kind and wonderful as they are. They put all the efforts on my studies, they believed on me all the time, even during the most challenging moments. They never let me give up, never accepted my excuses to not follow on my dreams, they challenged me so much to be better, to go further. They never let me forget how much I strived for my studies in Brazil to then get to Ireland.

I express my love and gratitude to Kamal, who made my path full of love, patience and courage.

Special thanks to Dr. Moïra Schuler for her support, friendship, discussions and kind and positive encouragement. Thanks to my friends Bianca, Cecilia, Claudia, Monika, Ross, Sahar and Tanja. We had such a good time together! Thanks to Layla, Renata and Gustavo, Camila and Karine for never stopping believing in me. Special thanks to my lab mates Aida and Markella, for their kindness and friendship! My sincere gratitude goes to the reviewers Camila, Cecilia, Ernane, Grace, Karine, Kamal, Lauren and Tanja.

I could go on with saying thanks, as I did have so much help indeed, but I cannot fit here the names of everyone. But I am deeply grateful for all of you who made this work possible. You will be always in my heart, and prayers.

I thank God who gave me strength and helped me to carry on through my PhD.

Abstract

The response of planktonic and aggregated bacterial cells in aqueous media to photodisinfection techniques

Ana Carolina Maganha de Almeida

Pseudomonas putida CP1 is an interesting environmental organism which auto-aggregates when grown under certain conditions. Laboratory studies were carried out to investigate the response of both the free-swimming and the aggregated form of the bacterium to photodisinfection. The response of the planktonic form of the organism was compared with that of *E. coli* which is widely reported in the literature. A variety of aqueous media were investigated including Milli-Q water, tap water, minimal medium, Phosphate Buffered Saline (PBS) and ¼ Strength Ringers solution. The response of the bacteria to UV-C was carried out in a Heraeus UV-RS3 system (700 ml capacity). Studies using UV-A/B in the presence and absence of 1g/l of TiO_2 (titanium dioxide) were carried out in an Aceglass (Vineland, New Jersey USA) reactor vessel model 7841-06 (290 mm and 1l capacity). Photodynamic inactivation was investigated using Rose Bengal and miniaturised LEDs (light-emitting diodes) with Petri dishes. Cell inactivation was determined using both culturable and non-culturable approaches. The response of the free-swimming form of *P. putida* CP1 to photodisinfection was similar to that for *E. coli* (DSMZ 498). The composition of the aqueous medium significantly affected the response of the cells to photodisinfection. The aggregated cells were significantly more resistant to photodisinfection than the planktonic cells. Resistance was attributed to the presence of an extracellular matrix comprising carbohydrate, protein and DNA. Photodisinfection using UV-C was the most effective method of disinfection. It was more effective than UV-A/B, in the presence or absence of TiO_2, and photodynamic inactivation using Rose Bengal, for the treatment of both planktonic and aggregated cells.

Abbreviations

- **AOPs** Advanced Oxidative Processes
- **cfu** Colony-forming unit
- **DBPs** Disinfection by-products
- **DSMZ** German Collection of Microorganisms and Cell Cultures
- **DNA** Deoxyribonucleic acid
- **DNS** 3,5-dinitrosalicyclic acid
- **EDTA** Ethylenediaminetetraacetic acid
- **EPA** Environmental Protection Agency (Ireland)
- **EPS** Extracellular polymeric substances
- **LED** Light-emitting diodes
- **LP** Low-pressure mercury lamp
- **LPS** Lipopolysaccharides
- **MP** Medium-pressure mercury lamp
- **$^{\bullet}OH$** Hydroxyl radicals
- **$^1O_2$*** Singlet oxygen
- **O.D.** Optical density
- **PBS** Phosphate Buffered Saline
- **PDI** Photodynamic inactivation
- **PDT** Photodynamic therapy
- **ppm** Parts per million
- **ROS** Reactive oxygen species
- **RB** Rose Bengal
- **RNA** Ribonucleic acid
- **SCVs** Small-colony-variants
- **TiO_2** Titanium dioxide
- **UV** Ultraviolet radiation
- **UV-A/B** Ultraviolet A and ultraviolet B wavelengths
- **UV-C** Germicidal ultraviolet radiation
- **USEPA** US Environmental Protection Agency
- **UV-VIS** Ultraviolet and visible wavelengths
- **VIS** Visible range wavelengths
- **VBNC** Viable but nonculturable
- **TNTC** Too numerous to count

List of Tables

List of Figures

1 Introduction

1 Introduction

1.1 UV disinfection and Photocatalysis

Terminology such as UV-disinfection, ultraviolet irradiation, photolysis or photodisinfection are used to define processes that rely on the ultraviolet region of the electromagnetic spectrum to eliminate undesired microorganisms from drinking and wastewaters, surfaces and air (Cutler and Zimmerman, 2011; Choi and Choi, 2010; Aidan *et al.*, 2007). At a molecular level, chemistry defines photolysis as the "*cleavage of one or more covalent bonds in a molecular entity resulting from absorption of light, or a photochemical process in which such cleavage is an essential part*" (McNaught and Wilkinson, 1997).

In 1887, Downes and Blunt were the first to demonstrate the natural killing effect of sunlight on microorganisms. The authors described the solar inhibitory effects over growth and regrowth of organisms in water and how these were related to wavelength region selected (Downes and Blunt, 1877). In 1910, after the invention of mercury bulbs, the first UV disinfection plant for drinking water treatment was built in Marseille (USEPA, 2006). Until the mid-20th century, the establishment of UV disinfection treatment plants was hampered by difficulties with UV plant operation and competition with chlorination. In 1955, the first reliable industrial applications of UV light for disinfecting water were rendered operational in Switzerland and in Austria. In the 1980s, with the discovery of disinfection-by-products, the popularity of UV disinfection increased as an alternative to chlorination. In the same decade, UV disinfection units were installed in Norway and in the Netherlands (USEPA, 2006). Over the course of the last 30 years, the UV disinfection process has been used as a reliable technology to disinfect water and wastewater in Europe and North America (M. Guo *et al.*, 2009; USEPA, 2006).

The ultraviolet region of the electromagnetic spectrum lies between the X-ray and visible region and is divided into four regions: UV-V vacuum (100-200 nm), UV-

C (200-280 nm), UV-B (280-315 nm) and UV-A (315-400 nm) (Figure 1.1). The subdivision of the UV region is related to physical, biological and medicinal effects. For instance, vacuum UV, X-rays and Gamma rays are ionizing electromagnetic radiation, which have an amount of energy high enough to eject electrons from irradiated molecules. As a result, they cause photo-ionization (Oppenländer, 2003).

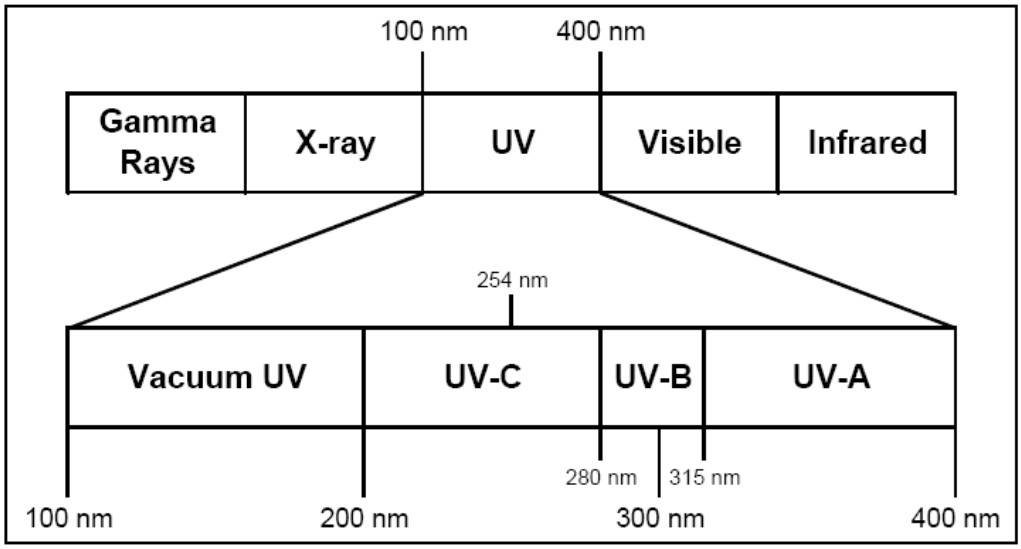

Figure 1.1 – Electromagnetic spectrum (USEPA, 2006).

The sun naturally generates ultraviolet radiation. Fortunately, negligible amounts of UV-C wavelengths (200-280 nm) which are very detrimental to organisms, reach the earth's surface (Smith *et al.*, 1992) as these wavelengths are not long enough (Cutler and Zimmerman, 2011). UV-C is referred to as the 'germicidal' spectrum for its high efficiency in inactivating bacteria (Cutler and Zimmerman, 2011). A term which is very useful referring to UV-C is 'UVGI' or 'ultraviolet germicidal irradiation' (Kowalski, 2009). UVGI distinguishes the germicidal wavelengths from the UV-A/B region (Cutler and Zimmerman, 2011).

UV-B (280-315) is detrimental to aquatic organisms and it is mostly absorbed by the ozone layer which reduces amounts of UV-B reaching the earth's surface. Contrary to that, UV-A as well as the visible wavelengths that reach the earth's surface are relatively independent of the ozone layer (Smith *et al.*, 1992). The UV-B region is responsible for the production of vitamin D and sun-tanning of

skin (Goodsell, 2001). UV-A (315-400 nm) is involved in photodamage/photorepair of living organism, whereas the visible wavelengths (400-700 nm) are responsible for photosynthesis (Smith *et al.*, 1992).

Photocatalysis is an advanced oxidative process (AOP). It involves the generation and subsequent reaction of very oxidizing species which includes the so-called $^{\bullet}OH$ hydroxyl radical (Malato *et al.*, 2007). $^{\bullet}OH$ radicals are highly reactive, non-selective, of electrophilic character, ubiquitous in nature and easy to produce (Oppenländer, 2003). The production of $^{\bullet}OH$ radicals is achieved by different oxidation processes, such as TiO_2/UV, H_2O_2/UV, photon-Fenton and ozone (O_3, O_3/UV and O_3/H_2O_2). As the production of ultraviolet radiation is costly, in recent years there has been an increasing amount of literature on AOPs driven by solar irradiation. In this scenario heterogeneous photocatalysis utilizing TiO_2 plays a major role (Malato *et al.*, 2007).

The appeal for applications of TiO_2 photocatalytic disinfection is a result of the unsuitability of current water treatment technologies. For instance, strong oxidants, such as chlorine, chlorine dioxide and ozone, produce disinfection-by-products. Another point is that the removal of pollutants by adsorption on carbon filters produces undesired accumulation of hazardous solids, which in turn still needs further disposal (Malato *et al.*, 2009). One major advantage of photocatalysis in this context is that it aims for the photomineralisation of organic pollutants which may reduce the problem of accumulation of hazardous products (Mills *et al.*, 1993).

The majority of studies on photocatalytic treatment of water have employed titanium dioxide (TiO_2) (Byrne *et al.*, 2011). TiO_2 is a polycrystalline, semi-conductor oxide with band-absorption mainly in the near UV (Josset *et al.*, 2008). The Degussa-P25 powder, which is formed by rutile and anastase crystalline form of the catalyst, offers a high surface area which enhances reactivity with bacterial cells. Therefore it is more efficient compared to other types of titanium for microbial inactivation (Gumy *et al.*, 2006). The activity of Degussa-P25, for disinfection purposes, has also shown to be relatively independent of initial pH of

the suspension (Gumy *et al.*, 2006). TiO_2 is found abundantly in nature, relatively cheap (Dalrymple *et al.*, 2010), non-toxic, chemically and biologically inert, photo-stable compound (Mills *et al.*, 1993). Moreover, photocatalytic activity of TiO_2 is preserved even after repeated usage (Gamage and Zhang, 2010). This feature allied with its mechanical properties allows for various applications of TiO_2 in photocatalytic water treatment (Chong *et al.*, 2010). TiO_2 has been used as slurry (Maness *et al.*, 1999), or immobilised in various surfaces, such as thin film coated onto an inert acetate sheets (Lonnen *et al.*, 2005), coated in glass slides (Lu *et al.*, 2003) or placed on membrane filter (Hara-Kudo *et al.*, 2006).

The surface area is one of the factors which determine photocatalyst efficiency (Bhatkhande *et al.*, 2002). In the case of TiO_2 slurry (suspended catalyst), more surface is available for reacting and for binding bacteria (Mccullagh *et al.*, 2007). Therefore the activity and efficiency of TiO_2 slurry has been generally found to be superior to that of the immobilised form. However, use of slurry has disadvantages. Dalrymple *et al.*, (2010) argued that the toxicity of nanoparticles and the need to recover them after treatment requires an additional separation method which put in additional complexity and costs to the photocatalytic process. Promising work has been carried out with immobilised TiO_2 (Mccullagh *et al.*, 2007) showing that this approach also offers advantages. Byrne *et al.*, (2011) proposed careful adaptation of reactor's design could prevent loss of efficiency caused by catalyst immobilisation, a premise also supported by Li *et al.*, (2008).

TiO_2 is photo-excited by UV-A wavelengths while the generation of hydroxyl radicals takes place at the surface of the catalyst in its interface with water. A relevant aspect of photo-excitation of TiO_2 by UV-A wavelengths is that ultraviolet emission represents only a minor part (<5%) of the sun irradiation spectrum (Dalrymple *et al.*, 2010). Thus, the use of photocatalytic materials which absorb in the visible range is of vital importance to the expansion of more cost-effective water treatment using solar irradiation. In this way, recent work has focused on shifting the absorption spectrum of TiO_2 to visible wavelengths (Byrne *et al.*, 2011). For example, N- and S- co-doped TiO_2 showed improved

disinfection of *E. coli* in visible wavelengths of doped material compared to the pure material (Rengifo-Herrera *et al.*, 2008). In another study a photocatalytic fibre composite material PdO/TiON showed a high photocatalytic disinfection rate of *E. coli* with visible irradiation (Pinggui *et al.*, 2009).

Upon absorption of UV-A photons (*hv*), with energy higher than its band gap (3.2eV) by TiO_2, one $e^-_{(cb)}$ electron is excited from the conduction band to an empty valence band leaving behind an electron hole $h^+_{(vb)}$ (Chong *et al.*, 2010). In this way, a positively charged 'hole' is formed in the valence band $h^+_{(vb)}$ and an $e^-_{(cb)}$ in the conduction band are generated (Seven *et al*,. 2004). A scheme of the main reactions during the electron-hole generation at the catalyst surface based in Min *et al.*, (2005) is illustrated in Figure 1.2.

Production of ROS and $^{\bullet}OH$ radicals by TiO_2 photocatalysis

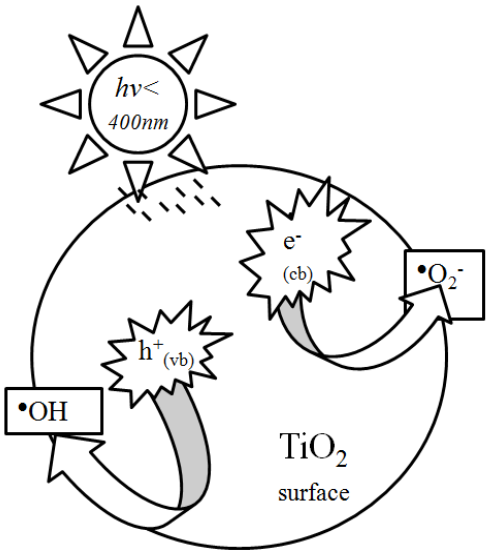

$TiO_2 + hv \rightarrow TiO_2 + e^-_{(cb)} + h^+_{(vb)}$

$O_2 + e^-_{(cb)} \rightarrow O_2^{\bullet-}$

$O_2^{\bullet-} + e^-_{(cb)} + 2H^+ \rightarrow H_2O_2$

$H_2O_2 + e^-_{(cb)} \rightarrow {}^{\bullet}OH + OH^-$

$O_2^{\bullet-} + H_2O_2 \rightarrow {}^{\bullet}OH + OH^- + O_2$

$h^+_{(vb)} + OH^- \rightarrow {}^{\bullet}OH$

$h^+_{(vb)} + H_2O \rightarrow {}^{\bullet}OH + H^+$

$2h^+_{(vb)} + 2H_2O \rightarrow 2H^+ + H_2O_2$

Figure 1.2 – UV generation of $^{\bullet}OH$ hydroxyl radicals at the surface of TiO_2 catalyst and reactions of the photocatalytic process.

In the conduction band, the electron $e^-_{(cb)}$ is available for electron transfer to reducible species that are adsorbed onto the TiO_2 surface. The $e^-_{(cb)}$ reduces oxygen to $O_2^{\bullet-}$(superoxide), and the further reduction of $O_2^{\bullet-}$ produces H_2O_2. Reduction of H_2O_2 by $e^-_{(cb)}$ can as well produce the $^{\bullet}OH$ radical. The superoxide can react with H_2O_2 to produce the $^{\bullet}OH$ radical (Haber–Weiss reaction) (Choi and

Choi, 2010). At the TiO_2 particle surface, the $h^+_{(vb)}$ hole abstracts electrons from absorbed oxidisable species, such as OH^- or H_2O and forming $^{\bullet}OH$ radicals. The recombination of $^{\bullet}OH$ radicals also produces H_2O_2. Therefore, the production of H_2O_2 can be ascribed to either a reductive pathway or an oxidative pathway (Choi and Choi, 2010). In the absence of electron acceptors, the electron-hole pair may recombine. The presence of oxygen might prevent this recombination by trapping electrons through the formation of superoxide ions. The final product of the reduction may also be a radical (Seven *et al.*, 2004).

By using semi-conductor photocatalysis, the organic pollutants (microbial or chemical origin) may be eventually photomineralised to CO_2, H_2O and mineral acids (Byrne *et al.*, 2011; Mills *et al.*, 1993). An attractive feature of heterogeneous TiO_2 photocatalysis is its ability to destroy simultaneously toxic pollutants and pathogenic microorganisms (Mccullagh *et al.*, 2007). This feature has been used in various applications such as water and wastewater treatment, self-cleaning surfaces and air cleaners (Fujishima *et al.*, 2000), in solar active materials to enhance degradation of pollutants on buildings roofs and surfaces and in bioufouling resistant materials (Li *et al.*, 2008). Additionally, photocatalysis has been claimed as a method to potentially help to inactivate airborne microbial pathogens and to combat the threat of bioterrorism agents such as anthrax (Gamage and Zhang, 2010).

1.1.1 Reactors

Oppenländer (2003) listed the basic models of photochemical reactors as batch reactor, mixed flow reactor, plug flow reactor and batch circulation reactor. The author explains that the choice for a reactor system depends of three variables: reaction system, lamp technology and photochemical engineering. In full-scale drinking water treatment a variety of UV reactor designs exist. The range of geometry of UV reactors results in different hydrodynamic within each system. As a result, the dose distribution, disinfection and oxidation may be different although the flow-rate, lamp power and water absorbance are the same (Wols *et al.*, 2011).

Studies of UV disinfection at bench scale often use a collimated beam apparatus (Braunstein *et al.*, 1996; Qualls *et al.*, 1983). It consists of a horizontally placed UV lamp, a shutter, a window, a collimated tube, power supply, platform (for stirring) and a Petri dish (Figure 1.3a). The collimated beam apparatuses are chosen more frequently because they are easier to construct and inexpensive compared to other UV reactors (Blatchley III, 1997).

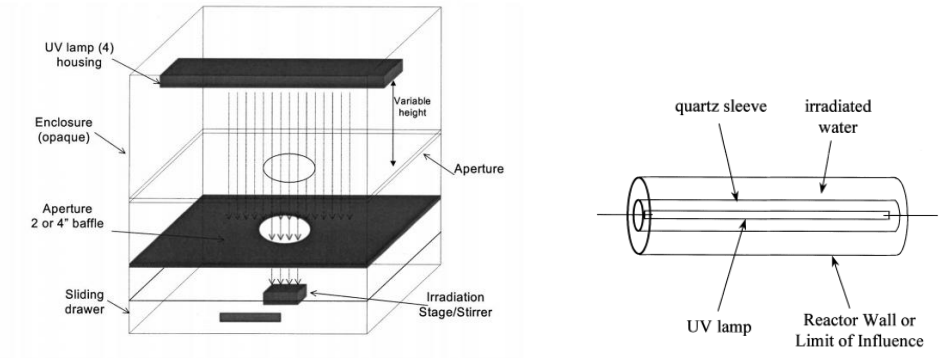

(a) (b)

Figure 1.3 – UV collimated beam apparatus (a) and annular UV reactor (b) (Bolton, 2000).

Another type of photochemical set up useful in bench-scale UV disinfection studies are the in-batch annular UV reactors (Figure 1.3b). Annular reactors are upscaled in comparison to the Petri dishes used in biodosimetry analysis, as they can hold a few litres of water (Labas *et al.*, 2009). They consist of an outside reactor vessel, an immersion well and a UV light source inserted into the quartz inner vessel. In UV annular reactors' fluence-rate varies from point to point in the reactor, but if the water is well mixed radially all the elements will receive the same average dose (Bolton, 2000).

In photocatalytic studies, when a catalyst such as TiO_2 is present in the reaction medium, the reactor configuration often differs from UV disinfection. In that case, two types of photocatalytic reactors are normally found; the slurry reactor type (Figure 1.4) and reactors with photocatalytic material immobilised in a solid carrier (Figure 1.5). The main difference between them is that in the slurry reactor type a separation unit is needed downstream in order to recover the photocatalyst. The slurry type of reactor is the one applied more frequently on photocatalytic

studies (Chong *et al.*, 2010). The reason, as aforementioned, is the larger surface of photocatalyst available for reaction and therefore more ROS (reactive oxygen species) are generated per volume of photocatalyst in suspension (Pozzo *et al.*, 1997).

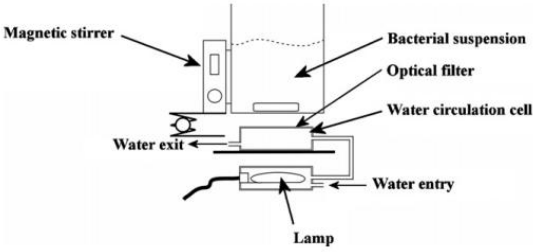

Figure 1.4 – Slurry reactor (Pyrex beaker) (Pinggui *et al.*, 2009).

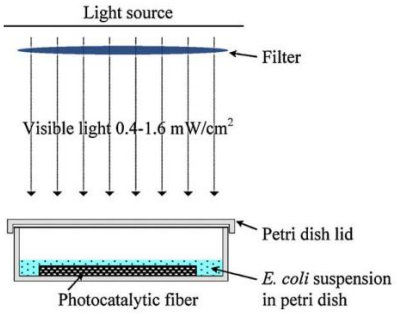

Figure 1.5 – Immobilised photocatalytic film (Benabbou *et al.*, 2007).

An effective reactor design will scale up laboratory bench scale processes to feasible industrial applications. Photocatalytic reactors have been used for various purposes including wastewater, potable water treatment and gaseous effluents. Examples of photocatalytic reactors employed in photocatalytic research are annular reactors, packed bed reactor, fluidised bed reactor, coated fibre optic cable reactor and swirl flow reactor (McCullagh *et al.*, 2011).

In the beginning of the 1980s the parabolic-trough collector (PTC) (Figure 1.6a, b) was believed to be the most appropriate hardware for the photocatalytic process. It followed the design of reactors used in solar thermal processes. However, drawbacks of the parabolic-trough collector included the large dimensions and area needed for installation, high cost, complicated maintenance, and the usage of photons was inefficient. Later, in the 1990s the focus of research turned to a new design of reactor, the non-concentrating collector (Figure 1.6c). This was static, simpler, and more cost-effective than the parabolic-trough collector. One type of collector that has shown major advantages against other systems is the compound parabolic collector (CPC) (Blanco-Galvez *et al.*, 2007) (Figure 1.6d). The CPC combines the capacity of concentrating the solar radiation and the ability to retain the stationary and diffuse-radiation collection properties

of flat plate collectors (Malato *et al.*, 2007). Advantages of the CPC include: turbulent flow conditions, absence of vaporization of volatile compounds, absence of tracking, absence of overheating, weatherproof resistance, low-cost, potential of capturing both diffuse and direct irradiance, absence of reactant contamination and high optical and quantum efficiency (Blanco-Galvez *et al.*, 2007).

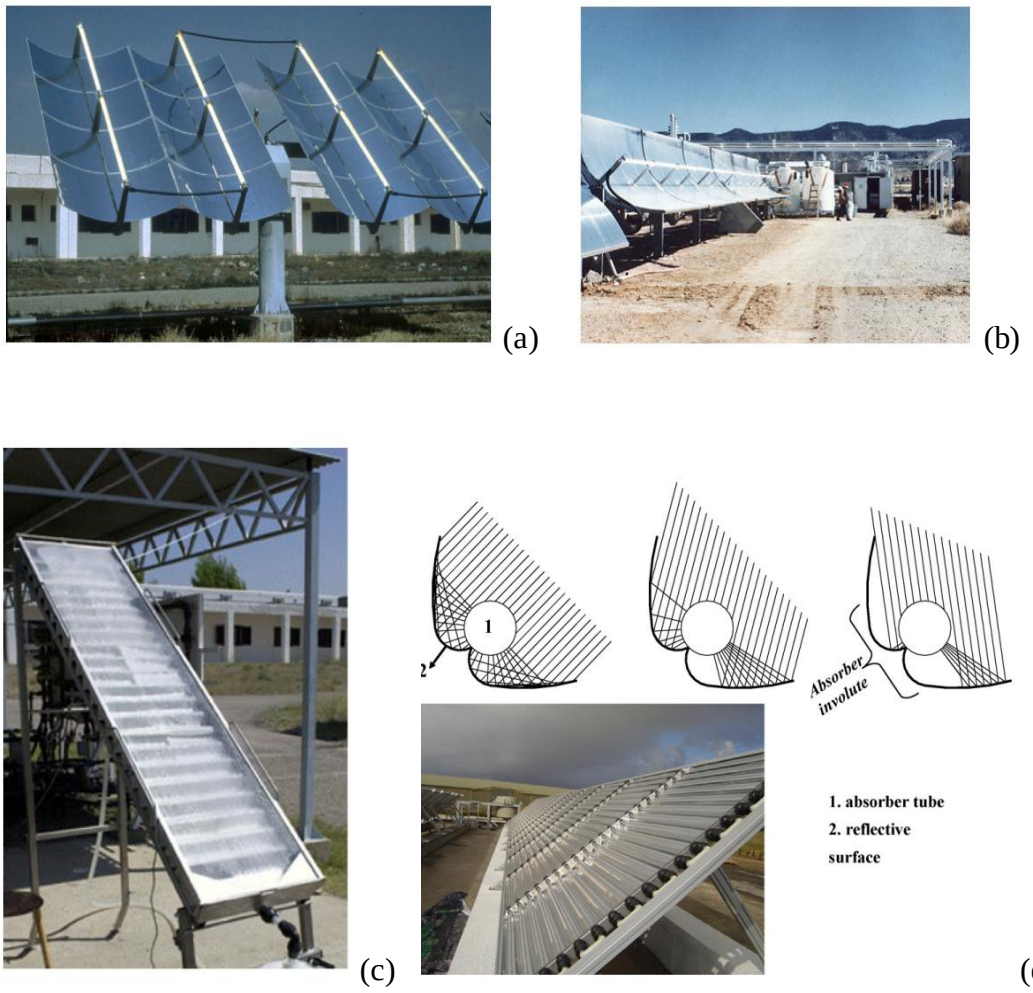

Figure 1.6 – A selection of solar reactors. Parabolic-troughs (PTC) with two axis solar tracking (a), Parabolic-troughs with single-axis solar tracking (b), Non-concentrating solar collector (c) and Compound parabolic concentrator (CPC) schematic drawing and photograph (d) (Malato *et al.*, 2007).

Much research has been carried out with CPC collectors in Plataforma Solar Almería (PSA), in Spain. The mirrors used in CPCs have been shown to be very effective in concentrating the solar spectrum (Navntoft *et al.*, 2008). The reactors have been used to enhance SODIS (solar disinfection) (Polo-López *et al.*, 2011; Navntoft *et al.*, 2008) , to reduce contamination of lettuce crops in reclaimed water irrigation (Bichai *et al.*, 2012) and to inactivate total coliform, *E. coli* and

Salmonella in natural water (Sciacca *et al.*, 2011). A new automated sequential batch CPC reactor for enhancing efficiency and application of SODIS has been recently demonstrated. In this work, the authors claimed an affordable solution to automatically carry out SODIS with reduction of exposure time and minimal user input (Polo-Lopez et al. 2011).

Mills and co-authors have suggested that the photocatalytic technology could be incorporated to alleviate fouling of membranes (Mills *et al.*, 1993). This was later demonstrated in practice by Zhang *et al.*, (2008). In addition, the work from Zhang *et al.*, (2008) investigated the concurrent filtration and photocatalytic degradation of humic acids. Li *et al.*, (2008) suggested that incorporating nanoparticles to membranes could prevent fouling and make the membranes "reactive instead of a simple physical barrier", which in turn would favour expansion of filtration in wastewater and water treatment. Furthermore, they claimed that nanoparticles, such as TiO_2 could be potentially combined with ultraviolet reactors to enhance detoxification and disinfection effects (Li *et al.*, 2008).

1.1.2 Light sources and measurement

UV disinfection units in water and wastewater disinfection plants use low (monochromatic) or medium-pressure (polychromatic) mercury lamps (Hijnen *et al.*, 2006; Sommer *et al.*, 2005).

Low-pressure mercury lamps (LP) are resonance lamps with emission peaks at 253.7 nm and 184.9 nm (USEPA, 2006). They contain mercury vapour at pressure of about $1.35x10^{-4}$ psi (USEPA, 2006) and power of 40-100 W (Bolton, 2000). LP lamps operate at an optimum temperature of $40^{o}C$. They are widely used in polymerization reactions and germicidal sterilization of water (Bolton, 2000), surfaces and food (Guerrero-Beltran and Barbosa-Cánovas, 2004). Two downsides of low-pressure mercury lamps are that monochromatic radiation at 253.7 nm is absorbed strongly by most organic system, the penetration of UV-C is low and limited, and in addition they emit lower fluence-rates compared to

medium-pressure mercury lamps (Phillips, 1983). Medium-pressure mercury lamps (MP) are high power (1-5 kW) (Bolton *et al.*, 2001) lamps that operate at elevated temperatures 600-900^{o}C. They are polychromatic and emit in the germicidal region between 200-300 nm and in the UV-A and B regions with overall high fluence-rate (intensity) (USEPA, 2006). Low-pressure mercury lamps have been used mainly in UV disinfection. Recently however, medium-pressure mercury lamps have been used more often. The reason for this is that they have a broader output power ranging between 200-300 nm (polychromatic) and consequently a higher germicidal UV power per unit length (Sommer *et al.*, 2005). Furthermore, medium-pressure lamps deliver UV-doses at lower contact times than low-pressure ones, thus fewer medium-pressure lamps are needed. In addition, costs associated with cleaning of quartz tubes used in medium-pressure lamps and replacement of the lamps is comparatively lower than the low-pressure lamps (Lingireddy, 2002) (Figure 1.7).

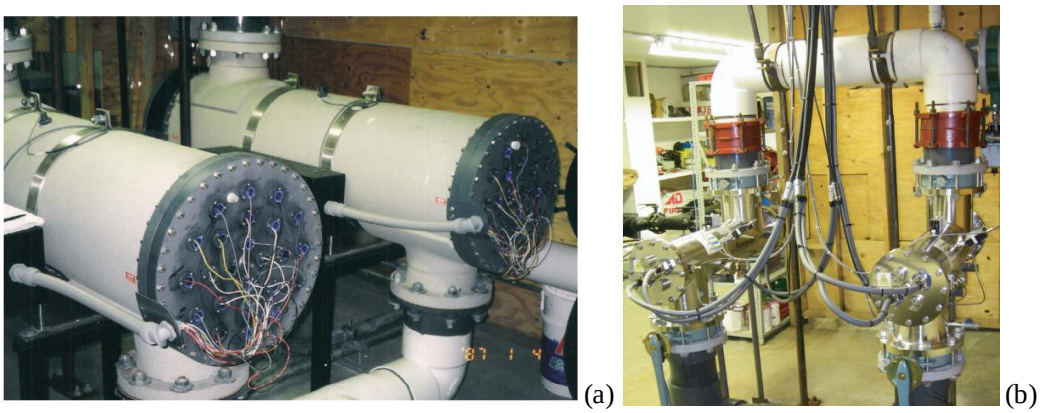

(a) (b)

Figure 1.7 – UV systems used to treat wastewaters in a low-pressure mercury lamp system with large number of lamps noted by the wires protruding from the ends of the UV chambers (a) and in a medium-pressure reactor system with only two lamps per chamber (b) (Aquionics, 2008).

The germicidal or UV-C emission of low-pressure mercury lamps is approximately 10%, whereas medium-pressure lamps have a germicidal efficiency of 30%. Other differences are that LP are indicated for lower water flows (<1000 m^3/h) while MP lamps are indicated for higher water flow (>1000 m^3/h) (Sommer *et al.*, 2005). The standards for efficiency of mercury lamps employed in UV disinfection plants are set by the Austrian National Standards ÖNORM M 5873-1 (ÖNORM, 2001) for low-pressure systems, and the ÖNORM M 5873-2 for

medium-pressure lamps (ÖNORM, 2003). In the US the standards for UV plants are set by the "Long Term 2 Enhanced Surface Water Treatment Rule" which was compiled by the US Environmental Protection Agency (USEPA, 2006).

The UV dose or "fluence" is calculated as a product of the fluence-rate (irradiance) and exposure time (Bolton and Linden, 2003). The SI unit of UV dose is J/m^2 (Joule per meter squared), conventionally adopted in Europe. On the other hand, the conventional unit of UV dose or fluence in North America is $mW\ s/cm^2$ (milliwatts seconds per centimeter squared) (Bolton, 2000). References for the validation of recommended UV doses on water treatment plants are available from the Austrian Standards Institute (ONÖRM, 2001) and the National Water Research Institute and the American Water Works Association (Jungfer *et al.*, 2007). Irradiance and intensity have been used in the UV literature; however the appropriate term in UV disinfection is 'fluence-rate'; as UV can hit the microorganism from any direction. On the contrary, radiometers measure the irradiance. In a well-designed collimated beam apparatus the fluence-rate and the irradiance are the same (Bolton and Linden, 2003).

Irradiance and intensity are terms used in the UV literature; however the appropriate term to be used in UV reactors is 'fluence-rate', since microorganisms can receive radiation from any direction, particularly when there are several UV lamps in the vicinity. Fluence-rate is the total radiant power passing from all directions through an infinitesimally small sphere of cross-sectional area d*A*, divided by d*A*. Irradiance is defined as the total radiant power incident from all directions onto an infinitesimal element of a surface area d*S* containing the point under consideration, divided by d*S*. Irradiance is the appropriate term when a surface is being irradiated by UV radiation coming from all directions above that surface (Bolton, 2000). The International System Units for fluence-rate is $W\ m^{-2}$ (Nic, Jirat and Kosata, 2010); however the unit mW/cm^2 is very common in UV disinfection studies. In a well-designed collimated beam apparatus the fluence-rate and the irradiance are the same. In this way, in a collimated beam apparatus, radiometers can be used to obtain the irradiance from each the fluence-rate is then extrapolated (Bolton and Linden, 2003).

In a collimated beam apparatus, the UV fluence-rate is obtained indirectly from a radiometric measurement of the UV fluence-rate reaching the water surface at the Petri dish (Lakretz *et al.*, 2010; Braunstein *et al.*, 1996). The radiometric measurement in a collimated beam apparatus needs to account for corrections which are the reflection factor, Petri factor, water factor and the divergence factor in low-pressure lamps and germicidal factor and sensor factor in medium pressure-lamps (Lakretz *et al.*, 2010; Bolton and Linden, 2003; Braunstein *et al.*, 1996). The Petri factor is a calculation representing a ratio which takes in accounts several measurements of average irradiance to the centre irradiance across the surface of a Petri dish. This factor compensates for the fact that the irradiance is not uniform over the entire surface area of the sample container, (e.g. a Petri-dish). The water factor determines the UV absorption by the liquid containing the test organism, a water factor was calculated by using an integrated form of Beer's Law that considers the absorption coefficient and the path length of the liquid (Zimmer and Slawson, 2002; Bolton, 2000).

Once these factors are taken into account the UV dose (mJ/cm^2) is obtained as a product of the average fluence-rate (mW/cm^2) value and exposure time in seconds. Radiometric measurements become a simple, cost-effective and routine measurement in full-scale UV plants. However, there are several problems with this method. The first is the number of sensors and the locations required to be monitored within the reactor as the variations in reactor geometry, reflection and water quality influence the actual fluence-rate. Secondly, UV sensors are not reliable in the long term due to fouling or degradation by exposure to UV wavelengths (Malley, 2002).

Other methods for measurement of UV-dose are biodosimetry, mathematical modelling and actinometry (Braunstein *et al.*, 1996). In biodosimetry, for instance, a surrogate microorganism (biodosimeter) is seeded in a collimated beam apparatus where a log inactivation is computed. The surrogate microorganism is then seeded in a full-scale UV system and the log inactivation obtained is correlated with the values of the collimated beam device in a

calculation called the Reduction Equivalent Fluence for obtaining the UV dose (USEPA 2006, Hijnen and Medema, 2010). Biodosimetry is already used in UV drinking water applications as a norm in Austria and as a guideline in Germany and in the USA (Hijnen and Medema, 2010). In mathematical modelling, refined and complex tools such as Multiple Point Source Summation (MPSS model), Line Source Integration (LSI model) or Multiple Point Source Summation modified model have been developed to obtain average fluence-rate of annular reactors, which then when multiplied by the hydraulic retention time yielded the ideal maximum UV dose (Bolton, 2000). In the case of chemical actinometry, an actinometer, such as potassium ferrioxalate or potassium iodide are used to determine experimentally the irradiance and dose delivery based on quantifiable, photochemically changes of the actinometer (Blatchley III *et al.*, 2006).

In photocatalytic disinfection a series of radiation sources able to emit in the UV range have been used. They include solar irradiation with CPC mirrors (Bichai *et al.*, 2012) , a Hanau Suntest (AM1) lamp (solar simulator) (Rincón and Pulgarin, 2004c), a high pressure mercury lamp (λ<300 nm cut off) (Lu *et al.*, 2003), F40BL blacklights (Huang *et al.*, 2000; Watts *et al.*, 1995), a xenon UVA lamp with 330-450 nm output (Robertson *et al.*, 2005) and low-pressure mercury lamp (Sun *et al.*, 2003). In photocatalytic studies, radiometric measurement is the choice of practice for obtaining fluence-rate values (Pinggui *et al.*, 2009; Rincón and Pulgarin, 2007; Gumy *et al.*, 2006), although chemical actinometry has been less reported (Gumy *et al.*, 2006; Cho *et al.*, 2004).

1.2 Photodynamic inactivation (PDI)

The principle of photodynamic inactivation (PDI) consists of irradiating a photosensitiser (PS) molecule with appropriate visible light (photosensitisation) and in the presence of molecular oxygen to generate singlet oxygen and other various reactive oxygen species (ROS). The singlet oxygen, which is a highly oxidizing excited state of molecular oxygen and the ROS formed react with biomolecules in the microbial cell and promote the photodynamic inactivation (Mantareva *et al.*, 2011).

Research in photosensitised production of singlet oxygen has made a substantial contribution to the medical and environmental fields. PDT (photodynamic therapy) is used to treat microbial infections, skin disease and tumours (Hashmi *et al.*, 2011; Dolmans *et al.*, 2003). PDT benefits agriculture in the production of sunlight-activated herbicides and insecticides, while other applications include remediation of wastewater and disinfection of drinking water (Magaraggia *et al.*, 2011). In addition, the photosensitized generation of singlet oxygen is applied in synthesis of fine chemicals to obtain products which would be more expensive or complex to obtain by other means (Oleinick, 2010).

Nowadays, the medical application of singlet oxygen is accepted namely as PDT. Nonetheless, PDT is a term also used in antimicrobial applications (Jori and Coppellotti, 2007). Wainwright (1998) named the destruction of microorganisms by singlet oxygen as "photodynamic anti-microbial chemotherapy" (PACT) (Wainwright, 1998), while other used terminologies used are anti-microbial therapy (aPDT) (Almeida *et al.*, 2011) and photodynamic inactivation (PDI) (Perussi, 2007).

The first record of medical usage of a photosensitiser dates from a painting of the ancient Egyptians. The plant extracts of *Amni majus* and sunlight were shown in that painting to be used in the treatment of a skin disease (Josefsen and Boyle, 2008; Oppenländer, 2003). Currently, the active principle of *A. majus* (psoralen) is successfully employed in the treatment of psoriasis (Josefsen and Boyle, 2008). In the beginning of the 20th century, Oscar Raad showed the first concrete evidence of toxicity of a sensitiser (acridine orange) against a microorganism (*Paramecium caudatum*) in the presence of light (Maisch, 2007). Later Raad's teacher Tappeiner named the effect observed as "photodynamic reaction" (Maisch, 2007). From the middle of 20th century, and with the discovery of antibiotics, research/studies with antimicrobial photodynamic therapy were put aside. When antibiotic misuse brought about emergence of drug resistant microbial species, studies on PDT were retrieved as an alternative to tackle the

problem of increased acquired antibiotic resistance (Schastak *et al.*, 2010; Maisch, 2007).

During the generation of singlet oxygen by photosensitisation, a photon of energy is absorbed by the photosensitiser S_0, which is excited to the singlet state (S_1). The S_1 short life-time and low-energy state sensitiser, either returns to ground state or, by intersystem crossing, passes to a lower energy but longer lived triplet state (T_1). T_1 sensitiser undergoes two types of photoreactions in the presence of oxygen- *type I* reaction - involves electron transfer between the T_1 photosensitiser and a substrate molecule (e.g. a membrane lipid) producing radical ions. In a chain of reactions, those radical ions react with oxygen to produce reactive oxygen species (ROS), such as superperoxide $O_2^{\bullet-}$, hydroxyl and hydroperoxide (Kuznetsova *et al.*, 2007). *Type II* reaction - involves energy transfer from the triplet state photosensitiser "T_1" to triplet state molecular oxygen $^3O_2$ "T_0". This transfer of energy generates singlet oxygen ($^1O_2$*) (Oleinick and Evans, 1998). In Figure 1.8, a detailed Jablonski diagram modified by Bonnet (1995) shows the reactions occurring during photosensitised generation of singlet oxygen.

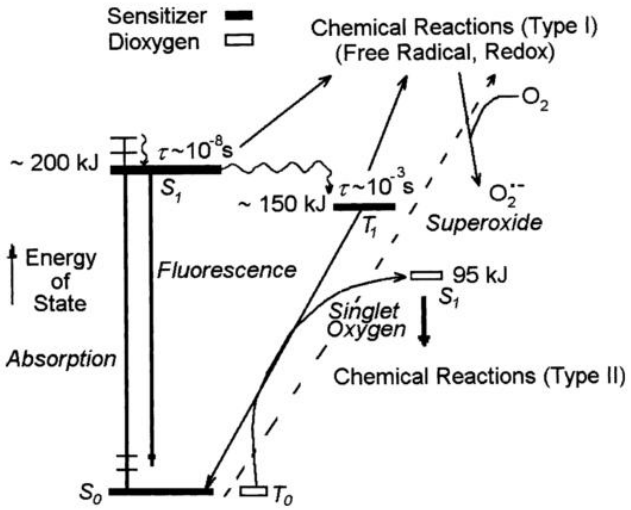

Figure 1.8 – Electronic transitions upon one photon of light absorption by a sensitiser during photosensitised generation of singlet oxygen (Bonnett, 1995).

Each photosensitiser molecule typically produces 10^3-10^5 singlet oxygen molecules $^1O_2$* before being photodegradaded or photobleached (Derosa and Crutchley, 2002). The singlet oxygen yield of singlet oxygen Φ_Δ is always equal

or less than a unit ($\Phi_\Delta \leq 1$). In other words, the Φ_Δ measures the efficiency of singlet oxygen generation during a photosensitised reaction (Josefsen and Boyle, 2008).

Any photosensitiser ought to have (1) high absorption coefficient in the spectral region of the excitation light; (2) a triplet state of appropriate energy to allow energy transfer to ground state oxygen; (3) high quantum yield of the triplet state and long triplet state lifetime (>1 μs); and (4) high photo-stability (Derosa and Crutchley, 2002). In the case of a photosensitiser used in the environment, e.g. to treat water, Almeida *et al.*, (2011) highlight other aspects which deserve attention. These include (1) the removal of the sensitiser after photodynamic action to avoid its release in effluent water; (2) the effect of physical and chemical parameters of environmental waters; (3) possibility of using sunlight as light source and (4) photostability of sensitiser and conjugates under sunlight irradiation. In medical applications, the photosensitiser has to be non-toxic under dark conditions and have high affinity to the tumour cells (Perussi, 2007). In addition, to minimise the risk of side effects it ought to have maximum absorption in the red region (λ>600 nm) which has a higher penetration power into most human tissue, and it should not be absorbed by endogenous cell/tissue constituents to a significant degree.

The efficiency of PDI depends on many factors including charge of the sensitiser, incubation time, light dose, and rate of drug uptake (Melo *et al.*, 2011). Another factor which has been found relevant in PDI of Gram-negative bacteria is increased lipophilicity which allows increased interaction with lipid-rich membranes (Wainwright *et al.*, 2010). In 2011 Wainwright and collaborators demonstrated (Wainwright *et al.*, 2011) through the study of methylene blue derivatives that increased amphiphilic character endowed higher microbial uptake by microbial cells, thus improving photo-antimicrobial activities. A sensitiser molecule which is successfully used in chemical assays may not perform well against microbial targets due to metabolism, reduction or because it is not localized in a non-vital area (Wainwright, 1998). Another point is that good yields of singlet oxygen production in an *in vitro* environment may not correlate

antimicrobial photodynamic efficiency given the differences with cellular environments (Wainwright *et al.*, 2010).

In general, positively charged photosensitisers are more effective in promoting PDI of bacteria and act in lower concentrations than anionic or non-charged photosensitisers (Perussi, 2007). Photosensitisers can be divided in three classes according to their level of microorganism association. There are photosensitisers which are tightly bound and penetrate into the microorganisms such as polycationic porphyrins conjugates, those which are only loosely bound such as toluidine blue or methylene blue, and those which do not demonstrate any level of binding such as Rose Bengal (Demidova and Hamblin, 2005). The higher efficiency of the polycationic porphyrins have demonstrated superior inactivation rates of *S. aureus*, *E. coli* and *C. albicans* at considerably lesser fluence of light and sensitiser concentrations (Ergaieg and Seux, 2009; Demidova and Hamblin, 2005).

Alternatively, chemical classification of photosensitisers used in PDI include halogenated xanthenes such as Rose Bengal, phenothiazinium photosensitisers such as methylene blue and toluidine blue (Perussi, 2007), cyclic terapyrroles or structural derivatives in particular porphyrin, chlorin, bacteriochlorin, expanded porphyrin, and phthalocyanines derivatives (Josefsen and Boyle, 2008).

Xanthene dyes such as erythrosine and Rose Bengal show strong absorption of light in the spectral range of 500-550 nm which corresponds to that emitted by light-emitting-diodes LEDs (blue and green lights) (Rossoni *et al.*, 2010). Rose Bengal possesses triplet states of appropriate energy for photosensitisation of oxygen and a high quantum yield in water ($\Phi_{\Delta=}0.76$) (Derosa and Crutchley, 2002) and very high molar extinction coefficient ε=99,800 M^{-1} cm^{-1} at 549 nm (Panzarini *et al.*, 2011). In photodynamic microbial inactivation for purposes of drinking water treatment, Rose Bengal (xanthenes) and methylene blue (phenothiazinium) are widely reported compounds (Josefsen and Boyle, 2008; Cooper and Goswami, 2002).

Wainwright and Crossley (2004) considered phenothiazinium photosensitisers, which include methylene blue, as very suitable for PDT applications. The reason is that methylene blue derivatives have often been used as microbial stains as they are highly selective to microbial cells, and they have high propensity for ROS production (Wainwright and Crossley, 2004). Methylene blue has a significant singlet oxygen yield in water (Φ_{Δ}=0.52) (Derosa and Crutchley, 2002). A new generation of derivatives from methylene blue (pentacyclic phenothiazinium compounds) have recently been developed and claimed to be highly effective in PDI applications. They have shown to have increased λmax and amphiphilic character, while maintaining intense light absorption and high singlet oxygen yields. Moreover, these phenothiazinium compounds present very low toxicity in the dark. One of compounds, 1,9-dimethyl-methylene blue, was more amphiphilic than methylene blue which could explain its improved efficiency in comparison to methylene blue. The discovery of such compounds is of great value as they can be used in red blood cells sterilisation for which there is no current clinic accepted protocol (Wainwright *et al.*, 2011). Porphyrins are a class of compounds which are found in nature and are composed of aromatic heterocyclic structures. The two important porphyrins are haem and chlorophylls. As porphyrins have unique physic-chemical properties they are used in diverse applications ranging from artificial photosynthesis, oxidation catalysis, sensors and in nanomaterials for PDT and PDI usage. For the purpose of PDT applications there are two groups of porphyrins: natural, natural but chemically modified porphyrins and synthetic porphyrins (neutral, anionic and cationic) (Almeida *et al.*, 2011).

Porphyrins and their analogues gained increased research attention because their presence in nature makes them ideal to be used in singlet oxygen generation in biological systems. They can absorb several wavelengths in the UV-VIS range and many have long triplet states which allow for high singlet oxygen quantum yield. When searching for specific applications, the properties of porphyrins can be modified by substituents on the macrocycle, such as metal ions coordinated at its centre, or ligands attached to axial positions (Derosa and Crutchley, 2002). Phthalocyanines are derivatives of the porphyrin skeleton and differ by having nitrogen atoms linking the individual pyrroles units. Phthalocyanines have the

property of absorbing the red region overlapping the region of max tissue absorption thus making them very useful in PDT applications (Derosa and Crutchley, 2002). Porphyrins and Phthalocyanines have been successfully used to promote inactivation of Gram-positive bacteria. When microbial inactivation in homogenous media takes place, the efficiency against Gram-negative bacteria, however, is dependent upon the addition of positive groups which are strongly linked with a negatively charged cell wall (Phoenix *et al.*, 2003).

Photosensitised generation of singlet oxygen from molecular oxygen using a suitable photosensitiser can be achieved in solution (homogeneous) and in a heterogeneous medium (immobilised sensitiser) (Burguete *et al.*, 2009). Photodynamic inactivation is efficient when the photosensitiser is water soluble, although the removal of water-soluble dyes and their photoproducts from treated solution is extremely difficult. In this way, the use of immobilised photosensitisers is of great interest as the immobilised chemical can be easily separated from the solution by filtration or centrifugation (Kuznetsova *et al.*, 2011). The first work demonstrating the utility of immobilised photosensitisers was carried out by Shaap and Neckers (1973) with Rose Bengal merrifield resin, a low cross-linked polystyrene bead. Since then, new solid supports or carrier systems have been developed to expand the applications of PDT or aPDT. Whether a sensitiser is immobilised in a solid support one factor to be considered is the diffusion length of the singlet oxygen which is about 200 nm (Kuznetsova *et al.*, 2011; Krasnovsky Jr, 1998). Kuznetsova *et al.*, (2011) discussed the need for ongoing research in the field as there is still a need to develop immobilised sensitisers able to generate better singlet oxygen yields in water (Kuznetsova *et al.*, 2011). Examples of solid supports include polymeric substances such as polycationic chitosan-conjugated (Shrestha and Kishen, 2012), porous silicon (Manjón *et al.*, 2007), polyacrylamine resins, polyacrylates, silica, gold nanoparticles, magnetic carriers, and quantum dots and porous monolithic polymer (Burguete *et al.*, 2009).

In order to achieve a successful level of microbial inactivation, an immobilised photosensitiser has to be in close contact with bacterial cells because of the short-

life of $^1O_2$* in water (3-4 μs) (Rengifo-Herrera *et al.*, 2007). This can be achieved by immobilising the sensitiser in a matrix which promotes interaction with the bacteria. PDI performed with immobilised sensitiser relies on the diffusion of singlet oxygen from the inside of the support to the peripheral area where bacterial cells must be located. It is important to note, however, that singlet oxygen can diffuse only through short distances ~0.2 μm (Kuznetsova *et al.*, 2011). In this way, PDI has so far reduced bacterial numbers in water, though more robust heterogeneous sensitiser/solid support systems need to be developed (Kuznetsova *et al.*, 2011; Bonnett *et al.*, 2006).

1.2.1 Reactors, light sources and measurement

As in photocatalysis, examples of reactor systems used in photodynamic inactivation studies are also divided into homogeneous (sensitiser in solution) and heterogeneous systems (sensitiser in solid carrier). Pyrex® glass with Pyrex lids irradiated by natural sunlight has been used into homogeneous PDI studies (Cooper and Goswami, 2002). Other homogeneous reactions with modified porphyrins in the inactivation of *Bacillus* spp. have used a fibre optic probe coupled with a halogen lamp with emission between 400-800 nm and measured irradiance (1690 W/m^2) obtained with radiometric measurement (Oliveira *et al.*, 2009).

Three PDI reactor systems for homogeneous solution of methylene blue used by de Paula *et al.*, (2010) are depicted Figure 1.9. The reactor used different lamps and a homogeneous solution of methylene blue. In the case of device (a) the equipment PHLS-halogen lamp and a metal carcass with lamp and cooler (1) was used with a magnifying glass (2), a glass box (3) and optical filter (4). In reactor (b) the LED600-LED had an arrangement of high brightness LED (1), a translucent mobile support for sample setting (2), a height groove (3) and a support setting (4). And in reactor (c) an AMS-II equipment-high intensity LED device made of an arrangement of high power LED (1) was used with a heat processor dissipater (2) and a groove for support setting for the insertion of the sample (3).

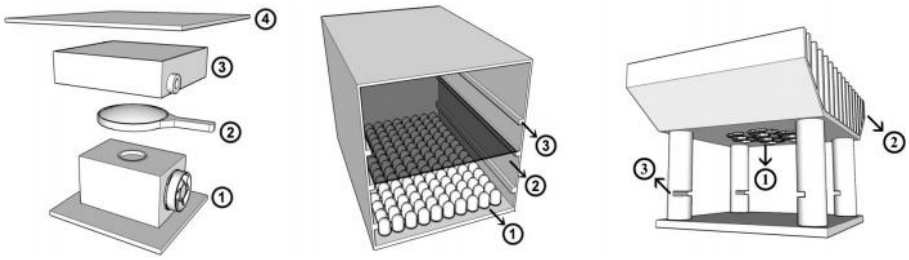

(a) (b) (c)

Figure 1.9 – PDI reactor systems for homogeneous solution of methylene blue: a PHLS-halogen lamp (a), a LED600-LED (b) and an AMS-II equipment-high intensity LED device (c) (de Paula *et al.*, 2010).

An alternative PDI system is illustrated in Figure 1.10. It consists of a heterogeneous reaction with circulating photoreactor system coupled with a chitosan membrane impregnated with either a modified porphyrin or phthalocyanine. The irradiation was provided by halogen lamp (Bonnett *et al.*, 2006).

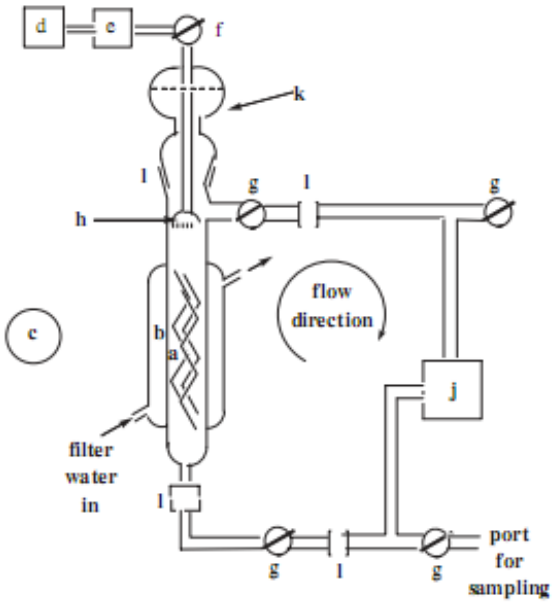

Figure 1.10 – Circulating water photoreactor system for the determination of photomicrobicidal activity under water flow conditions. a—reinforced membrane under study; b—water jacket, continuous flow, infra-red filter; c—light source; d—air pump; e—bacterial air filter; f—3-way tap/pressure release; g—2-way taps; h—frit for aeration; j—peristaltic pump; k—reservoir; l—ground glass joints, for ease of cleaning and sterilization.

In PDI studies radiation sources include lasers (coherent) and lamps and light emitting diodes (non–coherent). Lasers which are non-coherent light sources allow the light delivering through a fibre optics fibre to the site where PDI effect is desired. Examples of lasers are helium neon-lasers and the semiconductor diode lasers (LEDs) (Calin and Parasca, 2009). The fluence-rate used to calculate the "dose" produced by the light sources used in PDI studies is routinely acquired by radiometric measurement (Cooper and Goswami, 2002).

Light-emitting diodes (LEDs) are solid-state sources consisting of a semi-conducting crystal which covert electrical energy into radiant flux. Common LEDs are gallium arsenide and silicon carbide. With appropriate mixing of these components the λmax can be shifted between 540 nm and 900 nm. LEDs are usually operated at very low voltage and they normally produce very narrow spectral emission bands (Grum and Becherer, 1979). Some advantages of LED systems are high physical resistance, long lifetime (~100,000 h), low heat emission and low cost per unit of power when compared to laser diode systems (de Paula *et al.*, 2010).

1.3 Microbes in the environment

In the natural environment, microorganisms are found in planktonic (free-swimming) forms, aggregated in clumps (Logan and Hunt, 1987) or anchored in biofilms (Flemming and Wingender, 2010; Rehm, 2008). The suspended portion of microorganisms in a water sample, which is not found attached to either each other or to particles, is the free-swimming or planktonic population, whereas the part which is attached to a surface is the so-called "sessile" population (Meltzer, 1997).

Despite the acknowledged significance of aggregated microorganisms in the natural environment, practice in the laboratory generally involves cultures of planktonic microorganisms as models (Schleheck *et al.*, 2009). Standard microbiological practice includes inoculating a pure culture in a defined medium

until it reaches the exponential phase of growth, generally monitored by turbidity (Lengeler, Drews and Schlegel, 1999). The inoculum is resuspended in water or in a nutritious medium until it develops to a certain number of cells; then it is used to the purposes of the research. Much of the current knowledge of microbial physiology is based on laboratorial studies of planktonic cells (Stoodley *et al.*, 2002). Central to the entire discipline of the microbial way of life, however, is the now well accepted concept that microorganisms rarely, or even not at all, live as pure cultures of dispersed single cells (Flemming and Wingender, 2010; Costerton *et al.*, 1978). Instead, microbial cells are believed to grow preferentially in communities associated in biofilms anchored to surfaces or in free-floating aggregates, while planktonic cells have been suggested as a microbial mechanism of dispersion in the environment (Stoodley *et al.*, 2002).

Cell aggregation is a widespread phenomenon in the microbial world (Burdman *et al.*, 1998). For example, ecological associations of single or multiple prokaryotic species are often observed as symbiotic, parasitic, commensalism and neutralism systems (Lengeler, Drews and Schlegel, 1999). In the case of cell aggregation the definition has been given by Calleja in 1984 as "the gathering of cells to form fairly stable, contiguous, multicellular association, occurring under certain physiological conditions" (Calleja, 1984). Aggregated cells are also referred to with terminologies such as film, floc, pellet, pellicle, cluster, slim and for instance granule (Yu and Joo-Hwa, 2002). Floc-forming bacteria are indigenous to natural waters. The flocculant growth habit of organisms is exploited in biological waste treatment processes (Friedman *et al.*, 1969), or in the production of inoculants for agriculture (Burdman *et al.*, 2000). Another example of the use of flocculant habit is found in industrial fermentation processes, where it facilitates the removal of yeast biomass from the final product (Logan and Hunt, 1987).

Aggregation is a vital aspect related to microbial sensitivity to disinfection (Behnke *et al.*, 2011; Bohrerova and Linden, 2006b; Hijnen *et al.*, 2006) and this is due to the presence of EPS (extracellular polymeric substances), which endows aggregated microbial cells with a higher resistance against disinfectants (Behnke *et al.*, 2011) and antibiotics (Nichols *et al.*, 1989). Autoaggregation or aggregation

of microorganisms to particles has also been shown to decrease inactivation by UV (Hijnen, Beerdonk and Medema 2006).

EPS is a polymer "self-generated" (Schleheck *et al.*, 2009) by microbial species including archae, bacteria and eukaryotes (Flemming *et al.*, 2007). EPS is a protective layer of substances which often found surrounding bacterial cells (Lengeler, Drews and Schlegel, 1999). EPS is divided in bound-EPS or capsule (macrocapsules and microcapsules) and free-EPS or slime (Wingender, Neu and Flemming, 1999). The bound-EPS is tightly connected to the cell surface by covalent links, but most often by ionic bonding (Lengeler, Drews and Schlegel, 1999). Conversely, the free EPS is not directly attached to the cell surface. Besides, as opposite to bound-EPS, the free-EPS can be removed from cells by a centrifugation step (Eboigbodin and Biggs, 2008; Wingender, Neu and Flemming, 1999).

The EPS composition includes carbohydrates, proteins and nucleic acids (Scott *et al.*, 2005; Liao *et al.*, 2001). Sheng *et al.*, (2010) has defined EPS from wastewater treatment systems as a "complex high-molecular weight mixture of polymers". Examples of two relevant polysaccharides present in EPS are alginate and cellulose. Alginate was found to be the most abundant EPS component of *Pseudomonas aeruginosa*, for instance (Donlan, 2002). Cellulose, which has an important role in aggregation, participates in EPS composition of various bacteria, algae and amoeba (Flemming *et al.*, 2007). EPS composition varies according to factors such as growth conditions and species composition (Steinberger and Holden, 2005).

The superior resistance of biofilms and, by extension, of aggregated microbial cells, (Alhede *et al.*, 2011) compared to planktonic cells, is well discussed in the literature (Mantareva *et al.*, 2011; Flemming, 2009). The EPS matrix can offer full or partial protection against desiccation, oxidizing or charged biocides, antibiotics, metallic cations, ultraviolet radiation, protozoan grazers and host immune defences (Flemming and Wingender, 2010). EPS acts as an efficient barrier and protects a high percentage of cells from bactericidal effects of conventional

chemotherapy; besides the EPS matrix undergoes little or no destruction (Flemming and Wingender, 2010). As a consequence, the remaining EPS matrix allows for further colonization (Wainwright *et al.*, 2002).

Biofilms are an attached form of aggregated microbial cells. They are the oldest and most successful way of bacterial life on earth (Flemming and Wingender, 2010). The observation of pure and mixed bacteria biofilms showed that cells grow enclosed in a matrix (the EPS), forming micro-colonies interconnected by water-channels (Stoodley *et al.*, 2002). They colonize surfaces exposed to water in industry and inert surfaces of medical implants where they may cause fouling/corrosion and infection, respectively (Nichols *et al.*, 1989). EPS and biofilm attachment constitute a severe problem especially in healthcare systems where contamination of implants, catheters or bones results in long-term infections with complex eradication measures (Flemming, 2009).

Bridier *et al.*, (2011) explains that biofilms are resistant to disinfectants currently in use and that therefore, new methods to control them need to emerge. One strategy they indicated as being efficient in eliminating surface contamination by biofilms is the application of combined chemical, natural and physical treatments. The authors mentioned, for example use of Cu^{2+} ions, quaternary ammonium compounds, eucalyptus oil and chlorhexidine, silver and surfactant, or bacteriophage and alkaline cleaner were able to act synergically to eradicate biofilms. Alternatively, UV disinfection in association with chlorine dioxine was also shown to be efficient (Bridier *et al.*, 2011).

In situ eradication of biofilms by photodisinfection is receiving growing attention. Street and Gibbs (2010) has defended the application of photodynamic inactivation of *Desulfovibrio vulgaris* and *Desulfovibrio desulfuricans* microbial species which cause corrosion in pipelines. The method consists of applying a photosensitiser and visible light to promote the generation of singlet oxygen and secondary reactive oxygen species. They claimed that developments in this technology may improve *in situ* inactivation and removal of biofilms (Street and Gibbs, 2010). Endeavour to use photodisinfection; this time with UV-C radiation,

in order to sterilize urinary catheters has also been recently undertaken (Bak *et al.*, 2010).

Besides the focused attention that the disinfection of biofilms and planktonic cells has received from the literature, free-floating aggregates are under-studied (Armbruster *et al.*, 2012; Behnke *et al.*, 2011). Favourably to using aggregated cells as a model Schleheck *et al.*, (2009) proposed that investigations with "suspended biofilms" could "help to address some important contemporary questions about formation, maturation and dispersion of attached biofilms". The authors demonstrated that *P. aeruginosa* PAO1 in batch cultures was dispersed in form of 'suspended biofilms' instead of free-swimming forms. They also noted that aggregated forms had similar behaviour and responses compared to surface associated biofilms. Their study highlighted that aggregates could be a valid model to address mechanisms and factors enrolled in the formation, maturation or dispersal of surface attached biofilms (Schleheck *et al.*, 2009). As aggregated cells share physiological conditions to anchored biofilms (Henriques and Love, 2007), the study of their disinfection may contribute to the understanding of the resilience associated with microbial communities colonizing engineered environments in biofilm form.

As well as that, aggregated cells may be a robust model with which to study the inactivation of detached biofilm clusters. The detachment of clusters is one of the strategies biofilms use to disperse. It occurs by the sloughing of clusters of cells (aggregates) and their envelopes or by the releasing of planktonic forms (Schleheck *et al.*, 2009; Costerton, 2007; Henriques and Love, 2007; Costerton *et al.*, 1999). The detachment of the biofilms' clusters, which occurs intermittently by shedding parts of the biofilm structure in the contacting water, compromises the microbial integrity of the liquid (Costerton, 2007; Costerton *et al.*, 1999). Moreover, even a small number of microorganisms may prove pathogenic to susceptible individuals (Meltzer, 1997). A cluster of biofilm which falls into the potable water stream can hold up to ~$1.6x10^3$ cells (Stoodley *et al.*, 2001). Considering that the minimum infectious dose depends on the host (age and health) and pathogen (Gadgil, 1998), ingestion of a number as low as ten cells

may cause waterborne disease (FDA, 2006). In this context, as indicated by Stoodley *et al.*, (2001) the ingestion of one cluster of biofilm may offer a high risk of infectivity (Stoodley *et al.*, 2001).

Detailed examination of the contamination of public water distribution was carried out by LeChevallier, Babcock and Lee (1987). Their studies led to the conclusion that the water was contaminated by intermittent release of coliforms from biofilms inhabiting the inner surfaces of pipes. Biofilms are not only restricted to public water distribution systems, they are also ubiquitous to industrial distribution systems (Murthy and Venkatesan, 2009). In their editorial article, Riedewald and Sexton (U.S. Pharmacopeia, 2000) explained that the growth of biofilms occurs even under limited nutrient conditions of compendial waters. The authors argued that as long as water was available and there was a surface to attach to, intrusive free-swimming cells may develop into biofilms and colonize the water distribution systems. Interestingly, the role of detached cellular clusters in infecting water streams and the relevance of free-floating aggregates in this context remains poorly understood (Stoodley *et al.*, 2001).

Water systems in industry require high levels of purity. For instance, an alert for action concerning the quality of the industrial unit takes place when bacterial numbers exceed 500 cfu/ml in drinking water, 100 cfu/ml in purified water and 10 cfu/100 ml in water for injection. In industrial settings, the presence of biofilms is constantly monitored by evaluating the presence of free-swimming bacteria in a sample of flowing water. The detection of an increased level of planktonic microorganisms indicates advances in the biofilm growth. In this case, remediation actions to decrease biofilm infestation are taken (U.S. Pharmacopeia, 2000).

Many of the contaminants associated with biofilms in water distribution systems are Gram-negative rods, in particular Pseudomonads (Meltzer, 1997). Pseudomonads are ubiquitous inhabitants of the most diverse environments. Some are pathogenic for humans, animals or plants (Bergey and Holt, 1994). *Pseudomonas aeruginosa* is the most important species. It is often associated with

infections of humans and mammals (Kiil *et al.*, 2008). *P. aeruginosa* is used as an indicator of the quality of recreational waters and its presence is normally associated with dermatitis and ear infection (APHA, AWWA and WPCF, 1998). *P. aeruginosa* is an opportunistic pathogen and it is noted for its antibiotic resistance (Pipes, 1982). The bacterium has also been reported to have superior resistance to oxidative stress, disinfectants, and more importantly antibiotics, as well (Nichols *et al.*, 1989). Recently, in an Ulster hospital, close to Belfast, three new borne infants died from an infection caused by *Pseudomonas aeruginosa*. The microbiological assessment linked the outbreak to contaminated tap water from the outlet in the neo-natal intensive care unit of the hospital (BBC-UK, 2012). *P. putida* is another key species and model bacterium. Unlike *P. aeruginosa*, *P. putida* is a non-pathogenic organism. *P. putida* has been isolated from most diverse environments, such as polluted soil, water and the rhizosphere (Kiil *et al.*, 2008). As distinct from *P. aeruginosa* and *P. fluorescens*, *Pseudomonas putida* cannot liquefy gelatine, nor produce phenazine pigments, to denitrify, to give an egg yolk reaction, and to grow at 41^{o}C (Bergey and Holt, 1994).

Kiil *et al.*, (2008) explained that among *P. putida* species, the strain KT2440, ubiquitous to soils, is a reference species for diverse biotechnological applications, such as bioremediation or bio-pesticides. Another environmental isolate is the strain *P. putida* CP1. This bacterium has been extensively studied in this research laboratory for the purpose of bioremediation (Fakhruddin and Quilty, 2007; Fakhruddin and Quilty, 2006; Fakhruddin and Quilty, 2005; Farrell and Quilty, 2002b; Farrell and Quilty, 2002a). The organism forms clumps of aggregated cells, visible to the naked eye, under certain environmental conditions (Farrell and Quilty, 2002a).

Found in very high numbers in all mammalian faeces, *E. coli* remains as a useful indicator of faecal contamination in drinking waters (Edberg *et al.*, 2000). In Ireland, *E. coli* is a central health indicator of drinking water quality. The presence of *E. coli* in treated drinking waters indicates either a failure of the treatment process, or that contamination has entered the water distribution system after

treatment (Environmental Protection Agency, 2010). The detection of *E. coli* in public waters is considered a threat to public health and further examination for the presence of pathogens should be carried out. Although most strains of *E. coli* are not regarded as pathogens, they can be opportunistic pathogens which cause infections in immunocompromised hosts. There are also pathogenic strains of *E. coli* that once ingested, cause gastrointestinal illness in healthy humans (Feng, Weagant and Grant, 2011).

Despite some controversies and disagreements about the reliability of indicator organisms (Sadowsky and Whitman, 2011), the "coliform indicator concept" remains an acceptable and useful tool for assessing the quality of drinking waters (Kay, Fricker and Royal Society of Chemistry, 1997). Within the coliform concept, samples of water are tested for the presence of indicator microorganisms. In this context *E. coli* remains as the most important indicator of faecal contamination (APHA, AWWA and WPCF, 1998). Pathogens associated with drinking water include bacterial species, enteric viruses and protozoan cysts (Hrudey *et al.*, 2003). Pathogens are usually present in water samples in low numbers and their detection may require examination of several litres of water. Pathogens may also die off very quickly thus requiring repeated analysis (Gleeson and Gray, 1997). Therefore, the isolation and cultivation of specific waterborne pathogens have often proven to be complicated and time-consuming. For these reasons, the detection of indicator organisms is found to be adequate in evaluating the quality of drinking waters (Hurst and Crawford, 2007; Hrudey *et al.*, 2003).

1.3.1 Production of safe water

Since ancient times, the need to protect the quality of water sources intended for human consumption is a well-known issue. But it was much later, in the 19th century, that microbiologists linked causes of human diseases to contamination of drinking water supplies by sewage (Gleeson and Gray, 1997). Fortunately, disinfectant residuals added to potable waters since the beginning of that century

greatly improved public health by decreasing waterborne diseases (Stewart and Olson, 1996).

Disinfection is defined as an agent or process which kills living opportunist or pathogenic organisms. Non-pathogenic organisms are therefore not necessarily killed by disinfection process. Disinfection is required to act in a relatively short period of time (e.g. 10 minutes). The application of disinfection is restricted to inanimate objects (Meltzer, 1997), such as water, surfaces or medical devices.

In order to comply with microbiological quality standards, potable waters do not need to be sterilized. Alternatively, microorganisms are removed or inactivated to a safe threshold that is achievable through disinfection. In a water treatment plant, firstly the water is screened to remove gross solids, and secondly it is conveyed into the plant. Thirdly it is stored and it receives a primary phase of treatment. This generally includes coagulation, flocculation, sedimentation and rapid sand filtration. These steps work to remove a great percentage of microorganisms. Finally, the last step is the disinfection unit which should guarantee that up to 99.9% of the microorganisms is removed before water delivery to final consumers. The most often applied methods for disinfection of drinking waters are chlorination, ozonation and UV disinfection (Gray, 2005).

Chemical disinfection ensures microbiologically wholesome water. Nonetheless it presents obstacles. For instance, residuals of chlorination and ozonation may combine with dissolved organic matter and generate disinfection by-products (DBPs) (Richardson *et al.*, 2000) such as trihalomethanes and bromate. In the European legislation parametric values of 100 µg/L (trihalomethanes) and 10 µg/L (bromate) are set for drinking waters. Therefore, in order to respect the allowed low levels of DBPs in drinking waters, a compromise between disinfectant levels and DBPs has to be made for ensuring quality of tap water reaching final consumers. In other words, any threats to human health by either microbiological contamination or DBPs residual should be avoided (Environmental Protection Agency, 2009; Gray, 2005).

To aggravate this problem, pathogens' resistance is found within the safe threshold of chemical disinfectants to avoid generation of DBPs (Shannon *et al.*, 2008). Besides the downsides of DBPs generation, chlorination may also cause a final odour and taste in treated waters (Turgeon *et al.*, 2004). Other inconveniences of chlorination are: chlorine and residuals manufacture, storage and transportation as they may offer a continuous threat to operators and the environment (APHA, AWWA and WPCF, 1998). Ozone is a more powerful oxidizing agent, however it does not has a residual effect (Gray, 2005; Wolfe, 1990) and it has to be produced *in situ*, at high cost with high electrical energy input (Environmental Protection Agency, 1998).

An alternative to chemical disinfection is photodisinfection. These photochemical processes such as UV and photocatalysis have been successfully employed in industrial and pilot scale water treatment (Oppenländer, 2003). These processes are acknowledged for the benefits of treating water for human consumption and pollutant destruction, respectively. The high energy needed to drive UV lamps (Environmental Protection Agency, 1998) and the effect of mutagenicity and selection of drug resistant microbial strains (Magaraggia *et al.*, 2011; Environmental Protection Agency, 1998) are serious constraints of these methods. An alternative that is less likely to result in these effects is photodynamic inactivation with singlet oxygen (Magaraggia *et al.*, 2011).

1.4 Effects of photodisinfection on microbial cells

UV disinfection is credited as a reliable technology to promote desired levels of inactivation of pathogens in drinking waters; which is 99.99% of bacteria and viruses and 99.9% of protozoa (Hijnen and Medema, 2010; Masschelein and Rice, 2002; Lingireddy, 2002). Ultraviolet disinfection is the most utilised alternative method of disinfection to chemical disinfectants (Hofmann *et al.*, 2004). The process is effective against bacteria and bacterial spores, *Cryptosporidium* spp. and *Giardia* spp. protozoan cysts (Hijnen *et al.*, 2006; USEPA, 2006; Cotton and Passantino, 2005) and viruses including Poliovirus 1, Coliphage, Hepatite A virus, and Rotavirus SA 11 (Wolfe, 1990). Not all microbial species are susceptible to

UV disinfection. Adenoviruses, for instance, are highly resistant to UV and UV combined methods (Shannon *et al.*, 2008).

All cells are rich in UV absorbing molecules such as DNA and protein. Therefore all living cells are vulnerable to the effects of UV radiation. Absorption of ultraviolet radiation may cause genotoxic and cytotoxic effects. Even one single UV photon hit may cause a carcinogenic or lethal effect in living organisms, ranging from bacteria to plants and animals (Sinha and Hader, 2002). Many organic compounds are unsaturated or composed of conjugated bonds. As a natural feature, they are highly absorbent of UV-C wavelengths between 200-280 nm (Cutler and Zimmerman, 2011). In the case of conjugated bonds, an electron pair, with opposite spins of equal energy each, is present and it is shared by the whole molecule (Cutler and Zimmerman, 2011), in a phenomenon so-called resonance. When an UV-C photon hits one electron of the pair, its level of energy is raised and it destabilises the entire molecule. As a consequence conformational changes may occur (Jagger, 1967). Table 1.1 shows examples of damage caused by the UV-A, UV-B and UV-C inactivation of microorganisms.

Table 1.1 – Effects of ultraviolet radiation in living systems.

Ultraviolet region	Damage caused to cells (prokaryotic and eukaryotic cells)
UV-A	Not absorbed directly by DNA. Causes photosensitising reactions with DNA sub-products and subsequently secondary damage to DNA by generation of reactive oxygen species and singlet oxygen (Sinha and Hader, 2002).
UV-B	It is absorbed by cellular DNA causing minor adverse effects to living systems (Sinha and Hader, 2002). Causes sun-burn and synthesis of D vitamin (Goodsell, 2001).
UV-C	Directly absorbed by DNA. Causes lesions to DNA strands, mutagenic, carcinogenic and lethal effects (Sinha and Hader, 2002).

The two major lesions of DNA caused by UV photons absorption are cyclobutane-pyrimidine dimers and 6-4-photoproducts. If this damage goes unrepaired it may interfere with DNA transcription and replication, leading to

misreading of the genetic code which can cause mutations, and ultimately cell death (Sinha and Hader, 2002).

While UV disinfection is highly efficient against microorganisms, the method is costly as high energy usage is needed to drive UV lamps (Dalrymple *et al.*, 2010). Alternatively, photocatalysis may be driven by solar renewable energy and therefore is more sustainable than UV disinfection. The method has shown promising applications in the treatment of water contaminated with toxic compounds and biological contaminants using solar collectors (Blanco *et al.*, 2009). Although solar collectors are not yet in widespread usage, their relevance in developing areas of the globe, with no straightforward access to electricity and with abundant solar irradiation, has been demonstrated as pointed out in recent reviews of Gamage and Zhang (2010), Dalrymple *et al.*, (2010) and Malato *et al.*, (2009).

1.4.1 Mechanism of photocatalytic disinfection

The first report in photocatalytic inactivation of bacteria was made by Matsunaga, et *al.*, (1985). The authors tested the sterilization properties of the titanium catalyst to disinfect *Lactobacillus acidophilus, Saccharomyces cerevisiae, Escherichia coli* and *Chlorella vulgaris*. The killing mechanism was fully effective after two hours of irradiation with a halide lamp. Photo-oxidation of sulfhydryl groups of intracellular Coenzyme A were found to have caused a disorder in the respiratory chain regulation and subsequently cell death (Matsunaga *et al.*, 1985).

Saito *et al.*, (1992) reported partial destruction of the cell wall of streptococci after 60 minutes of photocatalysis and total disruption of the cell after 120 minutes of treatment. In addition, they reported rapid leakage of potassium and slow release of proteins and RNA. With their findings they proposed that the mode of bactericidal action of TiO_2 photocatalysis included disarranging the cell permeability and destruction of the cell wall.

Microorganisms with the thickest and densest cell walls are expected to be more resistant to attack of $^{\bullet}OH$ radicals produced during the photocatalytic process. For example, *E. coli* strain DH5 was reported to be less resistant than *P. aeruginosa*, *A. polyphaga* (trophozoite), *C. Albicans* (yeast), *F. solani* (fungus), *B. subtilis* (spore) and A. *polyphaga* (cyst) (Lonnen *et al.*, 2005). An example of the damage caused to *E. coli* by photocatalytic treatment is shown in Figure 1.11.

(a) 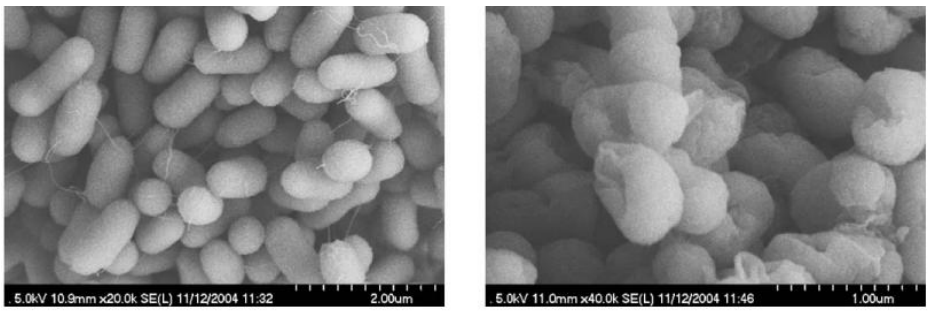

(b)

Figure 1.11 – Scanning electron microscopy of *E. coli* cells prior (a) and following (b) photocatalytic process treatment with PdO/TiON films.

Following this, Maness, *et al.*, (1999) reported that photocatalytic bactericidal activity was a result of lipid peroxidation, which occurred simultaneously with losses in membrane respiratory activity and cell viability (Maness *et al.*, 1999). In another study Huang, *et al.*, (2000) showed, by using a substrate probe to β–D-galactosidase, that photocatalytic treatment caused immediate increases in permeability of the substrate for the enzyme, and leakage of the enzyme after 20 minutes. In that study, the mechanism of cell disruption was proposed as sequential events which started with cell wall damage, followed by damage of the cytoplasmatic membrane which then allowed for intracellular injure (Huang *et al.*, 2000). This conclusion was reinforced by Sunada, Watanabe and Hashimoto (2003) who demonstrated that photocatalytic damage in bacteria followed a two-step process. The first was the disordering of the outer membrane of *E. coli* following illumination on TiO_2 films, which allowed penetration of ROS through the peptidoglycan and to the inner membrane. The second was the disordering of the cytoplasmatic membrane. In support to those studies, Kiwi and Nadtochenko (2005) have found that during photocatalytic inactivation peptidoglycan was the most resistant component of the cell wall, when compared to phospholipids and lipopolysaccharides (LPS).

Cho *et al.*, (2004) have reported quantitatively for the first time that concentration of $^{\bullet}OH$ radicals and the inactivation of *E. coli* were linearly correlated. The steady-state concentrations of $^{\bullet}OH$ radicals in UV-illuminated TiO_2 suspensions could be quantified from the measured photocatalytic degradation rates of *p*-chlorobenzoic acid (a probe compound). The results also indicated that the $^{\bullet}OH$ radical is the primary oxidant species responsible for inactivating *E. coli*. Moreover, the calculated *CT* value for the hydroxyl radical with the delayed Chick-Watson model was approximately 1,000 to 10,000 times as effective as other chemical disinfectants, such as chlorine, chlorine dioxide and ozone (Cho *et al.*, 2004).

Hydroxyl radicals are encountered in bulky-phase and on the surface of photo-excitated titanium dioxide (Min *et al.*, 2005). Surface-bound and bulky $^{\bullet}OH$ radicals were acknowledged as major contributing factors for the inactivation of *E. coli*, but only bulky $^{\bullet}OH$ participated in the inactivation of MS-2 Phage inactivation. That study concluded that differences in the cell structure and size of the two organisms were plausible explanations to the diverse photocatalytic inactivation behaviour. In addition, reactive oxygen species $O_2^{\bullet-}$(super anion) and H_2O_2 (hydrogen peroxide) were found to participate of the inactivation of *E. coli*, however to a lesser extent than $^{\bullet}OH$ radicals (Min *et al.*, 2005).

The role of adsorption in bacterial inactivation by TiO_2 photocatalysis was determined in a study from Gogniat, *et al.*, (2006). They proposed that $^{\bullet}OH$ has an extremely short life to allow it to travel long distances in order to reach targets on the bacterial cells. Therefore, the mechanism of kill was closely linked to the adsorption of bacterial cells to catalyst surface, where the generation of $^{\bullet}OH$ was taking place. In their findings, it has been demonstrated adsorption of bacterial cells depends upon aqueous media composition. While in NaCl-KCl medium cells immediately attached to the catalyst and lost their membrane integrity; in sodium phosphate solution both attachment and loss of membrane integrity were delayed (Gogniat *et al.*, 2006).

The major interaction between nanoparticles and microbial cells has been suggested as a particle-microbe interaction whereas the intracellular intrusion of nanoparticles has a lesser participation (Hessler *et al.*, 2012). It is unknown the predominant way nanoparticles get access into the intracellular environment. It may be either via membrane damage followed by penetration of the nanoparticles or via mechanical transport of the nanoparticles into the cell (Hessler *et al.*, 2012; Huang *et al.*, 2000).

The response of free-swimming bacteria in aqueous media to photocatalytic inactivation is well documented (Alrousan *et al.*, 2009; Guillard *et al.*, 2008; Mccullagh *et al.*, 2007). Fewer investigations have been carried out regarding the response of biofilms (Liu *et al.*, 2007; Raulio *et al.*, 2006). Interestingly, no studies to date have examined the response of aggregated cells, or the role of EPS in this context.

1.4.2 Dark repair in UV and photocatalytic disinfection

Remarkably, microbes are endowed with the capacity to recovery DNA damage by two processes: dark repair and photo-repair following UV treatment. Photorepair occurs when UV photolysed cells are post-irradiate with visible light sources (λ=380 nm and λ=440 nm) which activate the repair enzyme photolyase (Sinha and Hader, 2002). Photorepair plays an important role in wastewater disinfection, where the water is potentially exposed to sunlight after UV treatment (Zimmer and Slawson, 2002). Although in drinking waters photorepair may not show as significant as dark repair, its occurrence cannot be ruled out (Bohrerova and Linden, 2007). Factors such as post irradiation conditions (dose, wavelengths, etc.), organism origin (lab or environmental), temperature (Shang *et al.*, 2009) , nutrient availability (Shang *et al.*, 2009; Bohrerova and Linden, 2007; Sanz *et al.*, 2007; Zimmer and Slawson, 2002; Chan and Killick, 1995) and time between exposure and repair (Hijnen and Medema, 2010) affect organism regrowth (M. Guo *et al.*, 2009).

Guo *et al.*, (2009) verified photo-reactivation of pure cultures of *E. coli* (CGMCC 1.3373) and total coliforms in wastewater after UV barrier with low and medium-pressure mercury lamps. Both lamps allowed photo-reactivation occurrence, however higher UV doses (reaching 40 mJ/cm^2) inhibited the recovery. In that study efficiencies of low-pressure and medium-pressure lamps were not significantly different. They also found that total coliforms were inactivated to a lesser extent than *E. coli* cultures in lab conditions and easily photo-reactivated in real wastewaters (M. Guo *et al.*, 2009). Hence, the authors warn of a possible underestimation of safety risks associated with the application of UV protocols used to inactivate pure cultures used in lab conditions so as to inactivate total coliforms in wastewaters. Experimental UV doses to inactivate lab strains and prevent their repair are often not sufficient to prevent repair in environmental strains (M. Guo *et al.*, 2009). In another study, this time with a non-pathogenic laboratory strain of *E. coli*, photo-reactivation was significantly higher after LP mercury lamps, for the same applied fluence with MP lamps. Differences in the inactivation response were attributed to a larger inhibition of repair mechanisms (proteins and RNA) by the broader emission spectra of MP mercury lamps (Zimmer and Slawson, 2002).

The second mechanism of bacterial repair is dark repair. The mechanisms of dark repair are more complex than photo-repair. It includes the base excision repair and the nucleotide excision repair (Sinha and Hader, 2002). Dark repair in water distribution systems is a cause of concern as treated drinking water can be subjected to longer incubation times before reaching the final consumers. During this time dark repair may occur (Zimmer and Slawson, 2002).

Repair of bacteria ought not to be overlooked even at low percentage. For instance, a repair of 1% from a number of 10^6cell/ml represents a final concentration of 10^4 cell/ml (Sanz *et al.*, 2007). If during UV or photodisinfectant treatment the dose applied allows bacteria to retain repair capability this may cause further problems. Taking this into account, the present work has studied the occurrence of dark repair during overnight incubation of *E. coli* and *P. putida* CP1 after undergoing photodisinfection treatment.

Dark repair has been investigated during photocatalytic studies too (Robertson *et al.*, 2005; Rincón and Pulgarin, 2004a). The effective disinfection time (EDT), defined as the time to achieve total inactivation without subsequent regrowth in a period of 48 hours of incubation in the dark, ought to be determined in order to avoid microbial regrowth and contamination of the potable water which has been treated by photocatalytic process (Rincón and Pulgarin, 2004a). These authors have observed that the dynamics of bacterial survival in the presence and absence of photocatalysts are different. They observed that *E. coli*, for instance, continued to decay after irradiation, while in the absence of a photocatalyst, *E. coli* population was able to regrow.

1.4.3 Mechanism of photodynamic inactivation

As mentioned before, photodynamic inactivation relies on the action of reactive oxygen species (ROS) and singlet oxygen $^1O_2$* which are generated through reactions *Type I* and *Type II*, respectively. The singlet oxygen $^1O_2$* is a very oxidising excited form of molecular oxygen, significantly more electrophilic, reacting rapidly with unsaturated carbon-carbon bonds, neutral nucleophiles such as sulphides and amines, and as well as with anions (Derosa and Crutchley, 2002). Inactivation of microbial cells by occurs by $^1O_2$* and ROS in a series of hit-events which have as examples lipid peroxidation causing loss of membrane integrity, inactivation of enzymes via protein cross-linking and even mutagenic effects due to DNA alteration (Phoenix et al 2003). The $^1O_2$* and ROS are cytotoxic species which cause lipid peroxidation and may lead to increased ion permeability and Na^+ and K^+ leakage (Wainwright 1998). Singlet oxygen denatures antioxidant enzymes such as superperoxide dismutase, peroxidase and catalase (Wainwright *et al.*, 2002). In fact, $^1O_2$* produced in the presence of either Rose Bengal or methylene blue dyes has been shown to inactivate these enzymes (Wainwright *et al.*, 2002; Kim *et al.*, 2001).

Unlike UV disinfection, photodynamic inactivation has a lower probability of inducing (Almeida *et al.*, 2011) and selecting resistant mutant microbial strains

(Schastak *et al.*, 2010). As damage caused by photoproducts of *Type I* and *Type II* reaction are relatively non-specific, emergence of bacterial resistance is less likely to develop following PDI treatment (Phoenix and Harris, 2003). The reason is a principle of multiple targeted action of singlet oxygen which damages different cell structures and interferes with several diverse metabolic routes (Almeida *et al.*, 2011). Perussi (2007) explains that microbial evolution is quicker than human evolution and in this way a small percentage of the bacterial population which are resistant to penicillin, for example, quickly it becomes the dominant population. However, as the photosensitiser action is based on the production of the singlet oxygen, there is no natural bacterial resistance to this reactive form of oxygen (Perussi, 2007).

In general, it is accepted that polycationic sensitisers are active against Gram-negative bacteria while both cationic and anionic sensitisers are active against Gram-positive varieties (Wainwright *et al.*, 2002). Sensitisers diluted in suspension may bind to cell membranes allowing for effectively attack of cell constituents by singlet oxygen. Nevertheless, in drinking water applications microbial inactivation by singlet oxygen should not demand the presence of a sensitiser in its suspended form (homogeneous reaction) (Bonnett *et al.*, 2006).

Photodynamic inactivation of Gram-negative bacteria depends upon the ionic charge of the photosensitiser, whereas in the case of Gram-positive it is related essentially to singlet oxygen quantum yields (Ergaieg and Seux, 2009). The balance between hydrophobic and hydrophilic portions of a photosensitiser which is, in general, modulated by the number of functional charged groups in the its molecule may affect the kinetics of interaction with microbial cells. Thus, the large number of positive charges in tetra or octo-cationic porphyrins or phthalocyanines, for instance, ensures that these sensitisers are highly efficient against Gram-negative bacteria; probably as a consequence of binding of cationic charges to negatively charged cells walls. Gram positive cells and yeasts, on the contrary, are preferentially bound to amphiphilic photosensitisers (Jori and Coppellotti, 2007).

The majority of studies concerning singlet oxygen destruction of aggregated bacterial forms, such as biofilms, have focused on the use of suspended photosensitiser (Street and Gibbs, 2010; Wainwright *et al.*, 2002). Recent work with a polycationic chitosan-conjugated photosensitiser has been shown to be advantageous over homogeneous methylene blue and Rose Bengal. The polycationic polymer could adhere to the bacterial cells and to EPS which resulted in uptake and PI damage to the biofilm structure and, in addition the author observed a synergetic effect of the chitosan and Rose Bengal induced PDI (Shrestha and Kishen, 2012).

1.5 Aim and objectives of the project

The majority of photodisinfectant studies to date have used *E. coli* as the model bacterium, because of its importance as an indicator of faecal pollution of water. In using this bacterium, planktonic cells have been studied. However, bacteria are often present in aqueous media in an aggregated form and few studies have investigated them in such a form. *Pseudomonas putida* CP1 has been characterised in our laboratory. The organism autoaggregates when grown on certain substrates (Farrell and Quilty, 2002a) and so is an excellent model organism for use in aggregation studies. By choosing *P. putida* CP1, it was possible to evaluate the response of a Gram-negative bacterium other than *E. coli* and also to determine the response of aggregated cells to photodisinfection. Three approaches to this process were investigated, including UV disinfection, photocatalysis and photodynamic inactivation. The aim of this study was to investigate the response of planktonic and aggregated forms of Gram negative bacteria to a range of photodisinfection methods in various aqueous media.

The objectives of the study were:

- To compare the response of planktonic cells of *E. coli* and *Pseudomonas putida* CP1 to UV-C and UV-AB disinfection and photocatalysis.
- To study the response of aggregated cells of *Pseudomonas putida* CP1 to UV-C and UV-AB disinfection and photocatalysis.
- To evaluate Rose Bengal in the photodynamic inactivation of both planktonic and aggregated forms of *Pseudomonas putida* CP1.
- To investigate the role of aqueous media including Milli-Q/Distilled Water, phosphate buffered Saline, ¼ Strength Ringers solution, Minimal Medium and Tap water in all photodisinfection studies.
- To explore both culturable and non-culturable approaches in determining the response of the bacterial cells to photodisinfection.

1.6 Outline of experimental design

Table 1.2 – Experimental design of the present research.

Experimental Conditions \ Photodisinfection Treatment		Ultraviolet C disinfection	Ultraviolet A/B disinfection	Ultraviolet A/B + TiO_2 (1 g/l) Photocatalysis	Photodynamic inactivation with Rose Bengal (0-100 µg/ml)
Free-swimming cells of *E. coli* and *P. putida* CP1	Aqueous Media	Ringers, PBS, Minimal Medium, Milli-Q		Ringers, PBS, Minimal Medium, Milli-Q, Tap water	Ringers, PBS, Minimal Medium, distilled water
	Methods of Evaluation	• Culturability: Drop-plate, Pour-plate • Viability: Live and Dead • Dark repair			• Culturability: Turbidity
	Sections	3.1.1, 3.1.2	3.2.1	3.3.1	3.4.1
Aggregated cells of *P. putida* CP1	Aqueous Media	Minimal Medium			
	Methods of Evaluation	• Culturability: Spread-plate • Dark repair • Viability: Live and Dead • Epifluorescence microscopy (EPS with fluorochromes) • Biochemical analysis of EPS • Phase-contrast microscopy			• Culturability: Turbidity • Dark repair • Phase-contrast microscopy • Epifluorescence microscopy • Absorption studies
	Sections	3.1.3	3.2.2	3.3.2	3.4.2

2 Materials and Methods

2 Materials and Methods

2.1 Materials

2.1.1 Bacterial cultures

The bacterial cultures used in this study were *E. coli* (DSMZ 498) and *P. putida* CP1. *E. coli* was obtained from the German culture collection (DSMZ) and *P. putida* CP1 was obtained from the laboratory culture collection.

2.1.2 Maintenance of cultures

For long term preservation, the bacteria were stored in 80% (v/v) glycerol (800 µl overnight culture and 200 µl glycerol) at -80^{o}C. The strains were stored at 4^{o}C on nutrient agar for short-term storage. The agar plates were kept for a maximum of three weeks and then subcultured.

2.1.3 Source of chemicals

Chemicals were obtained from a number of sources including Sigma-Aldrich, Reidel-de-Haen, BDH and Fluka analytical unless otherwise stated. All chemicals were at analytical grade.

2.1.3.1 Titanium Dioxide

Titanium dioxide, Degussa P25, sold under the trade mark AEROXIDE® P25 (Evonik Industries, formerly the Degussa Corporation, Essen, Germany) was used. Degussa P25 had a mixture of anatase and rutile in the region of 70-90% anatase and it has an average particle diameter of 35–40 nm (anatase), 85–95 nm (rutile) and a specific surface area of 50 (±14) m^2/g.

2.1.3.2 Rose Bengal

Rose Bengal (grade/purity=95%) or 4,5,6,7-Tetrachloro-2′,4′,5′,7′-tetraiodofluorescein disodium salt is a xanthene dye which is known also as Acid Red 94 or Bengal Rose B sodium salt (CAS Number: 632-69-9) was obtained from Sigma-Aldrich (Figure 2.1). The empirical formula of Rose Bengal is $C_{20}H_2Cl_4I_4Na_2O_5$ and the molecular weight 1017.64 g/mol.

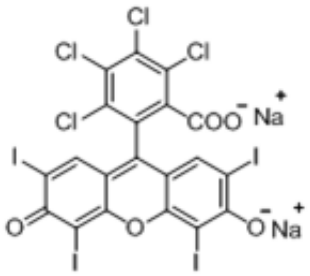

Figure 2.1 – Rose Bengal.

2.1.4 Media

All media unless stated otherwise were obtained from Oxoid and all media were sterilised by autoclaving at 121°C for 15 minutes.

2.1.4.1 Pseudomonas Minimal Medium

The ingredients of the minimal medium (Goulding *et al.*, 1988) were combined in distilled water and the pH was adjusted to 7.0 with 2 M NaOH. The trace salts solution was prepared separately in distilled water and was stored in a dark bottle for 6-8 weeks.

Minimal Medium

	(g/l)
K_2HPO_4	4.36
NaH_2PO_4	3.45
$(NH_4)SO_4$	1.26
$MgSO_4.6.H_2O$	0.912
pH	7.0
Trace salt	1ml/l

Trace salts

	(g/100ml)
$CaCl_2.2H_2O$	4.77
$FeSO_4.7H_2O$	0.37
$CoCl_2.6H_2O$	0.37
$MnCl_2.4H_2O$	0.10
$Na_2MoO_4.2H_2O$	0.02

2.1.4.2 Aqueous media used in photodisinfection studies

Ultra-pure water was obtained from a Milli-Q Academic water purification system (Millipore, Molsheim, France). Tap water was obtained from the Dublin City Council water supply. PBS (Phosphate Buffered Saline) (pH 7.3) was prepared by adding 1 Dulbecco 'A' tablet (Oxoid) per 100 ml of distilled water and autoclaved for 15 minutes at 115^{o}C. ¼ Strength Ringers solution (pH 7.0) was prepared by adding 1 tablet per 500 ml of distilled water and autoclaved for 15 minutes at 115^{o}C.

2.1.4.3 Sodium phosphate buffer

Sodium phosphate buffer (0.01 M) was prepared by dissolving Na_2HPO_4 (0.01 M) and NaH_2PO_4 (0.01 M) in distilled water. The pH of the resulting solution was then adjusted to 7.0 by adding sodium hydroxide 0.1 M.

2.2 Methods

2.2.1 *Determination of bacterial numbers*

Four methods were used to determine bacterial numbers. They included the pour-plate method, the Miles-Misra technique (drop-plate), the spread-plate method and turbidity. All four methods relied on cell cultivation.

2.2.1.1 Pour-plate method

Samples were serially diluted in 9 ml ¼ Strength Ringers solution and plated (one ml) in triplicate on nutrient agar. The plates were incubated at 30^{o}C for 24 hours and counted. Colonies were counted and cell numbers were expressed as cfu/ml (colony-forming units/ml). An advantage of the method is that bacterial cells are trapped immersed into the agar and their growth is limited. This prevents overlapping of the colonies and facilitates enumeration. Another advantage is the limited growth of colonies allows longer incubation of pour-plated samples and the possibility of recovery cells which were previously damaged (Josset *et al.*, 2008).

2.2.1.2 Miles-Misra (drop-plate) method

Samples were serially diluted. 10 µl of a dilution was dropped onto the surface of nutrient agar plates (5 up to 10 drops). Drops were let dry and plates were incubated upward at 30^{o}C for 24 hours (Bohrerova and Linden, 2006a; Collins and Lyne, 1976). The upper limit for counting was 30 colonies per drop, while the

lower limit was 3 colonies. Colonies were counted and cell numbers were expressed as cfu/ml (colony-forming unit/ml). The drop-plate is a robust and practical culturability method (Barbosa *et al.*, 1995). Advantages of the method include time and materials saving.

2.2.1.3 Spread-plate method

Aliquots (0.1 ml) of a bacterial suspension were spread on nutrient agar plates with a sterile glass spreader. The glass spreader was flamed and heat sterilized with IMS (methylated spirit) before and after use. Plates were allowed to dry on the bench and incubated for 24 hours at 30^{o}C. Colonies were counted and cell numbers were expressed as cfu/ml (colony forming units/ml). Unlike the pour-plate, the spread-plate method uses small sample volumes and because it uses solidified agar, the method avoids heat stress on the bacterial cell.

2.2.1.4 Measurement of turbidity

Turbidity of bacterial suspensions was investigated by inoculating 200 µl of sample in 9 ml sterile nutrient broth tubes. Tubes were allowed to incubate overnight at 30^{o}C and turbidity was checked at 24-48 hours. Turbid medium were marked as (+) for growth whereas absence of turbidity, i.e. translucent nutrient broth tubes were marked as (-) indicating negative growth. Turbidity was a useful method to quickly scan the result of photodisinfection studies without the need to quantify the number of inactivated/surviving organisms.

2.2.1.5 Evaluation of dark repair

At the end of each photodisinfection treatment, the reactors were switched off and the treated microbial suspension was incubated in the dark for 24 hours with no stirring. After the incubation period the suspension was stirred for 5 minutes and then sampled for further analysis. Cell numbers were determined by one of the above methods.

2.2.1.6 Determination of number of cells in aggregates of P. putida CP1

P. putida CP1 aggregated cells were disrupted by sonication prior to measurement of cell numbers (Fakhruddin and Quilty, 2007). The procedure started by adding 25 ml of minimal medium containing aggregated cells to 50 ml sterile centrifuge tubes (U-shape). The centrifuged tube was kept in a glass beaker containing crushed ice during the whole procedure. An ultrasound probe (Labsonic 2000 U, Standard 19 mm probe) was introduced into the minimal medium suspension and kept functioning at low power (50 W) during 30 seconds. Defloculation of aggregates was observed using phase-contrast microscopy. Cell numbers were determined by serial dilution and the pour-plate method. Sonication procedure was solely used to evaluate the number of cfu/ml in intact aggregated cells. As sonication is a method which could potentially impact cell survival (Salhani and Uelker-Deffur, 1998), it was not used to quantify the number of cells during photodisinfection procedures; however, sonication was useful to disrupt untreated aggregated cells to provide an estimation of the initial overall cfu/ml concentration.

2.2.2 Determination of viability

The viability assay using the LIVE/DEAD® Bacterial Viability Kit (*Bac*Light™) relies on the premise that the damage of cell membrane is associated with loss of viability of bacteria cells (Boulos *et al.*, 1999).

Planktonic cells

A cell suspension was stained using the LIVE/DEAD® Bacterial Viability Kit (*Bac*Light™) containing SYTO 9 and propidium iodide. Prior to staining, a stock solution of SYTO 9 and propidium iodide was prepared by mixing together the two *Bac*Light stains (30 µl+30 µl). The stock solution was kept at -20^{o}C and protected from light. One ml of bacterial suspension was mixed with 3 µL of *Bac*light dye mixture in an eppendorf covered with tin foil and incubated in the dark for 20 minutes. The stained cells were visualized using by two approaches:

(a) 3 µl of stained cells were placed on a clean glass slide and covered with a coverslip (18 mm x 18 mm).

(b) 1 ml of stained culture (~10^6cell/ml) was filtered through a 0.2 µm Nuclepore Track-Etch polycarbonate membrane (Whatman) in Millipore a 47 mm plastic filter holder. The filter was washed with sodium chloride (0.9% w/vol) solution in order to allow cells to be evenly spread on the filter surface. The membrane was filtered to dryness, removed with a forceps and laid on a drop of Baclight mounting oil drop, on a microscope slide (Boulos *et al.*, 1999). In all cases, slides were examined prior to 24 hours after staining had been carried out.

Aggregated cells

Stained aggregated cells (30 µl) were placed on a clean glass cavity slide and covered with a coverslip (18 mm x 18 mm).

Live cells fluorescence green whereas dead cells fluorescence red. The filter FITC was used to capture green signal (live cells) whereas the TRITC filter was used to capture red signal (dead cells). Each selected field was recorder in both FITC and TRITC signal and merged in a single image afterwards. A Nikon Eclipse Ti-E® inverted Epifluorescence Microscope was used to observe cells. Pictures for documenting cell numbers were taking using a colour video camera Digital Sight DS-2U attached to a Nikon Eclipse T*i*-E® inverted Research Epifluorescence Microscope equipped with FITC and TRITC filters. The images were stored in either in TIFF/JPEG/JP2 format files and processed with a software (NIS-Elements Advanced Research (Ver. 3.00) using a Dell Optiplex Computer.

In the case of planktonic cells, at least 10 randomly selected fields containing 10-50 planktonic were examined on the filter using the 100X oil immersion lens. The number of bacteria per ml of sample was calculated using the formula (Boulos *et al.*, 1999):

T= N x A/a ÷ V, where,

T= number of bacterial cells/ml

N= Number of bacteria/field

A=area of filter (mm^2)

a=area of the microscope field (mm^2)

V=volume of the sample filtered (ml).

In the case of aggregated cells, 5-10 fields were observed using 10X or 40X magnification lens. The red and green intensity of merged images were acquired by selecting 30-50 randomly aggregates. The results were expressed as percentage of live or dead cells.

2.2.3 Photochemical reactors

2.2.3.1 UV-C disinfection

A UV-Reactor System Heraeus UV-RS3 (Heraeus Noblelight GmbH, Hanau, Germany) comprising a quartz sleeve, a glass reactor vessel (700 ml capacity) and a 15 W UV-C low-pressure mercury lamp (253.7 nm) was used for the photolytic studies (Figure 2.2).

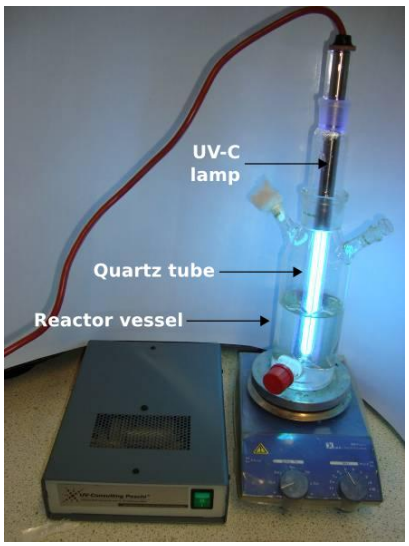

Figure 2.2 – In-batch UV-C disinfection reactor.

Measurement of emission spectrum of UV-C lamp

The emission spectrum of the UV-C lamp (Figure 2.3c) was obtained by using a spectrometer system from Ocean Optics (Dunedin, Florida, USA). The system was equipped with an USB2000 spectrometer, a LS-1-CAL calibrated light source (figure), a FOS 1 Integrated sphere, a UV-NIR fibre optics cable (600 µm) and the Spectra Suit software. The method provided by the manufacturer was followed (Spectroscopy TV, 2010).

1) The first step to calibrate the spectrometer was to obtain a reference light spectrum from a reference light (LS-1-CAL) (Figure 2.3a). As the fibre optics probe used to measure the reference light was easily saturated by the strong emission of the LS-1-CAL reference light, the method of manufacture was modified. This modification included placing a light filter, made of cling film, between the reference light source and the detector in order to attenuate light intensity.
2) The second step to calibrate the spectrometer was to obtain a dark spectrum which was acquired by exposing the fibre optic probe to the dark.
3) Thirdly, the emission spectrum of the UV-C lamp was measured by exposing the fibre optic probe (at 10 cm) to the UV-C lamp (Figure 2.3b).

(a)

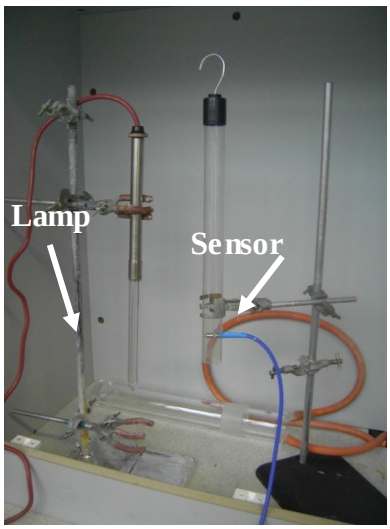

(b)

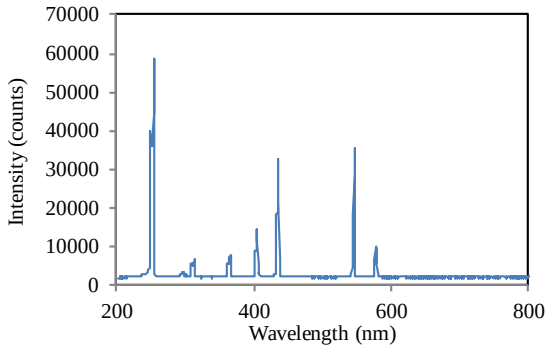

(c)

Figure 2.3 – Measurement of emission spectrum of UV-C lamp low-pressure mercury lamp. The reference light source with cling filter used in the calibration step (adaptation of Ocean Optic's method) (a), a fiber optics probe (blue cable) positioned to measure the UV-C (b). Emission spectrum of UV-C low-pressure mercury lamp (c).

The low-pressure mercury lamp emitted a strong single line at 253.7 nm and residual lines in the UV-A and the visible area.

Measurement of fluence-rate of UV-C lamp by radiometry

In order to measure the fluence-rate of the UV-C lamp a UV sensor (Solarmeter® model 8.0 from Solartech) with a detector at 254 nm µW/cm^2 was used. Radiometric measurement was taken by placing the UV-C lamp at 10 cm of distance from the radiometer. Distance for measurement was set as the medium distance between the quartz glass immersion well and the inner reactor wall. After 10 minutes the lamp was switched on, at least 10 successive measurements have

been taken. The resultant value of irradiance measured was 0.730(±0.014) mW/cm^2.

UV-C disinfection rates

In UV-C disinfection studies, where the irradiance of the low-pressure mercury lamp was acquired from a single emission wavelength at 254 nm, calculation of UV-doses was acquired by multiplying the value of measured irradiance (0.730 mW/cm^2) by time in seconds. UV-dose values obtained were then plotted in the x-axis versus a representative number expressing bacterial survival at related applied UV-dose. The representative reduction of cells was expressed as the Log of the survival ration or Log_{10} (N_0/N_D), which is equal to Log_{10} (counts of untreated sample)-Log_{10} (counts of treated sample dose D). Disinfection rate was equal to the slope of the resulting inactivation curve. Inactivation rate is determined according equation 1 described below Lakretz *et al.*, (2010):

(Equation 1) $Log_{10}\ N_0/N_D = k \times (I_{avg} \times t) = k \times$ UV-dose, where:

N_0 = untreated cells/ml,
N_D = treated cell/ml after dose D,
k = disinfection rate= cm^2/mJ,
I_{avg} = mW/cm^2,
UV-Dose = I_{avg} (mW/cm^2) x time (s),
t = time (s).

2.2.3.2 UV-A/B disinfection and photocatalysis

In the UV-A/B disinfection and photocatalysis experiments, an Aceglass (Vineland, New Jersey USA) reactor vessel model 7841-06 (290 mm and 1L capacity) was used (Figure 2.4). The reactor vessel was constructed of borosilicate glass Aceglass®. The immersion well or 'cooling finger' model 7857-10 was doubled-walled made in borosilicate glass with an inlet and an outlet tubes for cooling water flow. The light source in photocatalytic studies was a 400 W

medium-pressure mercury lamp (Photochemical Reactors LTD, Berkshire, UK.). The bulb had an overall length of 380 nm, discharge length 18 mm. The light output according to information provided by the lamp supplier is $5x10^{19}$ photons/s (measured by ferrioxalate actinometry in a quartz immersion well). The power supply model 3140 (Photochemical Reactors LTD) provided 400 W of electrical input.

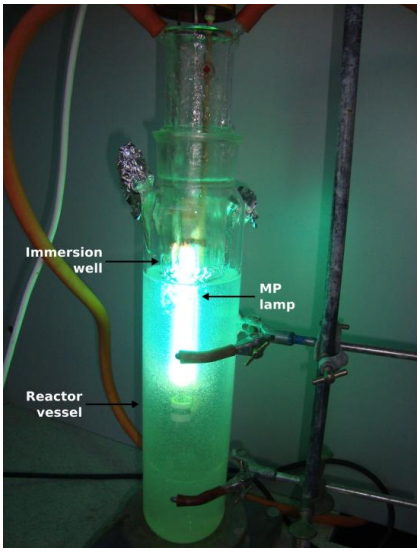

Figure 2.4 – UV-A/B photocatalytic in batch annular reactor.

Measurement of emission spectrum of UV-A/B lamp

The emission spectrum of the UV-A/B medium-pressure mercury lamp (Figure 2.5) was measured using the same spectrometer system from Ocean Optics (Dunedin, Florida, USA. The spectrometer could detect wavelengths above 300 nm which was the region of interest for the UV-A/B studies. The emission spectrum of the medium-pressure mercury lamp showed polychromatic emission with lines in the UV-B region at 312 nm, UV-A at 333 nm and 365 nm and in the visible range at 433, 436, 546 and 576 nm.

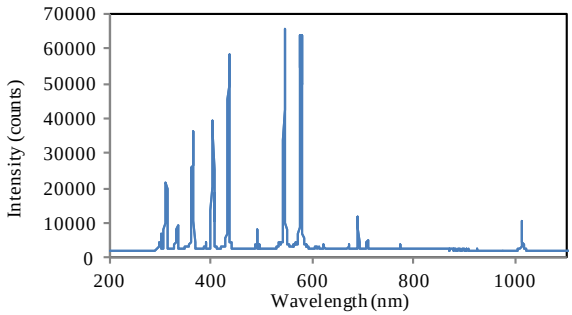

Figure 2.5 – Emission spectrum of UV-A/B medium-pressure mercury lamp.

UV-A/B disinfection and photocatalysis disinfection rates

During UV-A/B disinfection studies and UV-A/B TiO_2 photocatalytic studies, the UV dose has been not considered into calculation of disinfection rate. Rather than that reduction in the log of the survival fraction -s expressed as Log_{10} (N_0/N_t) and which is equal to Log_{10} (counts of untreated sample)-Log_{10} (counts of treated sample after an exposure time) – was plotted against time in minutes (min^{-1}). Data points included in a linear portion of the inactivation curve were used to generate a linear-regression curve respecting a limit of the >95% to r^2-value (>0.95). The slope of curves were considered as the inactivation rate values (k) and were used to compare different kinetics of UV-A/B disinfection and photocatalytic treatment (Lakretz *et al.*, 2010; Mamane-Gravetz and Linden, 2004). The disinfection rate was determined in Equation 2:

(Equation 2) $Log_{10}\ N_0/N_t = k \times t$

Where:

N_0 = untreated cells/ml,
N_t = treated cells/ml at exposure time t,
k = disinfection rate (min^{-1}),
t = time (min).

2.2.3.3 Photodynamic inactivation

A miniaturised LEDs system was constructed by Dr. Mary Pryce's research group, in the School of Chemical Sciences, Dublin City University (Figure 2.6). 100 LEDs with emission in the 525 nm region were assembled in 7 rows and arranged in a metal box which blocked all the external light. The voltage of each green LED was 2.1 V. A power source was connected to the LEDs. The reactor used to irradiate bacterial suspensions in photodynamic inactivation (PDI) studies was Petri dishes (20 ml capacity). The dimensions of the polystyrene Petri dish were diameter = 89.42 mm, height = 15.9 mm and the area = 62.74 cm^2.

(a)

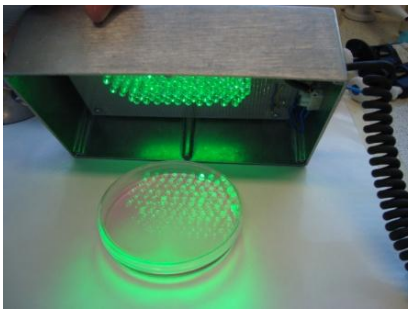

(b)

Figure 2.6 – The LEDs miniaturised device and power source (a), LEDs device detail of green light irradiating the top of Petri dish containing microbial suspension (b).

Measurement of emission spectrum, luminance and calculation of fluence-rate of LED system

The emission spectrum of the LEDs device (Figure 2.7) was measured using the spectrometer system from Ocean Optics (Dunedin, Florida, USA).

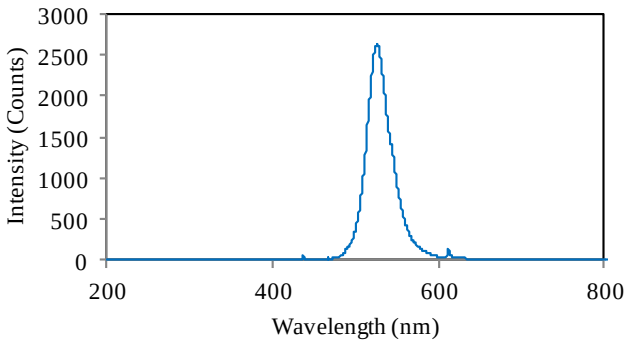

Figure 2.7 – Emission spectrum of light source of LEDs system used in photodynamic inactivation studies.

A digital light meter (Iso Tech model Lux-1337) was used to measure luminance (Lux) of the LED radiation source. The meter was placed at 10 cm of distance at the middle of the circular area of ~63 cm^2 of light produced by the LED system. The average luminance of the LED device was 4,700 Lux. According to the luminous function (Ohta and Robertson, 2005; Stimson, 1974) at 525 nm 1 Lux has a fluence-rate of ~1.16 mW/m^2. Thus, at 525 nm, 4,700 Lux are correspondent to a fluence-rate equal to:

Fluence-rate at 525 nm = (4,700 Lux x 1.16 mW/m^2) ÷ 1 Lux =

5,405 mW/m^2 i.e. = **<u>0.540 mW/cm^2.</u>**

2.2.4 Inoculum preparation

2.2.4.1 Free-swimming cells (E. coli and P. putida CP1)

Two loops of culture were aseptically transferred into 10 ml universals containing nutrient broth. The organisms were grown overnight on a shaker incubator (150 rpm) at 30°C. After an incubation period of 18-24 hours (late-exponential/stationary-phase) the microorganism suspension was centrifuged at 4,000 rpm (15 minutes, 4°C). The supernatant was removed and the pellet was washed twice with Phosphate Buffered Saline (PBS). Cells were resuspended in

buffer and diluted to achieve desired optical density (O.D.). The overnight O.D. (~1.0) at 600 nm of *E. coli* corresponded to a number of 2.60 (±0.38) $x10^9$cell/ml. For *P. putida* CP1 grown overnight, optical density was normally~0.9 at 660 nm and equivalent to 3.6 (±0.72) $x10^8$cell/ml.

2.2.4.2 Aggregated cells (P. putida CP1)

P. putida CP1 was grown overnight in nutrient broth. The culture was centrifuged at 4,000 rpm (15 minutes, 4°C) and washed twice in 0.01 M sodium phosphate buffer (pH 7.0) and then resuspended twice to give an optical density of 0.7±0.04 correspondent to 2.79 (±0.11) $x10^7$cell/ml at 660 nm. 500 ml of minimal medium flasks were inoculated with 5% (v/v) of this inoculum. A 50% (w/v) fructose solution was filtered through a membrane filter (Whatman GF/C 0.2 µm, 47mm membrane filters) and added to minimal medium to give a final concentration 1% (w/v). Flasks were incubated at 150 rpm at 30°C overnight for 24 hours.

2.2.5 Reactor set up

2.2.5.1 UV-C disinfection

In UV-C disinfection experiments the reactor was rinsed and washed with detergent and hot tap water and disinfected with 1% (w/v) Virkon®, and finally rinsed out twice with sterile Milli-Q water. 500 ml of sterile aqueous media containing a magnetic bar was added to the reactor and the medium was aseptically inoculated with free-swimming bacteria *E. coli* or *P. putida* CP1 (10^7, 10^6 or 10^5cell/ml) or aggregated cells of *P. putida* CP1 (~10^8cell/ml). The inoculated was placed in a closed wood cabinet and wrapped with tissue paper to avoid light transmission during operation. The reactor was stirred throughout the experiment. The low pressure mercury lamp was introduced into the immersion well and the power source turned on for the desired period of time. No light was used in the dark controls. The initial sample was taken at 10 minutes and at intervals following. Cell numbers and disinfection rate were determined.

2.2.5.2 UV-A/B disinfection and photocatalysis

In UV-A/B disinfection and photocatalysis the reactor was rinsed and washed with detergent and hot tap water and disinfected with 1% (w/v) Virkon®, and finally rinsed out twice with sterile Milli-Q water. 1 l of sterile aqueous media containing a magnetic bar was added to the reactor and the medium was aseptically inoculated with free-swimming bacteria *E. coli* or *P. putida* CP1 (10^7, 10^6 or 10^5cell/ml). In the case of aggregated cells of *P. putida* CP1 (10^8cell/ml), the reactor was inoculated with 1 l of aggregates grown for 24 hours in minimal medium and fructose medium. A magnetic bar was aseptically added into the reactor, afterwards. 1 g/l of Degussa P-25 TiO_2 was added to photocatalytic disinfection studies. The cooling finger was rinsed and washed with detergent and hot tap water and disinfected with 1% (w/v) Virkon® and then added into the photochemical reactor. Tap water was connected to the cooling finger and allowed to flow in and out throughout the experiment to allow cooling of the medium-pressure lamp. The inoculated reactor was placed in a closed wood cabinet and wrapped with tissue paper to avoid light transmission during operation. The reactor was stirred throughout the experiment. The lamp was introduced into the immersion well and the power source turned on for the desired period of time. No light was used in the dark controls. The initial sample was taken at 10 minutes and at intervals following. Cell numbers and disinfection rate were determined.

The first step during the photocatalytic investigations with the reactor system used in this work was to determine a standard load of TiO_2 to be used to inactivate free-swimming bacteria. For doing this, *E. coli* (10^7cell/ml) was inoculated in Ringers solution and photocatalysed in the presence of 0.2, 0.5, 1.0, 1.5 or 2.0 g/l. Preliminary investigations showed that the load of 1.0 g/l of TiO_2 provided the most satisfactory inactivation of bacteria. Therefore, 1.0 g/l of catalyst was the concentration used throughout this section.

As UV irradiation causes severe eye and skin burns, precautions were taken during Ultraviolet and Photocatalysis disinfection studies. A strict and detailed SOP used during manipulation of annular photochemical reactors was put in place in order to ensure safety. UV goggles, gloves and white coat protected any area of skin exposed.

2.2.5.3 Photodynamic inactivation (PDI)

In photodynamic studies sterile ¼ Strength Ringers solution containing a magnetic bar was added to sterile plastic Petri dishes (20 ml). The medium was aseptically inoculated with 0.5 ml (of O.D. at 660 nm) of free-swimming bacteria *P. putida* CP1 (10^6cell/ml). Alternatively, aggregated cells of *P. putida* CP1 (10^8cell/ml) were inoculated into Petri dishes. In this case, a magnetic bar was aseptically added into the reactor, afterwards. A volume of a stock solution of Rose Bengal (1 mM) was added to achieve concentrations between 10 to 100 µg/ml.

Preliminary investigations showed that concentrations of Rose Bengal below 10 µg/ml (e.g. 0.1, 0.2, 0.25, 0.5, 0.75, 1, 3, 5 or 7.5 µg/ml) were not effective in killing free-swimming cells within an hour of photodynamic treatment in Ringer Solution. Therefore, the studies with free-swimming cells were carried out with concentrations between 10 and 100 µg/ml of Rose Bengal. In the case of aggregated cells, it was found that due to their greater resistance to photodynamic inactivation in minimal medium, and to the uptake of Rose Bengal by the aggregates higher concentrations, (25, 50 and 100 µg/ml) of Rose Bengal were used.

Prior to irradiation bacteria and sensitiser suspension were kept stirring in the dark for 10 minutes. The Rose Bengal bacterial suspension was kept under stirring throughout. Every treatment included dark and light controls. Besides that all the treated suspensions were kept in the dark after treatment and occurrence of dark repair was verified. Samples were collected at different time intervals and evaluated by culturable or turbidity technique for evaluation of growth.

2.2.6 Determination of aggregates size

30 µl of aggregated cells of *P. putida* were placed on a clean glass cavity slide and covered with a coverslip (18 mm x 18 mm). The size of the aggregated cells CP1 was evaluated using phase-contrast microscopy with a Nikon Eclipse T*i*-E® inverted Research Epifluorescence Microscope. Preferably magnification 10X was used. All the aggregates from at least 5 microscope fields were selected and averaged, maximum, minimum and standard deviation values were automatically processed by the software NIS-Elements Advanced Research (Ver. 3.00) using a Dell Optiplex Computer.

2.2.7 Dry-weight of aggregates

A specific volume of suspended aggregated cells was filtered through two tarred filters (Whatman GF/C and Gelman 0.2 µm, 47 mm membrane filters), dried at 85^{o}C for 2 hours and then reweighed.

2.2.8 Analysis of extracellular polymeric substances (EPS)

2.2.8.1 Determination of bound and free EPS

The extracellular polymeric substances (EPS) of *P. putida* CP1 aggregated cells were extracted by adaptation of the methods from (Eboigbodin and Biggs, 2008). 10 ml of overnight grown fructose flocs suspension were harvested by centrifugation at 4000 rpm add x g for 15 minutes at 4^{0}C. The pellet was used for extraction of bound EPS while the supernatant was used for extraction of free EPS. For the extraction of the bound EPS, pellet was washed twice in NaCl (0.9 % w/vol) to remove traces of growth medium. The washed cells were resuspended in 1:1 volume of a solution 0.9% NaCl and 2% EDTA then incubated for 60 minutes at 4^{0}C. The supernatant was then harvested by centrifugation at 4,000 rpm at 4^{0}C for 30 minutes and then filtered through 0.45 µm sterile membrane

(Pall). For the extraction of extraction of free EPS, supernatant collected was centrifuged again during 4,000 rpm for 30 minutes at 4^0C to remove residual cells. The new supernatant containing free EPS was precipitated with 1:3 volume ethanol and stored at -20^0C for 18 hours. The sample was centrifugation at 4,000 rpm for 14 minutes at 4^0C. The extract was resuspended in ultrapure water and dialyzed against ultrapure water to removed ethanol. Both bound and free EPS were stored at -20^0C until needed for further analysis. The total EPS content was taken as the sum of the bound and free EPS.

2.2.8.2 Biochemical analysis

Dubois assay for the determination of carbohydrates

The Dubois assay or phenol sulphuric acid method (DuBois *et al.*, 1956) was used to determine the concentration of carbohydrates in the free and bound EPS. 2 ml of standard/sample was added to a universal, followed by the addition of 0.5 ml of 5% (w/v) phenol solution and 2.5 ml of concentrated sulphuric acid. Then the universal was allowed to stand for 10 minutes. After that, the universal was placed into a water bath at 30^0C for 20 minutes. The absorbance was measured at 490 nm. The concentration of carbohydrates was determined according to a standard curve with glucose (at 0, 20, 40, 60, 80 and 100 µg/ml).

Bradford assay for the determination of proteins

The concentration of proteins in the free and bound EPS was determined with the Bradford assay (Bradford, 1976). 1 ml of Bradford reagent (Sigma) was added to 1 ml of sample and immediately vortexed. The mixture was left at room temperature for 5 minutes and the absorbance was measured at 595 nm. The concentration of proteins was determined by comparison to a calibration curve with bovine albumin serum (BSA) from Sigma (at 0, 20, 40, 60, 80 and 100 µg/ml).

Dinitrosalicylate (DNS) colorimetric method for determination of fructose

Bacterial cells were removed from samples by centrifugation (13,000 rpm for 4 minutes) before assaying. The fructose concentrations were determined by the dinitrosalicylate (DNS) colorimetric method (Miller, 1959). The DNS reagent was prepared by dissolving 1 g of 3,5-dinitrosalicylic acid and 30 g potassium sodium tartrate in 50 ml distilled water and 16 ml of sodium hydroxide (10% w/v). The solution was warmed not to boil and when dissolved, the volume was completed up to 100 ml. 1 ml of standard or diluted samples and 1 ml of water was placed in a test tube. 2 ml of DNS reagent was added. The tubes were then capped and placed in boiling water bath for 10 minutes. The tubes were readily cooled and 10 ml of water added to each. Absorbance was read at 540 nm. The fructose concentration was determined against a calibration curve of corresponding known fructose concentrations (0.25; 0.50, 0.75; 1.0; 1.5 and 2.0 mg/ml).

2.2.8.3 Staining of aggregated cells with fluorochromes

The staining procedure was performed on aggregated bacterial cells as previously described by Chen *et al.*, (2007). A volume of 1 ml of aggregates was carefully collected from the reactors with a wide-mouthed pipette. The aggregates were kept fully hydrated during the staining procedure. 2.5 µl of FITC solution (10 g/l) was added first and left to incubate for 1 hour. FITC stains all protein and amino-sugars of cells and EPS. A second sample of aggregates was stained for polysaccharides by the addition of 10 µl of calcofluor-white solution (Fluka). The incubation time was 30 minutes. DNA was stained by addition of propidium iodide (1.5 µl) per each 1 ml of aggregates suspension and incubated for 15 minutes to stain the nucleic acid. After each staining step, the aggregates were let settling down for 2 to 5 minutes and washed with PBS (Oxoid) thrice for complete de-staining or until total removal of colour from supernatant was achieved. The incubation was carried out in the dark at room temperature. The aggregated cells were stained either by a single fluorochrome or by multiple fluorochromes, which were then applied in the order above described. The stained aggregates (30 µL)

were added to a cavity slide sealed with a coverslip and nail polish. Slides were visualized at 10X magnification with epifluorescence microscopy. The observations were performed with a Nikon Eclipse T*i*-E® inverted Research Epifluorescence Microscope with FITC, DAPI and TRITC filters. The filter FITC was used to capture green signal (proteins) whereas the TRITC filter was used to capture red signal (DNA) and the DAPI filter was used to capture blue signal (proteins). Each selected field was recorded in FITC, TRITC and DAPI signal which were merged in a single image afterwards. The green/blue/red intensity of all the aggregated cells present in a field were recorded automatically by the package NIS-Elements Advanced Research (Ver. 3.00)

2.2.9 Determination of Rose Bengal interactions with aggregated cells

2.2.9.1 UV-Vis analysis of supernatant of Rose Bengal and aggregated cells

Suspensions of aggregated cells of *P. putida* CP1 and Rose Bengal were centrifuged in a *Biofuge 13* microfuge (Heraeus Instruments) at 13,000 x *g*. The absorption spectrum of the supernatant was read between 200 and 800 nm. The supernatant was diluted if necessary. The blank sample (supernatant of aggregated cells without sensitiser) presented a strong UV absorption below ~370 nm (Figure 2.8).

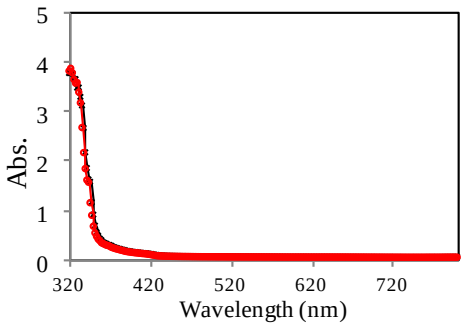

Figure 2.8 – Absorption spectrum of minimal medium used to grow aggregated cells of *P. putida* CP1.

From the absorption spectrum two information were obtained; the percentage of photosensitiser uptake by the biomass and the absorbance ratio.

Percentage of uptake of Rose Bengal by aggregated cells

The percentage of uptake of Rose Bengal by the aggregated cells of *P. putida* CP1 was monitored in relation to the maximum absorbance of the sensitiser (549 nm). The percentage of uptake of Rose Bengal (or the removal of colour) during interaction of aggregated cells and photosensitisers was calculated at different contact times using the Equation (3) described by Cripps (1990) where:

A_0= Initial absorption of Rose Bengal in the supernatant at time 0.
A_t= Absorption of Rose Bengal in the supernatant after time t.

(Equation 3) $(A_0-A_t/ A_0) \times 100$

Biodegradation and biosorption of Rose Bengal by aggregated cells

Occurrence of biosorption or biodegradation during interaction of photosensitisers and aggregated cells was inferred by evaluation of absorbance ratio (Glenn and Gold, 1983). If biosorption was the predominant process occurring, absorbance at all wavelengths are expected to decrease similarly. This would reflect in constant absorbance rates values. However, if absorbance at different wavelengths decreases irregularly absorbance ratio values should vary too. In this case chromophores groups were being broken down by enzymatic action indicating biodegradation (Glenn and Gold, 1983). The calculation of absorbance rate values was obtained from Equation 4:

(Equation 4) Absorbance ratio= $(Abs\ \lambda^{Max}/Abs\ \lambda^{Max/2})$, where:

$Abs\ \lambda^{Max}$ = Maximum absorption at the wavelength of 549 nm.
$Abs\ \lambda^{Max/2}$ = Maximum absorption at the wavelength of 428 nm.

In equation 4, $Abs\lambda^{Max}$ is the highest value of absorbance at wavelength of 549 nm for Rose Bengal whereas $Abs\ \lambda^{Max/2}$ was the value of absorbance correspondent to a half of λ wavelength, i.e. 428 nm.

2.2.9.2 Epifluorescence microscopy of Rose Bengal attached to the aggregated cells

During photodynamic studies, the attachment of Rose Bengal (50 or 100 µg/ml) to aggregated cells was observed. 30 µl of bacterial suspension was added to cavity slide sealed with a coverslip and nail polish. Slides were visualized at 10X magnification with epifluorescence microscopy Nikon Eclipse T*i*-E® inverted Research Epifluorescence Microscope equipped with TRITC filters. The images were recorded automatically by the package NIS-Elements Advanced Research (Ver. 3.00).

2.2.10 Data analysis

All experiments were carried out in duplicates. All data points were analysed in triplicates. Microsoft Office Excel 2007 was used to determine the values of mean, standard deviation and regression coefficients. Two-way and one-way ANOVA together with Post-Hoc testing was used to determine relationships between independent variables aqueous media and microorganisms (Field, 2005). ANOVA testing was carried out with the software IBM® SPSS® Statistics 19.

3 Results

3 Results

The study investigates the responses of planktonic and aggregated bacterial cells to photodisinfection. The results are described in four sections. The first section 3.1 describes the response of bacteria to UV-C, the response of the bacteria to UV-A/B disinfection is described in section 3.2, TiO_2 photocatalysis of the bacteria is described in section 3.3 and photodynamic inactivation of the bacteria is described in the final section 3.4.

3.1 UV-C disinfection

UV-C disinfection was carried out using free-swimming, *E. coli* (DSMZ 498) and both free-swimming and aggregated forms of *P. putida* CP1. Studies were conducted at room temperature in a variety of aqueous media including Milli-Q water, Tap water, Phosphate Buffered Saline (PBS), ¼ Strength Ringers solution and Minimal Medium. The reactor used was a Heraeus UV-RS3 (Heraeus Noblelight GmbH, Hanau, Germany) comprising of a quartz sleeve, a glass reactor vessel (700 ml capacity) and a 15 Watt Ultraviolet-C low-pressure mercury lamp (λ=253.7 nm). The response of the cells to UV-C disinfection was monitored by determining cell number following growth and cell viability was determined using the LIVE/DEAD® Bacterial Viability Kit (*Bac*Light™). In the case of aggregated cells changes in the composition of the EPS (extracellular polymeric substances) was noted using epifluorescence microscopy and biochemical analysis. The size of aggregated cells during UV-C disinfection was monitored using phase-contrast microscopy.

3.1.1 Study of aqueous media suitability for ultraviolet disinfection studies

Prior to carrying out UV disinfection studies of free-swimming *Escherichia coli* (DSMZ 498) and *Pseudomonas putida* CP1, the suitability of four aqueous media was investigated. Milli-Q water, Tap water, Phosphate Buffered Saline (PBS), ¼ Strength Ringers solution were inoculated with pure cultures of each bacterium

(10^6cell/ml) and incubated, with stirring in the dark for a period of 60 minutes. Samples were taken at intervals and checked for cell number. There was no significant fall in cell numbers for both bacteria in Milli-Q water, Phosphate Buffered Saline (PBS) and ¼ Strength Ringers solution. However no growth of either culture was detected in tap water (Table 3.1).

Table 3.1 – Numbers of *E. coli* and *P. putida* CP1 (10^6cell/ml) after 1 hour of incubation in various aqueous media.

Organism / Aqueous medium	*E. coli* (DSMZ 498)	*P. putida* CP1
Milli-Q water	+	+
¼ Strength Ringers Solution	+	+
Phosphate Buffered Saline (PBS)	+	+
Tap water	-	-
Minimal Medium (up to 6 hours)	+	+
(+): No significant reduction, (-) no organisms detected.		

The viability of the *P. putida* CP1 cells in Milli-Q and Tap water was evaluated using the LIVE/DEAD® Bacterial Viability Kit (*Bac*Light™) for up to 4 hours (Figure 3.1). The result showed sustained viability in the Milli-Q however an absence of any viable cells in the tap water after 2 and 4 hours of incubation. The findings led to the exclusion of tap water as a medium for the UV-C disinfection studies.

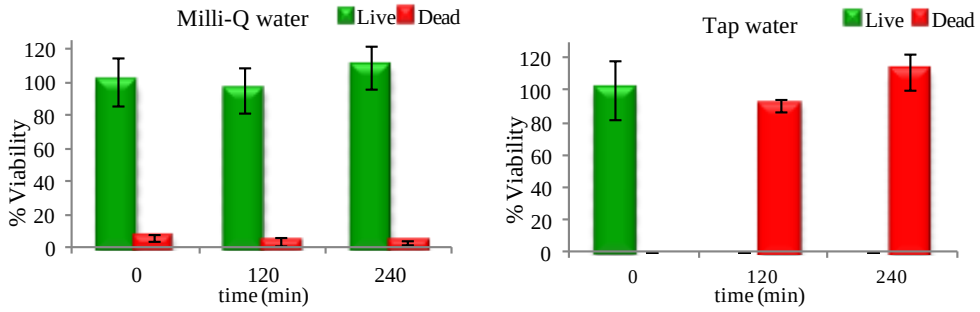

Figure 3.1 – Live and dead profile of *P. putida* CP1 free-swimming cells incubated in (left) Milli-Q water and (right) Tap Water over time as determined by LIVE/DEAD® Bacterial Viability Kit (*Bac*Light™).

3.1.2 UV-C disinfection of free-swimming cells

The response of *E. coli* and *P. putida* CP1 to UV-C disinfection was investigated in Ringers, Phosphate Buffered Saline and Milli-Q water. When the response of the cells was monitored using the plate count technique, a rapid fall in the numbers of cells was observed within seconds for both bacteria. No significant reduction in cell numbers was observed for dark controls. An inoculum of 10^6cell/ml took no longer than 7 seconds to be inactivated (Table 3.2 and Table 3.3). The inactivation rate (k) for each bacterium in all three media was calculated by plotting the decimal logarithm of the fraction of surviving organisms (N_0/N_D) against UV-C dose using the following Equation 1:

(Equation 1) $\text{Log}_{10}\ N_0/N_D = k$ x (I_{avg} x t) = k x UV-dose, where:

N_0 = Number of cells/ml at time dose "0",
N_D = Number of cells/ml at dose D,
k = disinfection rate= cm^2/mJ,
I_{avg} = Irradiance averaged value= mW/cm^2,
Dose of UV-C = I_{avg} (mW/cm^2) x time (s) = mJ/cm^2,
t = time (s).

Table 3.2 – Number of *E. coli* (DSMZ 498) following UV-C photolytic disinfection in Milli-Q ultrapure water, Phosphate Buffered Saline and ¼ Strength Ringers solution.

UV-C treatment		**Counts (cfu/ml)**		
UV-dose (mJ/cm^2)	Time (sec)	Milli-Q water	Phosphate Buffer Saline (PBS)	¼ Strength Ringers solution
0	0	$1.46(\pm0.66)x10^6$	$2.32(\pm0.05)x10^6$	$2.07(\pm0.05)x10^6$
0.73	1	$3.87(\pm0.73)x10^5$	$1.22(\pm0.12)x10^6$	$4.43(\pm0.97)x10^5$
2.19	3	$1.55(\pm0.16)x10^3$	$1.08(\pm0.13)x10^4$	$1.05(\pm0.05)x10^4$
3.65	5	0.00	$3.57(\pm0.05)x10^1$	$2.08(\pm0.52)x10^1$
5.11	7	0.00	0.00	0.00
7.3	10	0.00	0.00	0.00
14.6	20	0.00	0.00	0.00

Table 3.3 – Number of *P. putida* CP1 following UV-C photolytic disinfection in Milli-Q ultrapure water, Phosphate Buffered Saline and ¼ Strength Ringers solution.

UV-C treatment		Counts (cfu/ml)		
UV-dose (mJ/cm^2)	Time (sec)	Milli-Q water	Phosphate Buffer Saline (PBS)	¼ Strength Ringers solution
0	0	$8.50(\pm0.98)x10^5$	$4.50(\pm0.58)x10^6$	$1.35(\pm0.06)x10^6$
0.73	1	$3.50(\pm0.37)x10^5$	$6.50(\pm4.12)x10^6$	$2.82(\pm0.41)x10^5$
2.19	3	ND	$2.34(\pm0.43)x10^4$	$1.03(\pm0.07)x10^3$
3.65	5	$5.23(\pm0.60)x10^1$	$3.30(\pm0.58)x10^2$	0.00
5.11	7	0.00	0.00	0.00
7.3	10	0.00	0.00	0.00
14.6	20	0.00	0.00	0.00
ND: not determined.				

The UV-C dose response curves are plotted in Figure 3.2. The inactivation rates are summarised in Table 3.4.

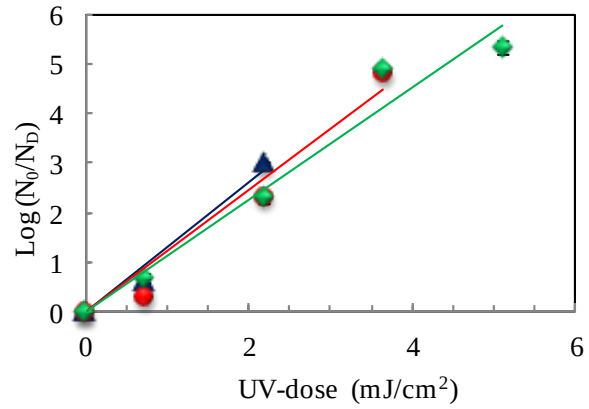

(a)

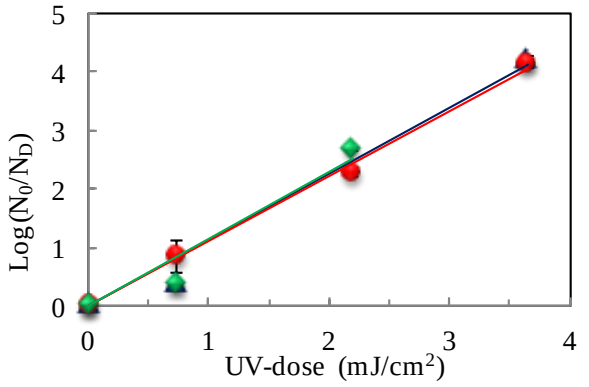

(b)

Figure 3.2 – UV-C dose response of free-swimming (a) *E. coli* (DSMZ 498) and (b) *P. putida* CP1. Decimal logarithm of survival fraction or Log_{10} (N_0/N_D) as a function of aqueous media composition: Milli-Q water (▲), Phosphate Buffered Saline-PBS (●) and ¼ Strength Ringers solution (◆) and UV-C dose in mJ/cm^2.

The inactivation rates "*k*" of free-swimming organisms were obtained from the log-linear regression of data points. The values of *k* ranged from 1.019 to 1.145 cm^2/mJ. Analysis of the data using the two-way ANOVA test showed there were no significant differences between the organisms, that the response was independent of medium composition and that no interactions between medium and organisms altered the inactivation rate (Table 3.4).

Table 3.4 – Inactivation rates of free-swimming *E. coli* and *P. putida* CP1 during UV-C disinfection in aqueous media.

Free-swimming organism	Milli-Q water	Phosphate Buffer Saline	1/4 Strength Ringers solution
E. coli (DSMZ 498)	1.145(±0.091)	1.105(±0.055)	1.019(±0.043)
P. putida CP1	1.130(±0.054)	1.085(±0.034)	1.089(±0.031)
Test Between-Subjects Effects tested by ANOVA-two-way: Organism p=.799; Medium p=.325; Organism*Medium, p=.521.			

Dark repair and viability of *P. putida* CP1 were evaluated following UV-C disinfection. When free-swimming *P. putida* CP1 (10^7cell/ml) was photolysed for 20 seconds in Ringers solution and then left for 24 hours in the dark, dark repair was observed using both a culturable and non-culturable approach (Table 3.5). Using a culturable approach, inactivation of *P. putida* CP1 in Ringers solution was seen to be complete in 10 seconds. Viability results however showed that approximately 40% of the cells remained in a viable state. The analysis of 24 hours samples incubated in the dark showed that viability of the cells recovered significantly and up to 86.26% of viable cells were detected. Cells numbers were also determined using the culturable approach, however the numbers detected were 6-Log units lower than the number of cells at the beginning of the experiment. A dose response curve for the organism is described in Figure 3.3. The mean value of the inactivation rate of 10^7cell/ml of *P. putida* CP1 was 0.872 (±0.05) cm^2/mJ. One-way-ANOVA analysis showed that this inactivation rate was significantly different to the value obtained when the inoculum size was 10^6/ml (Table 3.5).

Table 3.5 – Number of *P. putida* CP1 following UV-C photolytic disinfection in ¼ Strength Ringers solution.

UV-dose (mJ/cm^2)	Time (sec)	Counts (cfu/ml)	Viability (%)
0	0	$1.78(\pm0.23)x10^7$	95.28(±13.11)
0.73	1	$1.33(\pm0.11)x10^7$	ND
2.19	3	$1.39(\pm0.28)x10^6$	ND
3.65	5	$1.67(\pm0.27)x10^5$	46.56(±11.57)
5.11	7	$1.09(\pm0.23)x10^3$	ND
7.3	10	0.00	43.04(±11.70)
14.6	20	0.00	38.52(±5.15)
24 hours dark repair		$8.00(\pm0.77)x10^1$	86.26(±16.19)
ND: not determined.			

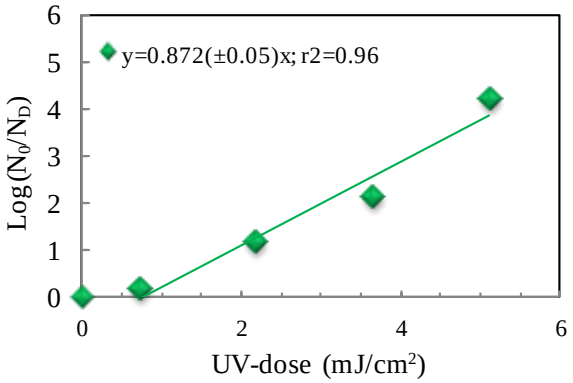

Figure 3.3 – UV-C dose response of free-swimming *P. putida* CP1 (10^7cell/ml) in ¼ Strength Ringers solution (◆).

3.1.3 UV-C disinfection of aggregated cells

The response of aggregated cells of *P. putida* CP1 to UV-C was investigated. In order to produce the aggregates the cells had been grown in minimal medium with fructose supplied as the sole carbon source and so the response of free swimming cells of *P. putida* CP1 in minimal medium to UV-C disinfection was first evaluated. The effect of UV-C on the aggregated cells was determined by monitoring cell growth, viability and the size and composition of the aggregates.

3.1.3.1 Response of free-swimming P. putida CP1 in minimal medium to UV-C disinfection

The response of free-swimming *P. putida* CP1 in minimal medium to UV-C disinfection was investigated using two inoculum sizes – 10^6cell/ml and 10^7 cell/ml (Table 3.6). The cells were checked periodically for growth using the Miles-Misra (drop-plate) technique and no growth was observed for the system inoculated with 10^6cell/ml at 10 seconds (7.3 mJ/cm^2) and for the system inoculated with 10^7cell/ml growth was detected up to 30 seconds and no growth was detected at 60 seconds (43.8 mJ/cm^2).

Following irradiation of the cells for 10 minutes, the cells were then left in the dark for 24 hours. Dark repair, 6.00 (±2.00) x10^2cell/ml, was observed when the inoculum size was 10^7cell/ml but no repair was observed for the system inoculated with 10^6cell/ml (Table 3.6). There was no reduction in cell numbers in the dark controls for a period of up to 8 hours. When the viability of the cells in the system with the higher inoculum was monitored, there was a drop in viability of the cells with time and no dark repair was observed.

The inactivation curves of UV-C disinfection of 10^7cell/ml and 10^6cell/ml of *P. putida* CP1 in minimal medium are described in Figure 3.4. In the case of the dose response curve of the inoculum 10^6cell/ml a shoulder was observed at lower fluence, whereas at 10^7cell/ml the inactivation curve acquired a tailing shape at UV-C doses higher than 10 mJ/cm^2. Neither tailing nor shoulder portions were

taken into consideration for the calculation of inactivation rates (Figure 3.4). The mean value of the inactivation rate of 10^7cell/ml was 0.798 (±0.02) cm^2/mJ while for 10^6cell/ml the value was 0.797 (±0.09) cm^2/mJ. No significant difference was determined for these two values (Table 3.7). When the inactivation rate for 10^6cell/ml was compared with the values obtained when the organism was grown on Ringers, Milli-Q and PBS (Table 3.4) a significant difference was determined.

Table 3.6 – Number of *P. putida* CP1 following UV-C photolytic disinfection in minimal medium.

UV-C treatment		**Counts (cfu/ml)**		**Viability (%)**
UV-dose (mJ/cm^2)	Time (sec)	10^6	10^7	10^7
0	0	$1.90(\pm0.27)x10^6$	$2.58(\pm0.40)x10^7$	81.62(±1.06)
0.73	1	$1.28(\pm0.37)x10^6$	$2.42(\pm0.13)x10^6$	ND
2.19	3	$6.00(\pm2.55)x10^5$	$1.48(\pm0.46)x10^6$	ND
3.65	5	$4.80(\pm1.48)x10^4$	$1.92(\pm0.43)x10^4$	ND
5.11	7	$1.60(\pm1.52)x10^3$	$5.80(\pm1.30)x10^3$	ND
7.30	10	0.00	$2.32(\pm0.47)x10^3$	76.27(±8.56)
14.6	20	0.00	$5.50(\pm1.20)x10^2$	38.52(±5.15)
21.9	30	0.00	$4.43(\pm1.27)x10^2$	ND
43.8	60	0.00	0.00	61.07(±8.70)
219.0	300	0.00	0.00	47.31(±18.47)
438.0	600	ND	0.00	0.00
24 hours dark repair		0.00	$6.00x10^2(\pm2.00)$	0.00
ND: not determined.				

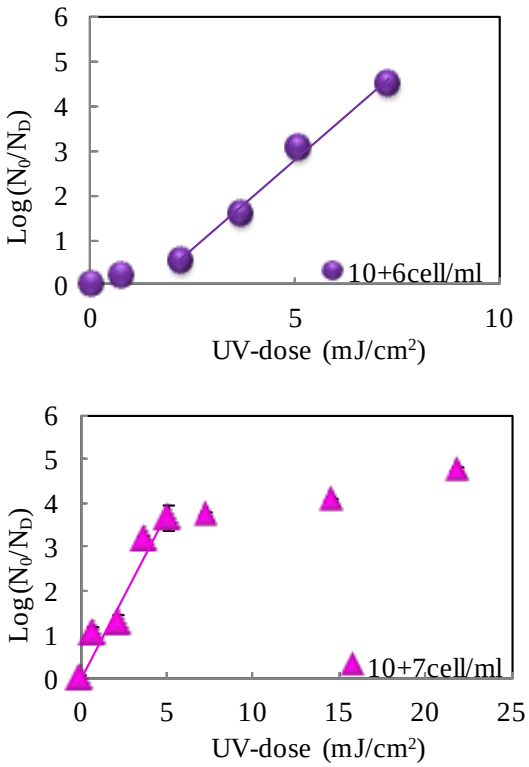

Figure 3.4 – UV-C dose response of free-swimming *P. putida* CP1 (10^6cell/ml) (●) and (10^7cell/ml) (▲).

Table 3.7 – Inactivation rates for 10^6cell/ml and 10^7cell/ml free-swimming *P. putida* CP1 following UV-C disinfection in minimal medium.

Inoculum size of *P. putida* CP1	**Inactivation rate (cm^2/mJ)**
10^7cell/ml	0.794 (±0.029)
10^6cell/ml	0.787 (±0.036)
Test Between-Subjects Effects and Dependent Variable: Inactivation rate tested by One-way-ANOVA. Inoculum size: p=.885.	

3.1.3.2 Growth and viability of aggregated cells following treatment with UV-C

Aggregated cells of *P. putida* CP1 were challenged by UV-C up to 6 hours in minimal medium. The number of cells in the aggregates at time 0 was 6.82 (±0.92) x 10^8cell/ml. The response of the cells to UV-C disinfection was determined by culturability method using the spread-plate technique. The time to achieve total inactivation of aggregated cells of *P. putida* CP1 was found to be 120 minutes. A rapid decay of cell survival was observed up to 30 minutes, with rate of inactivation k_1 estimated as being 0.0048 cm^2/mJ (Figure 3.5). From 30 minutes and up to 105 minutes, a second and lower inactivation rate k_2 was calculated. The k_2 value was 0.0006 cm^2/mJ and 8 times smaller than the initial rate (Figure 3.5). Dark repair was observed following 24 hours of incubation (Table 3.8). In dark control samples changes in culturability was not observed.

Table 3.8 – Number of *P. putida* CP1 aggregated cells following UV-C photolytic disinfection.

UV-C dose (mJ/cm^2)	**Time (min)**	**Counts (cfu/ml)**
0	0	$6.82(\pm0.92)x10^6$
1,314	30	$2.97(\pm1.73)x10^2$
1,971	45	$1.42(\pm3.46)x10^2$
2,628	60	$6.73(\pm2.13)x10^1$
4,599	105	$1.16(\pm2.02)x10^1$
5,256	120	0.00
10,512	240	0.00
13,140	300	0.00
15,768	360	0.00
24 hours dark repair		$1.88(\pm2.85)x10^2$

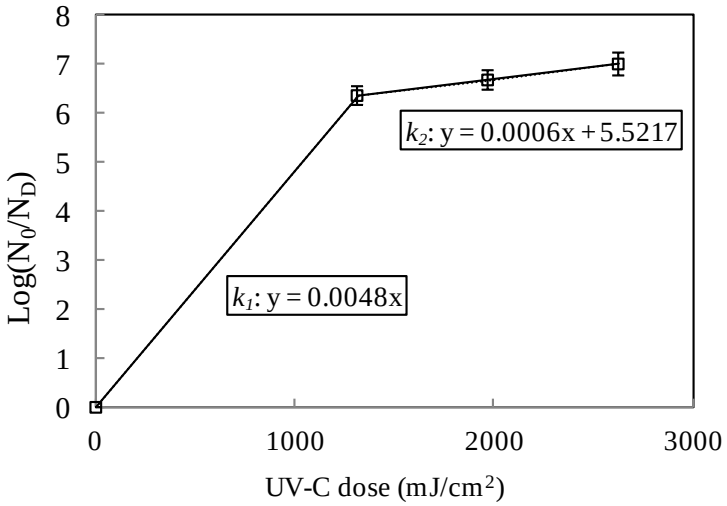

Figure 3.5 – UV-C dose response of aggregated cells of *P. putida* CP1 (~10^8cell/ml) in minimal medium.

UV-C treatment, which took up to 6 hours, did not cause changes in viability of aggregated cells (Table 3.9). Viability of the overnight incubated sample was not altered when compared to viability of untreated aggregated cells.

Table 3.9 – Percentage of viable cells in aggregates of *P. putida* CP1 following UV-C disinfection.

UV-C dose (mJ/cm^2)	Time (min)	Viability (%)
0	0	68.45(±11.68)
7,884	180	48.42(±15.19)
15,768	360	57.50(±9.01)
24 hours dark repair		62.73(±9.38)

3.1.3.3 Size of aggregates

When *P. putida* CP1 was added into minimal medium containing fructose, after 24 hours, it clumped forming aggregates. Comparatively to free-swimming cells (Figure 3.6a), aggregates were four orders of magnitude greater (Figure 3.6b). A three-dimensional structure, with curved edges, though not circular in the overall, with area size ranging from 10^3 to 10^4 μm^2 well defines an aggregated cell. Examination by phase-contrast microscopy showed that they could present variable forms such as an elliptical shape of similar size (Figure 3.6b) or as great

chunks (Figure 3.6c). The presence of "inclusions", dark circular structures immersed within the aggregates was evident (Figure 3.6c and d). The inclusions were less transparent to light than the overall structure of the aggregates and with diameter of approximately 20 µm to 50 µm (Figure 3.6d). At 100X magnification, the detail of an inclusion was demonstrated as a patched of parallel and intercrossed patterns, resembling a ball of thread.

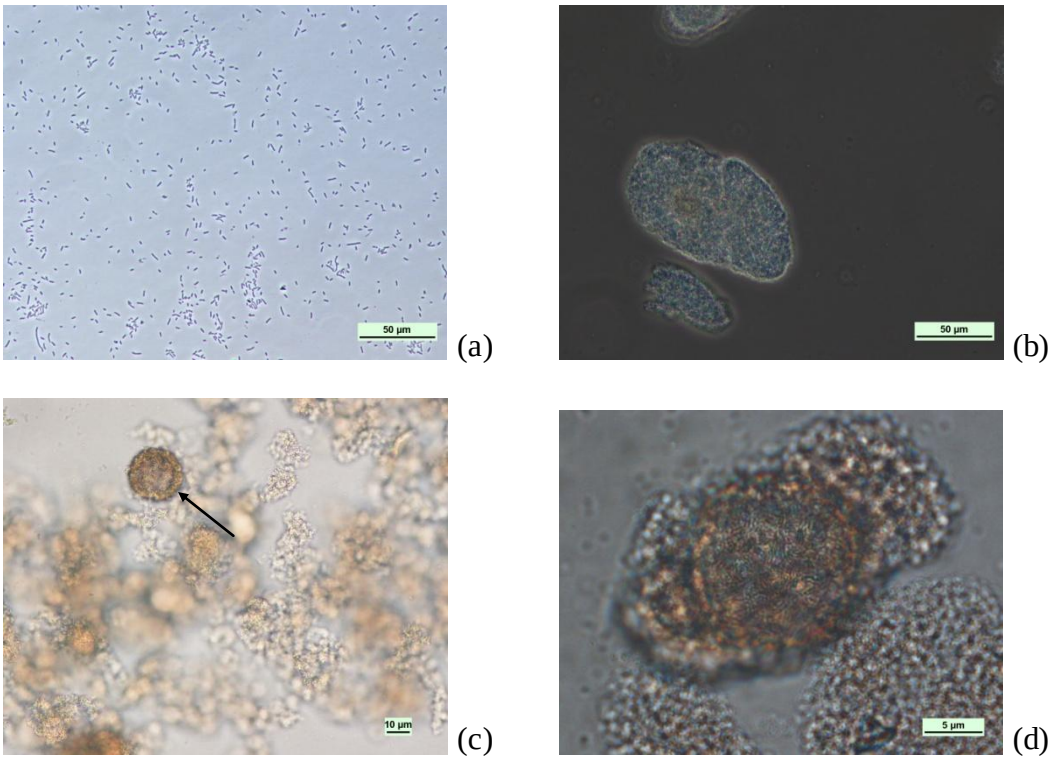

Figure 3.6 – Phase-contrast microscopy at 40X of cells of *P. putida* CP1 in free-swimming (a) and in aggregated form (b). Light-microscopy of aggregated cells of *P. putida* CP1 at 40X (c) and at 100X (d).

The number of aggregates was distributed in ranges between 0-5,000 μm^2, 5,000-10,000 μm^2, 10,000-20,000 μm^2 and 20,000-100,000 μm^2 during UV-C treatment. The results showed in Table 3.10 pointed to a reduction in the number of larger aggregates. Simultaneously, an increased number of smaller aggregates were formed. The greatest reduction in the aggregates size was observed following 1 hour of UV-C treatment when the average size changed from 3.34 (±3.68) x 10^4 μm^2 to 9.36 (±9.80) x 10^3 μm^2. Further changes in aggregate size were more gradual and the changes were not significantly different for the remainder of the experiment (Table 3.10). Agitated and non-agitated dark controls were monitored

for up to eight hours. The dominant aggregate size was in the range 20,000-100,000 μm^2. The average aggregate size was significantly different at eight hours indicating that agitation did not contribute to the change in aggregate size observed following UV-C treatment (Table 3.11). Images of the aggregates show the presence of inclusions (Figure 3.7a). They too were found to be disrupted by UV-C treatment and are illustrated in Figure 3.7b.

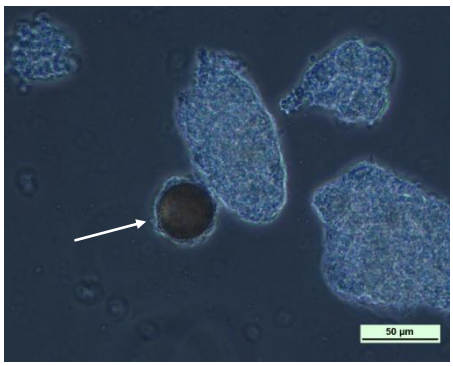

(a)
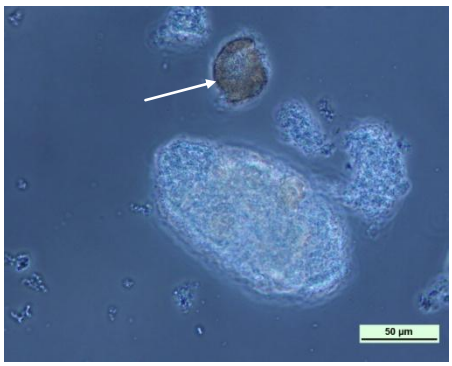

(b)

Figure 3.7 – Phase-contrast microscopy of aggregated cells during UV-C disinfection at time 3 hours (a) and 6 hours (b). Arrows indicate inclusions.

Table 3.10 – Effect of UV-C disinfection on aggregates size of *P. putida* CP1. Scale-bar=100 µm.

Time (h)		Size range of aggregates				Average aggregates size (μm^2)	Phase-contrast 10X
		0-5,000 μm^2	5,000-10,000 μm^2	10,000-20,000 μm^2	20,000-100,000 μm^2		
0	Number of aggregates	1.2(±1.3)	1.2(±1.3)	0.8(±0.4)	4(±1)	$3.34(\pm3.68)x10^4$	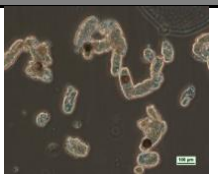
1		6(±5.2)	4(±3.8)	5(±3.6)	0.00	$9.36(\pm9.80)x10^3$	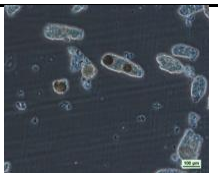
2		11(±5.78)	3.8(±1.94)	3.2(±1.64)	1.8(±1.64)	$6.93(\pm7.67)x10^3$	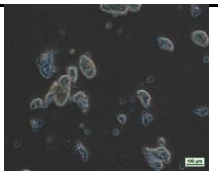
3		7.6(±4.49)	5.2(±1.64)	3.4(±2.50)	1.6(±2.50)	$6.03(\pm4.97)x10^3$	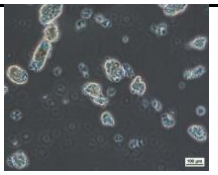
6		28.6(±9.8)	3.4(±1.81)	2(±1.58)	1(±1.22)	$3.50(\pm5.54)x10^3$	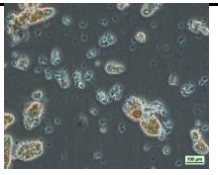

Table 3.11 – Effect of agitation and non agitation on the size of *P. putida* CP1 aggregated cells. Scale-bar=100 µm.

Time (h)		Size range of aggregates				Average aggregates size (μm^2)	Phase-contrast 10X
		0-5,000 μm^2	5,000-10,000 μm^2	10,000-20,000 μm^2	20,000-100,000 μm^2		
0 h	Number of aggregates	0.00	0.00	0.00	1.0±(0.00)	$3.27(\pm 5.70)x10^4$	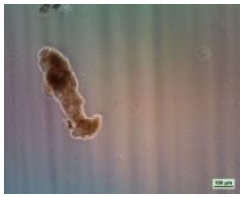
8 h no agitation		1.5(±1.29)	0.5(±1.0)	0.25(±0.5)	0.75(±0.95)	$2.82(\pm 1.62)x10^4$	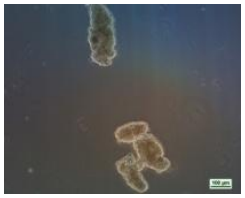
8 h agitation		0.00	0.00	0.00	1.4(±0.89)	$5.69(\pm 2.92)x10^4$	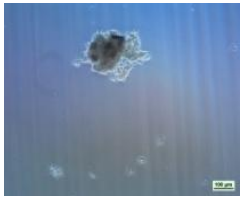

3.1.3.4 Composition of aggregates

When the mixed liquor was examined, the dry-weight of the biomass was 0.63±0.12 mg/ml and a residual level of fructose, 3.19±0.08 mg/ml was detected. The total EPS detected was determined as 17.91±0.35 mg/g or 11.24±0.22 µg/ml. On examination, the main components of the EPS were found to be carbohydrate and protein. Levels of protein were higher than carbohydrate and were mainly present in the free-EPS. The levels of carbohydrate were similar in the bound and free-EPS. The levels of protein and carbohydrate in the aggregates did not change significantly following 6 hours of treatment with UV-C (Figure 3.8).

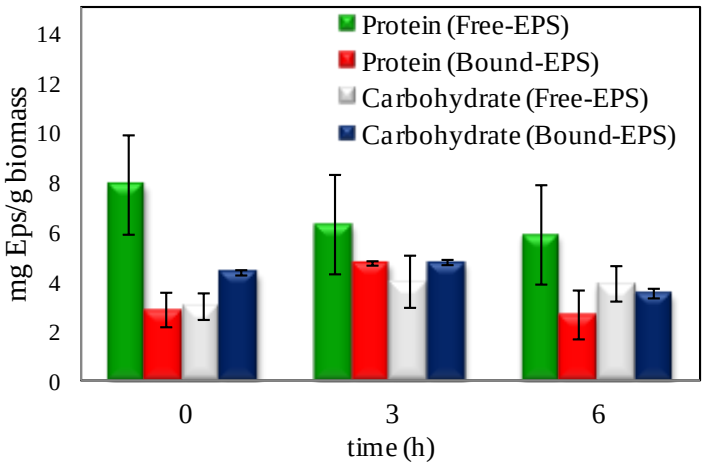

Figure 3.8 – Biochemical analysis of carbohydrates and proteins of extracellular polymeric substances of aggregated cells of *P. putida* CP1 during UV-C disinfection.

When calcofluor-white and FITC were used to stain the aggregates, the presence of carbohydrate and protein was evident. The presence of both carbohydrate and protein following 6 hours of treatment with UV-C was also evident using the stains while the size of the aggregates was clearly reduced (Figure 3.9). The pH of the mixed liquor was 6.7 and did not change during irradiation of the aggregated cells or in the dark controls.

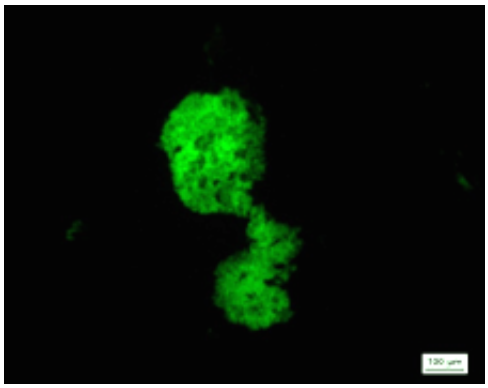
(a)

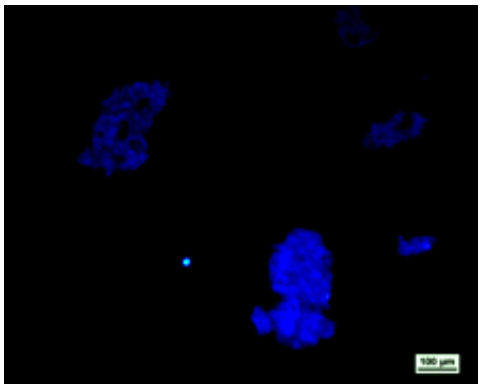
(b)

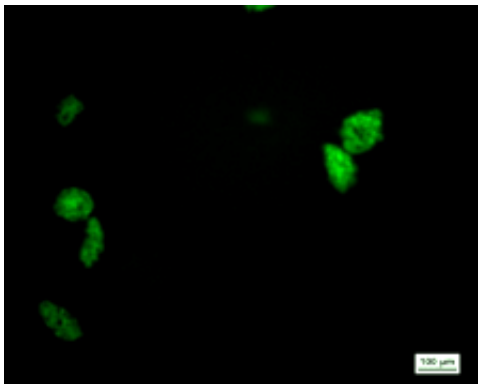
(c)

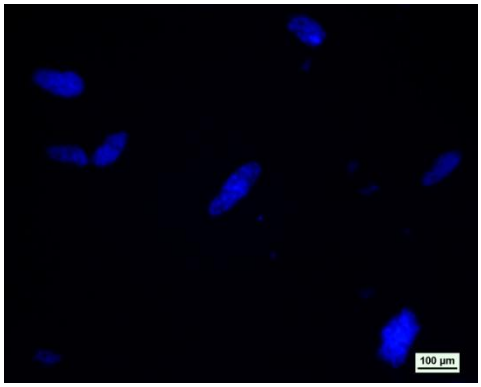

(d)

Figure 3.9 – Single fluorescent staining of aggregated cells of *P. putida* CP1 during UV-C disinfection at t=0 h with FITC (a), at t=0 h with calcofluor-white (b), at t=6 hours with FITC (c) and at t=6 hours with calcofluor-white (d).

3.2 UV-A/B disinfection

UV-A/B disinfection was investigated as an alternative route to achieve inactivation of free-swimming cells of *P. putida* CP1 and *E. coli* and aggregated cells of *P. putida* CP1. The same media used in UV-C disinfection, Milli-Q water, Phosphate Buffered Saline, ¼ Strength Ringers solution and minimal medium (for *P. putida* CP1 only), were used in the studies. An Aceglass (Vineland, New Jersey USA) reactor vessel constructed of borosilicate glass Aceglass® (1 l capacity) together with a 400 W polychromatic medium-pressure mercury lamp with ($\lambda \geq 300$ nm) was used. The response of the cells to UV-A/B disinfection was monitored by determining cell number following growth and by using the LIVE/DEAD® Bacterial Viability Kit (*Bac*Light™). In the case of aggregated cells changes in size and composition were observed using epifluorescence microscopy and biochemical analysis.

3.2.1 UV-A/B disinfection of free-swimming cells

Milli-Q water, Phosphate Buffered Saline and 1/4 Strength Ringers solution were inoculated with pure cultures of free-swimming *E. coli* or *P. putida* CP1 (10^7cell/ml), incubated with stirring and underwent UV-A/B treatment for a period up to 120 minutes. Samples were taken at intervals and checked for cell growth using the Miles-Misra (drop-plate) method. Results showed that when *E. coli* was challenged in Milli-Q water and PBS total inactivation occurred after 60 minutes, while in Ringers disinfection was quicker and it took 15 minutes (Table 3.12). In the case of *P. putida* CP1 no growth was detected at 15 minutes in Milli-Q water and at 30 minutes in PBS and Ringer solution (Table 3.13).

Table 3.12 – Number of *E. coli* (DSMZ 498) following UV-A/B photolytic disinfection in Milli-Q ultrapure water, Phosphate Buffered Saline and ¼ Strength Ringers solution.

UV-A/B treatment	**Counts (cfu/ml)**		
Time (min)	Milli-Q Water	Phosphate Buffer Saline (PBS)	¼ Strength Ringers solution
0	$5.29(\pm1.49)x10^{7}$	$3.75(\pm0.96)x10^{7}$	$5.58(\pm1.30)x10^{7}$
1	$6.11(\pm1.76)x10^{7}$	$2.42(\pm0.27)x10^{7}$	$1.86(\pm0.27)x10^{7}$
5	$8.25(\pm3.79)x10^{6*}$	$2.17(\pm0.65)x10^{7}$	$1.81(\pm0.27)x10^{6}$
10	$1.22(\pm0.31)x10^{6*}$	$5.42(\pm2.19)x10^{5*}$	$1.04(\pm0.90)x10^{5*}$
15	$2.80(\pm0.83)x10^{5}$	$1.68(\pm0.37)x10^{4}$	0.00
30	ND	$2.33(\pm1.52)x10^{2}$	0.00
60	0.00	0.00	0.00
90	0.00	ND	0.00
120	0.00	ND	ND
* Presence of small-colonies-variants (SCVs). ND: not determined.			

Table 3.13 – Number of *P. putida* CP1 following UV-A/B photolytic disinfection in Milli-Q ultrapure water, Phosphate Buffered Saline and ¼ Strength Ringers solution.

UV-A/B Treatment	**Counts (cfu/ml)**		
Time (min)	Milli-Q Water	Phosphate Buffer Saline (PBS)	¼ Strength Ringers solution
0	$5.55(\pm2.50)x10^{7}$	$2.12(\pm0.26)x10^{7}$	$1.65(\pm0.32)x10^{7}$
1	$1.66(\pm0.36)x10^{7*}$	$1.56(\pm0.19)x10^{7}$	$1.80(\pm0.34)x10^{7}$
5	$5.44(\pm1.67)x10^{6*}$	$1.04(\pm0.56)x10^{7*}$	$2.33(\pm1.53)x10^{5*}$
10	$6.50(\pm1.87)x10^{5*}$	ND	ND
15	0.00	$2.67(\pm4.16)x10^{5*}$	$6.16(\pm1.16)x10^{3*}$
30	0.00	0.00	0.00
60	0.00	0.00	0.00
90	0.00	0.00	0.00
120	0.00	0.00	0.00
24 hours dark repair	ND	ND	$1.24(\pm0.28)x10^{3}$
* Presence of small-colonies-variants (SCVs). ND: not determined.			

Dark repair and viability of *P. putida* CP1 were evaluated following UV-A/B disinfection in Ringers solution (Table 3.13). Although no cells were culturable after 120 minutes, the LIVE/DEAD® Bacterial Viability Kit (*Bac*Light™)

detected 44% cell viability. When these cells were left for 24 hours in the dark to allow dark repair, repair was identified using both the plate count technique and the Live Dead method (Table 3.14).

Table 3.14 – Reduction in the number of culturable free-swimming cells of *P. putida* CP1 obtained during UV-A/B photolytic disinfection in ¼ Strength Ringers solution.

Time (min)	Viable cells (%)
0	81.07(±7.60)
1	ND
3	ND
5	ND
10	ND
30	36.22(±5.01)
60	ND
90	ND
120	43.43(±7.57)
24 hours dark repair	49.63±(7.91)
ND: not determined.	

Interestingly, colonies of bacteria photolysed by UV-A/B showed a small colony variants (SCVs) phenotype. SCVs of *E. coli* were manifested at 5 and 10 minutes in Milli-Q water, while in Phosphate Buffered Saline and in Ringers solution, at 10 minutes (table). In the case of *P. putida* CP1, SCVs were observed at 1, 5 and 10 minutes in Milli-Q and at 5 and 15 minutes in PBS and Ringers solution (table). Examples of SCVs in UV-A/B photolysed *E. coli* are displayed in Figure 3.10. Colonies produced by the organisms in the dark controls were of normal size.

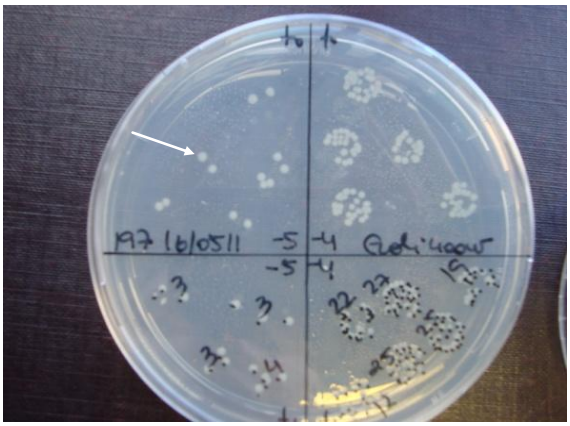
(a)

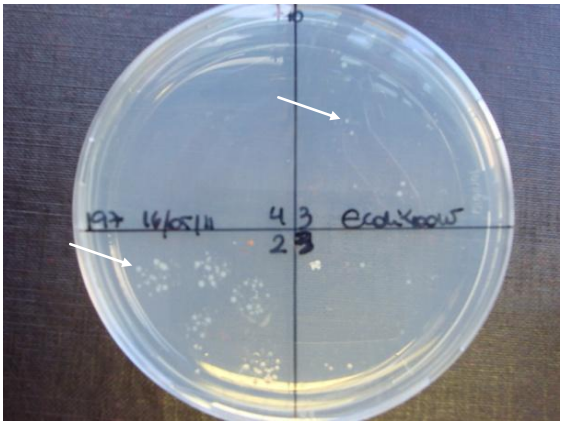
(b)

Figure 3.10 – Observation of small colonies variants (SCVs). Size of untreated *E. coli* colonies at t=0 h (a) and size of *E. coli* colonies following 10 minutes of UV-A/B disinfection treatment (b).

The inactivation rate (k), for each bacterium and in all three media, was calculated from the linear regression of the decimal logarithm of the fraction of surviving organisms (N_0/N_t) versus time (t) of UV-A/B exposure, where:

(Equation 2) $\text{Log}_{10}\, N_0/Nt = k \times (t)$, where

N_0 = Number of cells/ml at time "0",

N_t = Number of cells/ml at time t,

k = disinfection rate= min^{-1},

t = time (min).

Figure 3.11a and Figure 3.11b display the inactivation curves of *E. coli* and *P. putida* CP1, respectively.

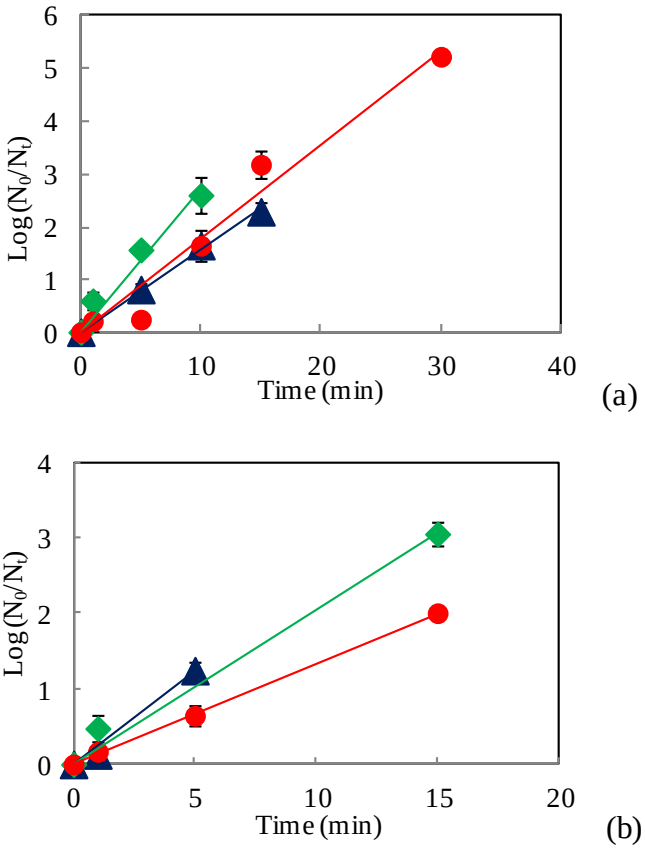

Figure 3.11 – UV-A/B disinfection inactivation curves of (a) *E. coli* and (b) *P. putida* CP1 in aqueous media. Milli-Q water (▲), PBS (●) and ¼ Strength Ringers solution (◆).

The mean values of the disinfection rates of free-swimming *E. coli* and *P. putida* CP1 in PBS, Milli-Q and Ringers solution are displayed in Table 3.15. Two-way analysis of variance (ANOVA) did not show any significant differences between the inactivation rates for the two bacteria (p=.132). However, there was a difference in the response of each bacterium between the media.

Table 3.15 – Inactivation rates of free-swimming *E. coli* and *P. putida* CP1 during UV-A/B disinfection in aqueous media.

Free-swimming organism	Milli-Q Water	Phosphate Buffer Saline	¼ Strength Ringers solution
E. coli (DSMZ 498)	0.157(±0.039)	0.170(±0.024)	0.222(±0.018)
P. putida CP1	0.253(±0.016)	0.168(±0.014)	0.212(±0.013)
Test Between-Subjects Effects tested by ANOVA-two-way: Organism p=.089; Medium p=.035; Organism*Medium p=.132.			

3.2.2 UV-A/B disinfection of aggregated cells

The effect of UV-A/B disinfection on aggregated cells was determined by monitoring cell growth, viability and the size and composition of the aggregates. Since the aggregated cells had been grown in minimal medium with fructose supplied as the sole carbon source, the response of free swimming cells of *P. putida* CP1 in minimal medium to UV-A/B disinfection was first evaluated.

3.2.2.1 Response of free-swimming P. putida CP1 in minimal medium to UV-A/B disinfection

The response of the free-swimming *P. putida* CP1 was determined by inoculating the photochemical reactor with two inoculum sizes, 10^7cell/ml and 10^6cell/ml. The microbial suspension was stirred into the UV-A/B reactor and sampled at various time intervals. The evaluation of culturability was carried out using the Miles-Misra (drop-plate) technique. The results obtained from UV-A/B disinfection of free-swimming *P. putida* CP1 in minimal medium are presented in Table 3.16. Total inactivation of *P. putida* CP1 free-swimming (10^6 and 10^7cell/ml) occurred in 60 minutes (Table 3.16). Dark repair of *P. putida* CP1 challenged in minimal medium was observed in the inoculum size of 10^7cell/ml though not when the inoculum size was 10^6cell/ml. Evaluation of viability, carried out for the higher inoculum size system (10^7cell/ml), showed that no viable cells were detected following 30 minutes of UV-A/B exposure. Furthermore, no viable cells were found in the overnight dark repair samples (Table 3.16). Small-colony-variants were also observed between 5 and 15 minutes of UV-A/B exposure in minimal medium.

Table 3.16 – Number of *P. putida* CP1 following UV-A/B photolytic disinfection.

Time (min)	Counts (cfu/ml)		Viability (%)
0	$8.83(\pm3.76)x10^{6}$	$1.48(\pm0.40)x10^{7}$	79.70(±6.96)
1	$7.40(\pm4.51)x10^{6}$	$1.12(\pm0.17)x10^{7}$	ND
5	$2.15(\pm0.35)x10^{6}$	$3.40(\pm1.25)x10^{6*}$	ND
10	$2.52(\pm0.35)x10^{5*}$	$9.80(\pm3.35)x10^{4*}$	ND
15	$1.22(\pm0.40)x10^{4*}$	$7.60(\pm3.13)x10^{4*}$	ND
30	$8.60(\pm2.30)x10^{2*}$	0.00	0.00
60	0.00	0.00	ND
90	0.00	0.00	ND
120	0.00	0.00	0.00
24 hours dark repair	0.00	$1.16(\pm0.41)x10^{3}$	0.00
* Presence of small-colonies-variants (SCVs). ND: not determined.			

The dose-response curves of free-swimming *P. putida* CP1 in minimal medium are presented in Figure 3.12. There was evidence of shouldering at longer exposure times > 10 minutes. The mean values of the inactivation rate for the inoculum size 10^{7}cell/ml was 0.147 (±0.006) min^{-1}, while for 10^{6} cell/ml the value was 0.149 (±0.006) min^{-1} (Table 3.17). There was no significant difference between the two values.

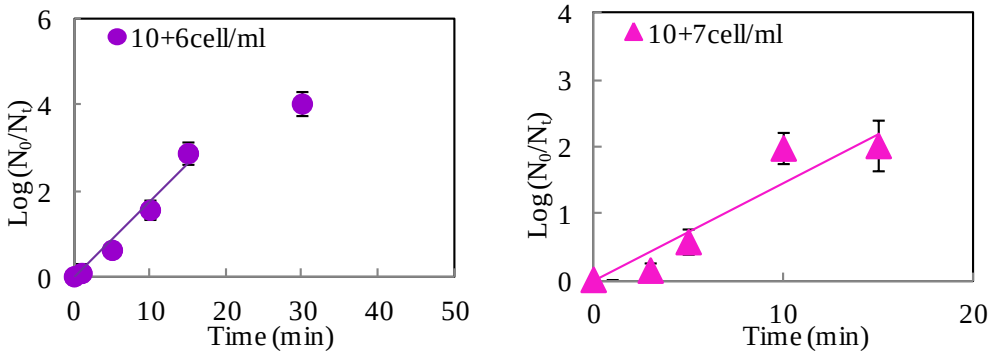

Figure 3.12 – UV-A/B disinfection inactivation curve of *P. putida* CP1 in minimal medium (10^{6}cell/ml) (●) and (10^{7}cell/ml) (▲).

Table 3.17 – Inactivation rates for 10^6cell/ml and 10^7cell/ml free-swimming *P. putida* CP1 following UV-A/B disinfection in minimal medium.

Inoculum size of *P. putida* CP1	Inactivation rate (cm^2/mJ)
10^7cell/ml	0.147(±0.006)
10^6cell/ml	0.149(±0.006)
Test Between-Subjects Effects and Dependent Variable: Inactivation rate tested by One-way-ANOVA. Inoculum size: p=.854.	

3.2.2.2 Growth and viability of aggregated cells following treatment with UV-A/B

Aggregated cells of *P. putida* CP1 underwent UV-A/B disinfection for up to 6 hours (Table 3.18). The initial number of cells in the aggregates was 6.82 (±0.92) x 10^8cfu/ml. The response of the cells was determined using the spread-plate technique. There was a six log reduction in the numbers of cells in the first 20 minutes. The cell numbers continued to fall until no growth was detected at 240 minutes. Cells which had been treated for 6 hours showed some dark repair. The inactivation curve shows two stages (Figure 3.13). The first stage represents the immediate dramatic fall in cell numbers in the first 20 minutes and the inactivation constant k_1 was calculated at 0.319 min^{-1}. The second stage, between 20 and 180 minutes, showed a lower inactivation rate, corresponding to a tailing behaviour. For this region, the calculated k_2 value was 0.0036 min^{-1}, approximately four times slower than the initial and fast-inactivation part of the curve. When the viability of the cells was monitored using the Live Dead stain, the percentage viability dropped while viable cells continued to be detected in the absence of growth. Cells that grew following dark repair also showed the presence of viable cells (Table 3.18).

Table 3.18 – Number of *P. putida* CP1 aggregated cells following UV-A/B photolytic disinfection.

Time (min)	Counts (cfu/ml)	Viability (%)
0	$6.82(\pm0.92)x10^{8}$	79.55(±13.74)
20	$8.62(\pm12.1)x10^{2}$	ND
60	$1.56(\pm1.65)x10^{2}$	ND
90	$3.55(\pm5.02)x10^{1}$	ND
180	$3.17(\pm4.49)x10^{1}$	74.56(±13.40)
240	0.00	ND
300	0.00	ND
360	0.00	64.53(±13.24)
24 hours dark repair	$8.8(\pm3.30)x10^{1}$	57.57(±3.76)
ND: not determined.		

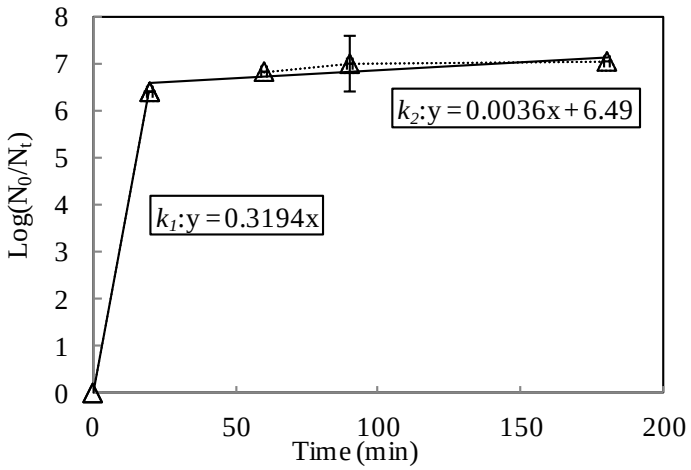

Figure 3.13 – UV-A/B disinfection inactivation curve of aggregated cells of *P. putida* CP1 (~10^{8}cell/ml).

3.2.2.3 Size of aggregates

As with UV-C disinfection, the number of aggregates in suspension were described in terms of size ranges of 0-5,000 μm^2, 5,000-10,000 μm^2, 10,000-20,000 μm^2 and 20,000-100,000 μm^2 (Table 3.19). Following UV-A/B treatment, there was an increase in the number of smaller aggregates and in the average size of the aggregates. The average size was reduced from 2.76 (±6.50) $x10^3$ μm^2 at time 0 to 1.93 (±3.83) x 10^3 μm^2 following 3 hours of treatment, and finally to 1.02 (±2.35) x 10^3 μm^2 after 6 hours. The presence of inclusion bodies in the aggregates was also noted during UV-A/B disinfection (Figure 3.14). However, disruption of these inclusions following six hours of UV-A/B treatment was not observed.

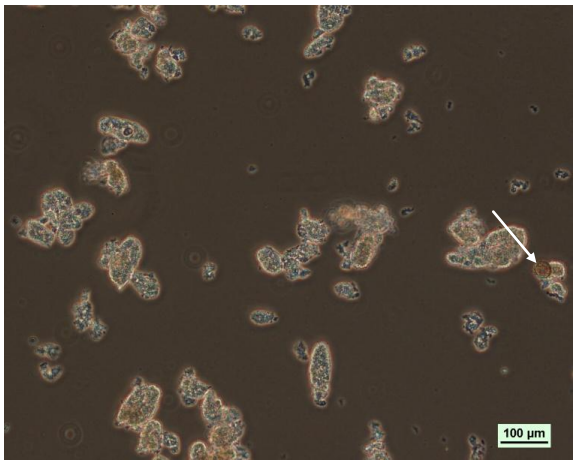

(a)

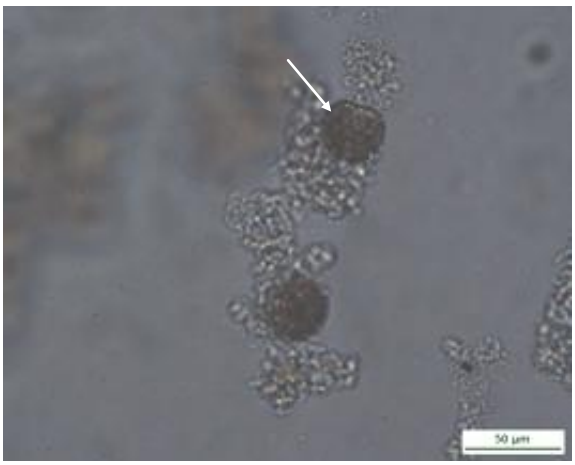

(b)

Figure 3.14 – Phase-contrast microscopy of aggregated cells of *P. putida* CP1 during UV-A/B treatment at t=0 h at 10X (a) and at t=3 hours with inclusions at 40X (b). White arrows indicate inclusions.

Table 3.19 – Effect of UV-A/B disinfection on aggregates size of *P. putida* CP1. Scale-bar=100 µm.

Time (h)		Size range of aggregates				Average aggregates size (μm^2)	Phase-contrast 10X
		0-5,000μm^2	5,000-10,000μm^2	10,000-20,000μm^2	20,000-100,000μm^2		
0	Number of aggregates	13.6(±11.32)	3(±2.23)	3.8(±4.20)	0.00	2.76(±6.50)x10^3	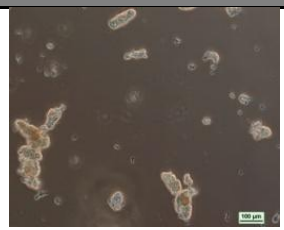
3		45(±12.72)	3.5(±0.70)	1.5(±0.70)	1.0(±1.4)	1.93(±3.83)x10^3	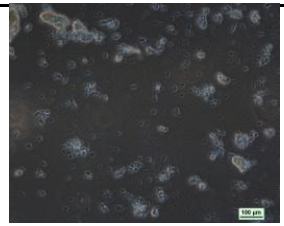
6		50(±10.82)	12.2(±18.57)	2.3(±0.57)	0.00	1.02(±2.35)x10^3	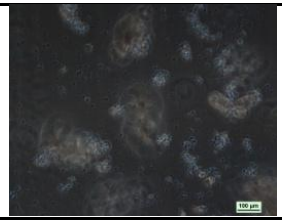

3.2.2.4 Composition of aggregates

When the composition of the aggregated cells was investigated during UV-A/B disinfection, the dry-weight was found to be 0.535±0.03 mg/ml, a residual amount of fructose was determined as 4.15±0.17 mg/ml and the total EPS detected was 61.38 (±0.48) mg/g or 32.83 (±1.04) µg/ml. The components of the EPS were carbohydrate and protein. Carbohydrate was the main component comprising ~80% of the total EPS at time 0. The carbohydrate was mainly in the form of bound EPS and the levels of carbohydrate in the bound fraction of the EPS increased fourfold during the six hours of UV-A/B exposure. Before UV-A/B, less than 20% of the total EPS was protein which was evenly distributed between the bound and free fractions (Figure 3.15). The levels of protein together with the carbohydrate in the free EPS did not change significantly during the UV-A/B treatment. The pH of the mixed liquor was 6.8 and did not change throughout UV-A/B exposure.

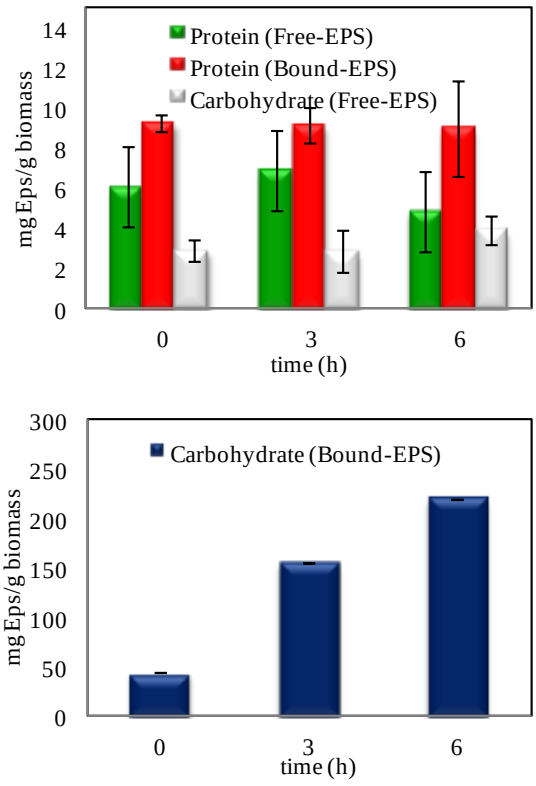

Figure 3.15 – Biochemical analysis of carbohydrates and proteins of extracellular polymeric substances of aggregated cells of *P. putida* CP1 during UV-A/B disinfection.

When the EPS was stained with a combination of FITC, calcofluor-white and propidium iodide, proteins and carbohydrates were the dominant components at time 0. Following UV-A/B treatment for six hours, an increased level DNA was observed suggesting an increase in the numbers of dead cells and cell lysis. The inclusions present in the aggregates were not stained by the fluorochromes (Figure 3.16).

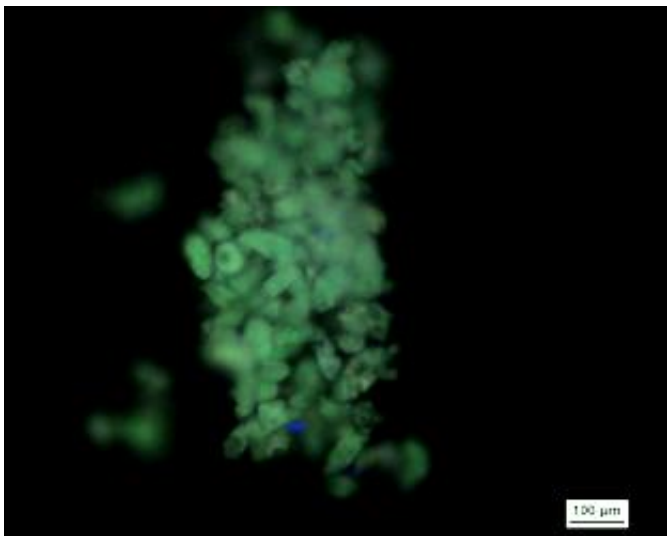

(a)

(b)

Figure 3.16 – Epifluorescence multistaining microscopy of UV-A/B photolysed aggregated cells. At t=0 h (a) and at t=6 hours (b).

3.3 Photocatalytic disinfection of bacteria

In this section, UV-A/B-TiO_2 photocatalysis was carried out on the free-swimming, *E. coli* (DSMZ 498) and both free-swimming and aggregated forms of *P. putida* CP1. The disinfection studies were conducted in a photochemical reactor Aceglass (Vineland, New Jersey USA) vessel with a 400 W polychromatic medium-pressure mercury lamp ($\lambda \geq 300$ nm), as was used UV-A/B studies. The studies were conducted in the presence of 1 g/l of TiO_2. The influence of aqueous media was first evaluated. The response of the bacteria was determined using culturability and viability using LIVE/DEAD® Bacterial Viability Kit (*Bac*Light™). The evaluation of survival of aggregated cells of *P. putida* CP1 was carried out by culturability and viability methods. Phase-contrast and epifluorescence microscopy was used to investigate interactions between the TiO_2 nanoparticles and the cell aggregates.

3.3.1 TiO_2 photocatalysis of free-swimming bacteria

3.3.1.1 Evaluation of aqueous media

Milli-Q water, PBS, Ringers solution and tap water were tested for their suitability as aqueous media. One litre quantities were placed in the reactor, inoculated with each bacterium (10^7cell/ml) and 1 g/l of TiO_2 and incubated, with stirring in the dark for a period up to 240 minutes. Samples were taken at intervals and checked for cell number. Unlike the previous studies, there was no significant change in the numbers of cells in the tap water. The other media were also found to be suitable and all four media were used in the TiO_2 photocatalysis studies (Table 3.20).

Table 3.20 – Numbers of *E. coli* and *P. putida* CP1 (~10^7cell/ml) after 240 minutes of incubation in the presence of 1 g/l of TiO_2 in various aqueous media.

Organism / Aqueous medium	*E. coli* (DSMZ 498)	*P. putida* CP1
Milli-Q water	+	+
¼ Strength Ringers Solution	+	+
Phosphate Buffered Saline (PBS)	+	+
Tap water	+	+
Minimal Medium (up to 6 hours)	+	+
(+): not significant reduction.		

3.3.1.2 TiO_2 photocatalysis of free-swimming bacteria in aqueous media

In photocatalytic studies of free-swimming bacteria, the aqueous media (Milli-Q, PBS, Ringers solution and Tap water) were inoculated with pure cultures of each bacterium (10^7cell/ml). The reactor was then incubated with stirring and underwent UV-A/B exposure in the presence of 1g/l of TiO_2 up to a period of 180 minutes. Samples were taken at intervals and checked for cell number using the Miles-Misra (drop-plate) technique. The results of photocatalytic studies of the free-swimming bacteria are depicted in illustrated by Table 3.21 and Table 3.22. For *E. coli*, complete inactivation was achieved in Ringers solution after 90 minutes. In Milli-Q, Tap water and Phosphate Buffered Saline, although total inactivation of *E. coli* did not occur over the course of 180 minutes, survival was greatly reduced (~5-Log) (Table 3.21). In the case of *P. putida* CP1, total inactivation in Ringers took place after 60 minutes. In Milli-Q a 4-Log reduction of *P. putida* CP1 was achieved after 60 minutes and beyond that, at 90 and 120 minutes, a statistically insignificant number of cells were detected. In Tap water and PBS the maximum inactivation achieved at 120 minutes was, 5-Log and 3-Log, respectively. No further inactivation occurred in PBS even at prolonged exposure (180 minutes) (Table 3.22). There was no dark repair for *P. putida* CP1 free-swimming cells in Ringers solution. There was no reduction in cell numbers in dark controls.

Table 3.21 – Number of *E. coli* following UV-A/B TiO_2 photocatalytic disinfection in the presence of 1 g/l of TiO_2 in Milli-Q water, PBS, ¼ Strength Ringers solution and Tap water.

UV-A/B+TiO_2 treatment	**Counts (cfu/ml)**			
Time (min)	Milli-Q Water	Phosphate Buffer Saline (PBS)	¼ Strength Ringers Solution	Tap water
0	$4.20(\pm1.30)x10^7$	$7.50(\pm2.42)x10^7$	$6.33(\pm2.96)x10^7$	$4.00(\pm1.00)x10^7$
10	$2.80(\pm0.70)x10^7$	$2.24(\pm0.63)x10^7$	$1.05(\pm0.71)x10^7$	$2.48(\pm0.42)x10^7$
20	$1.56(\pm0.41)x10^7$	$6.50(\pm1.73)x10^6$	$1.20(\pm0.27)x10^4$	$2.10(\pm0.33)x10^5$
30	$2.70(\pm0.30)x10^6$	$1.32(\pm0.21)x10^6$	$7.20(\pm3.10)x10^3$	$6.33(\pm1.53)x10^3$
60	$1.00(\pm0.28)x10^4$	$2.20(\pm0.37)x10^3$	$3.50(\pm1.27)x10^3$	$1.08(\pm0.27)x10^3$
90	$5.20(\pm1.64)x10^2$	$1.84(\pm0.30)x10^3$	0.00	$7.20(\pm3.27)x10^2$
120	$3.00(\pm1.00)x10^2$	$6.78(\pm3.15)x10^2$	0.00	$5.20(\pm2.28)x10^2$
150	$3.00(\pm0.57)x10^2$	$4.00(\pm0.70)x10^2$	ND	$3.86(\pm1.21)x10^2$
180	ND	$3.80(\pm1.64)x10^2$	ND	ND
ND: not determined.				

Table 3.22 – Number of *P. putida* CP1 following UV-A/B TiO_2 photocatalytic disinfection in the presence of 1 g/l of TiO_2 in Milli-Q ultrapure water, Phosphate Buffered Saline, ¼ Strength Ringers solution and Tap water.

UV-A/B+TiO_2 treatment	**Counts (cfu/ml)**			
Time (min)	Milli-Q water	Phosphate Buffer Saline (PBS)	¼ Strength Ringers Solution	Tap water
0	$7.00(\pm4.08)x10^{6}$	$1.46(\pm0.32)x10^{7}$	$1.12(\pm0.33)x10^{7}$	$4.20(\pm2.17)x10^{7}$
10	$2.05(\pm0.13)x10^{6}$	ND	$4.75(\pm1.50)x10^{6}$	$7.50(\pm3.03)x10^{6}$
20	$5.60(\pm2.61)x10^{4}$	$4.6(\pm0.57)x10^{6}$	$1.84(\pm0.20)x10^{4}$	$5.00(\pm1.41)x10^{5}$
30	ND	$1.50(\pm0.50)x10^{6}$	$6.00(\pm0.00)x10^{2}$	$8.33(\pm3.04)x10^{5}$
60	$1.50(\pm0.57)x10^{3}$	$4.00(\pm1.80)x10^{5}$	0.00	$2.26(\pm0.49)x10^{3}$
90	$1.00(\pm1.00)x10^{2}$	$1.57(\pm0.37)x10^{5}$	0.00	ND
120	$1.00(\pm1.00)x10^{2}$	$1.86(\pm0.48)x10^{4}$	ND	$4.67(\pm0.57)x10^{2}$
150	ND	$5.40(\pm2.30)x10^{2}$	ND	ND
180	ND	$5.33(\pm1.15)x10^{2}$	ND	ND
24 hours dark repair	ND	ND	0.00	ND
ND: Not determined.				

When photocatalytic treatment of *P. putida* CP1 (10^7cell/ml) free-swimming cells in Ringers solution and 1.0g/l TiO_2 was evaluated using the LIVE/DEAD® Bacterial viability kit (*Bac*Light™), while viable cells were detected at 30 minutes, viability was seen to be completely lost at 120 minutes and no viable cells were detected following dark repair (Figure 3.17).

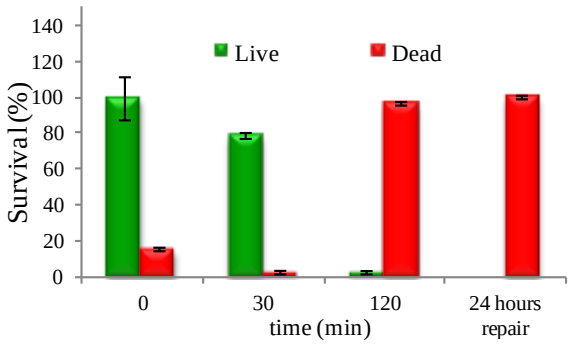

Figure 3.17 – Percentage of survival of *P. putida* CP1 as determined by LIVE/DEAD® Bacterial Viability Kit (*Bac*Light™) during photocatalytic treatment in the presence of 1g/l of TiO_2 ¼ Strength Ringers Solution.

The inactivation rate (k) for each bacterium was calculated by plotting the decimal logarithm of the fraction of surviving organisms (N_0/N_t) against time (t) of UV-A/B photocatalytic exposure, with Equation 2, where:

(Equation 2) $Log_{10}=N_0/N_t= k\ x\ (t)$, where

N_0 = Number of cells/ml at time "0",
N_t = Number of cells/ml at time t,
k = disinfection rate= min^{-1},
t = time (min).

The inactivation curves of *E. coli* and *P. putida* CP1 in the presence of 1 g/l of TiO_2 in the various aqueous media can be seen in Figure 3.18a and Figure 3.18b, respectively. In Milli-Q water, Tap water and Ringers solution inactivation curves were not linear. The inactivation rates were calculated from the initial linear portion which preceded a tailing of the curve as described in Figure 3.18a and b. The fastest inactivation was obtained for Ringers. The data obtained for the response of the bacteria in PBS generated a completely linear

response. The inactivation rate was significantly lower than for the other media.

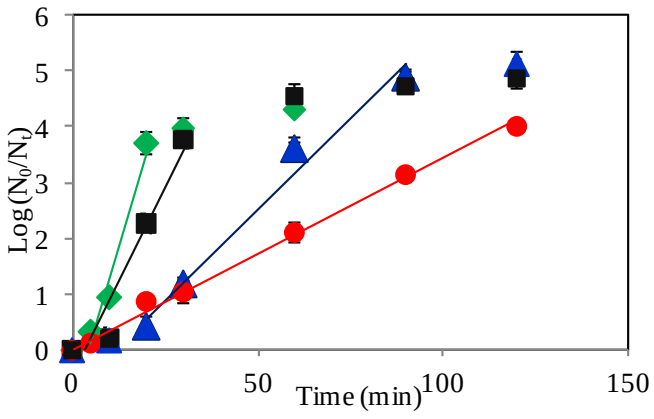

(a)

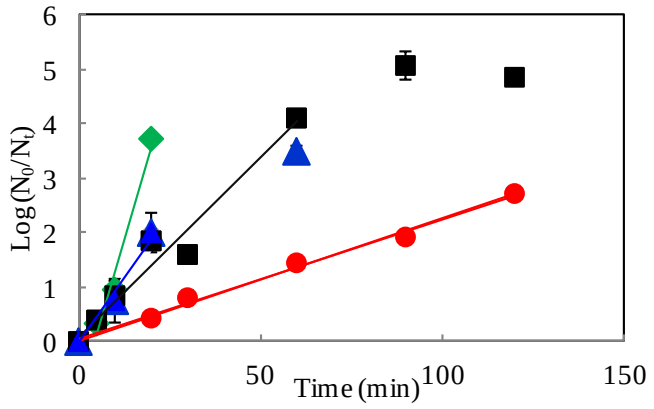

(b)

Figure 3.18 – UV-A/B TiO_2 photocatalysis inactivation curve of *E. coli* (a) and *P. putida* CP1 (b) in aqueous media in ¼ Strength Ringers solution (◆), Milli-Q water (▲), Tap water (■) and PBS (●).

Statistical analysis using two-way-ANOVA determined highly significant differences in inactivation rates dependent upon (1) aqueous media composition ($p=0.000$), (2) microorganisms ($p=0.000$) and (3) interactions between organisms and aqueous media ($p<0.000$). Post-Hoc Tukey's test, showed that inactivation rates were quicker in Ringers, followed by Milli-Q, Tap water and lastly by PBS (Table 3.23).

Table 3.23 – Inactivation rates of free-swimming *E. coli* and *P. putida* CP1 during photocatalytic disinfection in aqueous media.

Organism	Milli-Q water	Phosphate Buffer Saline (PBS)	1/4 Strength Ringers solution	Tap water
E. coli (DSMZ 498)	0.080 (±0.006)	0.034 (±0.005)	0.231 (±0.004)	0.149 (±0.011)
P. putida CP1	0.095 (±0.003)	0.025 (±0.003)	0.187 (±0.003)	0.069 (±0.004)
Test Between-Subjects Effects tested by ANOVA-two-way: Organism p=.000; Medium p=.000; Organism*Medium p<.000.				

3.3.2 TiO_2 photocatalysis of aggregated cells

Aggregated cells of *P. putida* CP1 were challenged by photocatalysis. The aggregated cells were present in minimal medium as before and so the response of free-swimming cells of *P. putida* CP1 in minimal medium to photocatalysis was first determined.

3.3.2.1 The response of free-swimming cells of P. putida CP1 in minimal medium to photocatalysis

Assessment of the survival of free-swimming *P. putida* CP1, following incubation with TiO_2 nanoparticles and under light conditions, was carried out in minimal medium. The photochemical reactor was inoculated with 10^7cell/ml of free-swimming bacteria *P. putida* CP1 and received 1.0 g/l of TiO_2, then stirred and samples were taken at different time intervals up to 240 minutes. Survival of bacteria following photocatalytic treatment was assessed by culturability and viability methods. Results of the culturability method are shown in Table 3.24. At the end of 120 minutes, a 5-Log inactivation of free-swimming *P. putida* CP1 was observed. A 24 hours dark incubated sample showed the presence of the same number of cells. There was no significant reduction in cell numbers in the dark control. While the viability of the cells was reduced following treatment, a residual (~23%) percentage of the cells remained viable at the end of exposure to

photocatalytic treatment at 120 minutes and also following 24 hours of incubation in the dark (Figure 3.19).

An inactivation curve of the plate count data showed a lag (shoulder area) of up to 10 minutes (Figure 3.20). The value of the inactivation rate which was computed between 10 and 60 minutes was $0.062(\pm 0.003)min^{-1}$. Rates of inactivation in minimal medium and in other aqueous matrices (Milli-Q water, Ringers solution, PBS and Tap water) were compared by analysis of variance one-way was and showed a highly significant difference between the media ($p<0.000$). Tukey's test classified the inactivation rate values as being quickest in Ringers solution, followed by Milli-Q water, then tap water and minimal medium. The slowest inactivation rate was obtained with PBS.

Table 3.24 – UV-A/B TiO_2 photocatalytic disinfection of free-swimming *P. putida* CP1 in minimal medium aqueous medium.

Time (min)	Counts (cfu/ml)
0	$2.58(\pm 0.68)x10^{7}$
1	$6.20(\pm 1.92)x10^{6}$
3	$5.80(\pm 1.92)x10^{6}$
5	$6.00(\pm 1.87)x10^{6}$
10	$6.00(\pm 2.35)x10^{6}$
15	$3.80(\pm 1.92)x10^{6}$
30	$3.40(\pm 3.88)x10^{5}$
60	$9.60(\pm 2.88)x10^{2}$
90	$1.20(\pm 1.64)x10^{2}$
120	$1.80(\pm 2.17)x10^{2}$
24 hours dark repair	$3.60(\pm 0.27)x10^{2}$

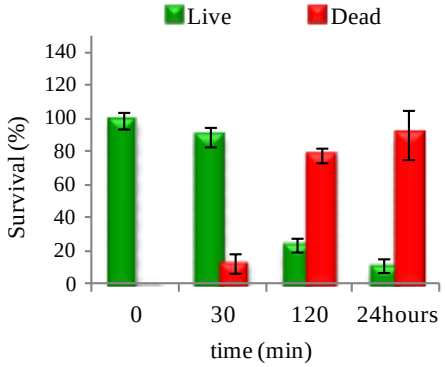

Figure 3.19 – Percentage of survival of *P. putida* CP1 as determined by LIVE/DEAD® Bacterial Viability Kit (*Bac*Light™) during photocatalytic treatment in the presence of 1g/l of TiO_2 in minimal medium.

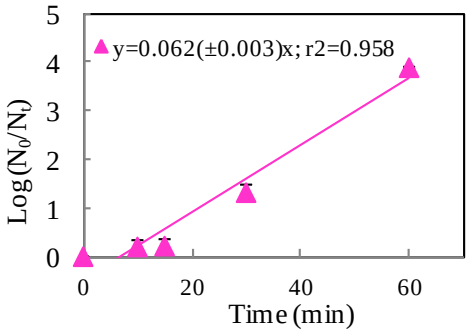

Figure 3.20 – UV-A/B TiO_2 photocatalysis inactivation curve of *P. putida* CP1 in minimal medium with 1 g/l of TiO_2 (▲).

3.3.2.2 Growth and viability of aggregated cells following photocatalysis

Photocatalytic treatment was performed by adding 1 g/l of TiO_2 to minimal medium containing aggregated cells (~10^8cell/ml). Then the cells and the catalyst were exposed to UV-A/B wavelengths and the reactor was sampled overtime up to 6 hours of exposure. The evaluation of survival following photocatalytic treatment was performed by culturability and viability methods. The samples were spread over nutrient agar plates and growth was checked following overnight incubation. Results which were interpreted as density of growth on the plates show no significant change in growth after 3 hours treatment (Table 3.25). There was a significant reduction in cell numbers, estimated at a 5-Log reduction, after 6 hours treatment and a similar level of growth was observed following 24 hour dark repair.

When cell viability of the aggregates was determined, approximately 80% viability was detected prior to treatment. A drop in viability to 45% was determined after 3 hours treatment and this level of viability did not change even following 24 hour dark repair (Table 3.26).

Table 3.25 – Culturability of aggregated cells of *P. putida* CP1 during photocatalytic treatment. 0.1 ml spread on nutrient agar plates.

Time (hours)	Density of agar plates and pictures.		Estimated Log reduction
0	TNTC all covered plates		0
3	TNTC all covered plates		0
6	TNTC > 300		5
24 hours dark repair	TNTC > 300		5

Table 3.26 – Percentage of viable cells in aggregates of *P. putida* CP1 following UV-A/B disinfection as determined by the LIVE/DEAD® Bacterial Viability Kit (*Bac*Light™).

Time (min)	Viability (%)
0	77.48(±10.3)
180	45.22(±11.9)
360	50.58(±2.30)
24 hours dark repair	45.34(±11.3)

The results of culturability and viability of the aggregated cells indicated that while there was a considerable reduction (~5-Log) in both viability and culturability after 6 hours treatment, total kill was not achieved.

A clear association between nanoparticles and the aggregated cells was evident when they were observed by phase-contrast microscopy. This association made sizing of the aggregates difficult, however microscopic observations show a clear reduction in the size of the aggregates after treatment (Figure 3.21). The inclusions, previously observed, also showed disruption (Figure 3.22). Observation of the aggregates using multistaining with epifluorescence microscopy confirmed the close association of the nanoparticles with the aggregates (Figure 3.23). The presence of the nanoparticles interfered with observations of the biochemical components. Photocatalytic treatment did not alter the initial pH value (~6.7) or the initial dry-weight (1.11 ±0.06) mg/ml.

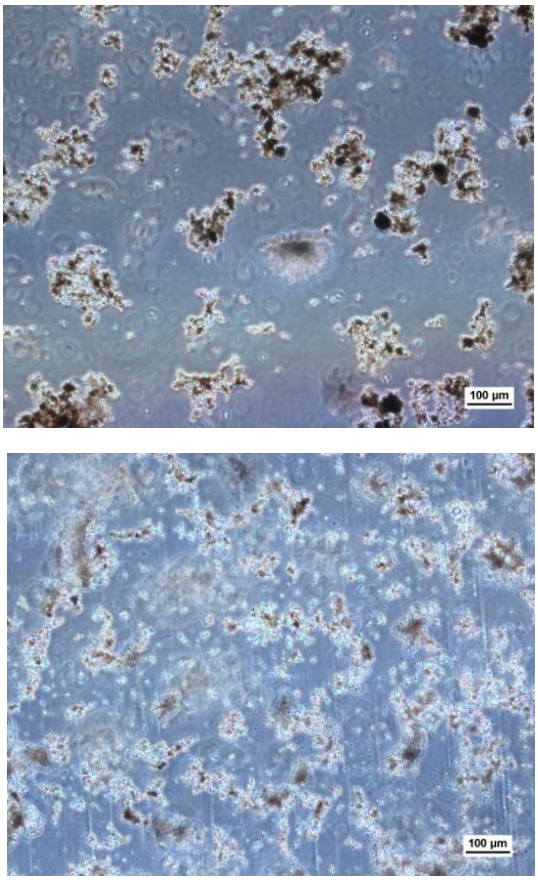

(a)

(b)

Figure 3.21 – Phase-contrast of aggregated cells of *P. putida* CP1 at 10X magnification following photocatalytic disinfection at t=0 h (a) and at t=6 hours (b).

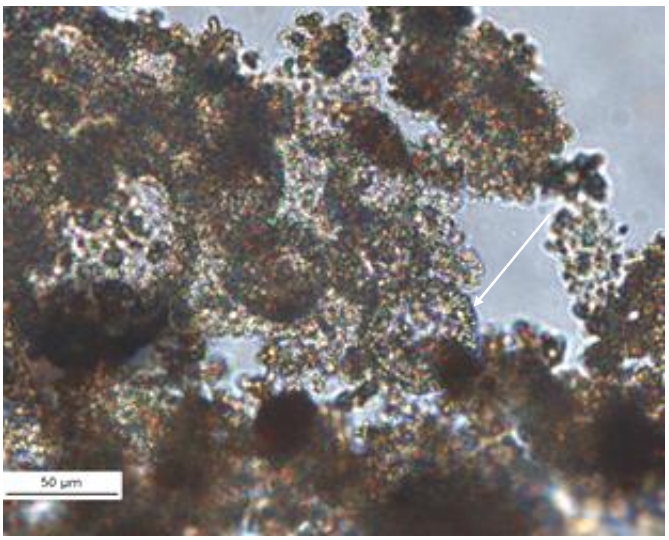

Figure 3.22 – Phase-contrast at 40X of aggregated cells of *P. putida* CP1 following 6 hours photocatalytic disinfection detail of an inclusion destroyed. White arrow indicating inclusion semi-destroyed.

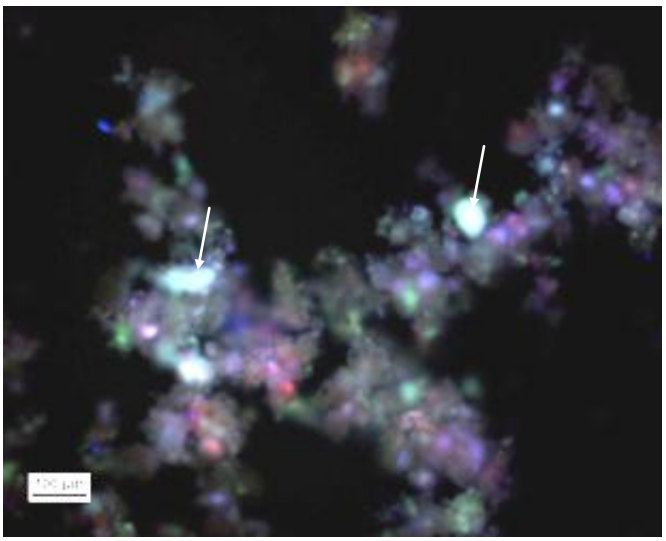

Figure 3.23 – Epifluorescence multistaining microscopy at 10X of aggregated cells of *P. putida* CP1 following 3 hours of photocatalytic treatment. The TiO_2 nanoparticles interactions with aggregates are indicated by white arrows.

3.4 Photodynamic inactivation of bacteria

Photodynamic inactivation of free-swimming and aggregated cells of *P. putida* CP1 was investigated. The response of free-swimming *P. putida* CP1 cells and aggregated cells of *P. putida* CP1 to Rose Bengal was studied in various media. The visible light source was a miniaturised LED system equipped with 100 light-emitting diodes at 525 nm and the reactors used included disposable or glass Petri dishes (90 mm diameter).

3.4.1 Photodynamic inactivation of free-swimming P. putida CP1 cells by Rose Bengal

Photodynamic inactivation of free-swimming *P. putida* CP1 cells (10^6cell/ml) by Rose Bengal (10 to 100 µg/ml) in quarter strength Ringers solution was studied in Petri dishes which were irradiated by an LED device and stirred. Samples were taken at time intervals and the maximum exposure time varied up to 120 minutes. Dark controls were carried out simultaneously. It was noted that the cells aggregated after 90 minutes incubation in both the light and dark treatments for all concentrations of Rose Bengal, except in the case of 10 µg/ml (Table 3.27). Undiluted bacterial samples were checked for growth using the drop-plate technique. Presence and absence of growth was noted using (+) or (-) symbols, and when possible, individual colonies on the drops were quantified (Table 3.28). The most effective concentration of Rose Bengal to enhance kill with light was 10 µg/ml. Inactivation of free-swimming bacteria at 10 µg/ml under light conditions took place at 45 minutes. The bacteria were also killed in the dark controls but at a slower rate. There was no survival following overnight incubation with the light treatment. There was recovery of the cells in the dark at low concentrations but not at high.

Table 3.27 – Aggregative behaviour of free-swimming *P. putida* CP1 following photodynamic inactivation with Rose Bengal (0-100 µg/ml) in ¼ Strength Ringers solution.

	Dose (J/cm^2)	0	0.48	0.97	1.46	2.93	3.90	NA
Experimental conditions	**Time (min) / [µg/ml]**	**0**	**15**	**30**	**45**	**90**	**120**	**24hours dark repair**
Light	**0**	○	○	○	○	○	●	●
	10	○	○	○	○	○	○	○
	50	○	○	○	○	●	●	●
	100	○	○	○	○	●	●	●
Dark	**0**	○	○	○	○	○	●	●
	10	○	○	○	○	○	○	○
	50	○	○	○	○	●	●	●
	100	○	○	○	○	●	●	●

Aggregation (●), no aggregation (○).

Table 3.28 – Photodynamic inactivation of free-swimming *P. putida* CP1 in ¼ Strength Ringers solution with Rose Bengal (0-100 µg/ml).

	Dose (J/cm^2)	0	0.48	0.97	1.46	2.93	3.90	NA
Experimental conditions	**Time (min)** / **[µg/ml]**	**0**	**15**	**30**	**45**	**90**	**120**	**24 hours dark repair**
Light	**0**	+	+	+	+	+	+	+
	10	+	+	+	4-Log reduction	-	-	-
	50	+	+	+	+	-	-	-
	100	+	+	+	+	+	+	-
Dark	**0**	+	+	+	+	+	+	+
	10	+	+	+	+	2-Log reduction	-	+
	50	+	+	+	+	4-Log reduction	4-Log reduction	-
	100	+	+	+	+	+	+	-
Growth (+), no growth (-).								

The response of the free swimming bacterium was further investigated at a concentration of 10 µg/ml Rose Bengal in Phosphate Buffered Saline and in distilled water (Table 3.29). Aggregation was noted in PBS at 60 minutes in the dark with no sensitiser. There was also aggregation in distilled water with light and no sensitiser. There was no reduction in growth in any treatment except in the case of distilled water in the presence of the sensitiser (Table 3.30). There was however a similar response in this case in both light and dark treatments. In the distilled water treatment in the dark without sensitiser there was evidence of kill following in the sample irradiated for 60 minutes and then incubated for 24 hours. This was not the case for the related treatment exposed to light which may have been due to the aggregation of the cells in this treatment.

Table 3.29 – Aggregative behaviour or free-swimming *P. putida* CP1 following photodynamic inactivation with 10 µg/ml of Rose Bengal in aqueous media.

	Dose (J/cm^2)	**0**	**0.48**	**0.97**	**1.46**	**1.98**	**NA**
Experimental conditions	**Time (min)** / **[µg/ml]**	**0**	**15**	**30**	**45**	**60**	**24 hours dark repair**
PBS (dark)	**0**	○	○	○	○	●3.86 (±4.50) $x10^{2*}$	●
PBS (light)	**0**	○	○	○	○	○	○
PBS (light)	**10**	○	○	○	○	○	○
PBS (dark)	**10**	○	○	○	○	○	○
Distilled water (dark)	**0**	○	○	○	○	○	○
Distilled water (light)	**0**	○	●	●	●	●7.21 (±1.64)x 10^{2*}	●
Distilled water (dark)	**10**	○	○	○	○	○	○
Distilled water (light)	**10**	○	○	○	○	○	○

Aggregation (●), no aggregation (○). *Size of aggregates (μm^2).

Table 3.30 – Photodynamic inactivation of free-swimming *P. putida* CP1 by Rose Bengal (at 10 µg/ml) in aqueous media.

	Dose (J/cm^2)	**0**	**0.48**	**0.97**	**1.46**	**1.98**	**NA**
Experimental conditions	**Time (min) / [µg/ml]**	**0**	**15**	**30**	**45**	**60**	**24 hours dark repair**
PBS (dark)	**0**	+	+	+	+	+	+
PBS(light)	**0**	+	+	+	+	+	+
PBS (light)	**10**	+	+	+	+	+	+
PBS (dark)	**10**	+	+	+	+	+	+
Distilled water (dark)	**0**	+	+	+	+	+	+/-
Distilled water (light)	**0**	+	+	+	+	+	+
Distilled water (dark)	**10**	+	+/-	+/-	+/-	+/-	+/-
Distilled water(light)	**10**	+	+/-	+/-	+/-	+/-	+/-

Growth (+), reduced growth (+/-).

3.4.2 Photodynamic inactivation of aggregated cells

The aggregated bacteria were present in minimal medium and so free-swimming cells of *P. putida* CP1 were first investigated for their response to Rose Bengal in minimal medium. The cells were exposed to the 525 nm LED system at various concentrations of Rose Bengal for up to 6 hours (Table 3.31). There was no evidence of photodynamic inactivation of *P. putida* CP1 free-swimming cells in any of the conditions tested, under light, under dark, with and without sensitiser and in overnight samples with and without sensitiser. Aggregation of *P. putida* CP1 in minimal medium was not observed in the presence of any concentration of Rose Bengal tested.

Table 3.31 – Photodynamic inactivation and aggregative behaviour of free-swimming *P. putida* CP1 in minimal medium with Rose Bengal (0-100 µg/ml).

	Dose (J/cm^2)	**0**	**0.48**	**0.97**	**1.46**	**1.98**	**3.90**	**5.86**	**9.77**	**11.72**	**NA**
Experimental conditions	**Time (min)** / **[µg/ml]**	**0**	**15**	**30**	**45**	**60**	**120**	**180**	**300**	**360**	**24 hours dark repair**
Light	**0**	+○	+○	+○	+○	+○	+○	+○	+○	+○	+○
	10	+○	+○	+○	+○	+○	+○	+○	+○	+○	+○
	50	+○	+○	+○	+○	+○	+○	+○	+○	+○	+○
	100	+○	+○	+○	+○	+○	+○	+○	+○	+○	+○
Dark	**0**	+○	+○	+○	+○	+○	+○	+○	+○	+○	+○
	10	+○	+○	+○	+○	+○	+○	+○	+○	+○	+○
	50	+○	+○	+○	+○	+○	+○	+○	+○	+○	+○
	100	+○	+○	+○	+○	+○	+○	+○	+○	+○	+○

Aggregation (●), no aggregation (○), growth (+).

When aggregated cells of *P. putida* CP1 underwent photodynamic inactivation in the presence of Rose Bengal (50 and 100 µg/ml) driven by irradiation of a visible light LED source at 525 nm there was still growth even after 6 hours irradiation. Growth was also observed in the 6 hours samples following 24 hours incubation in the dark (Table 3.32). A reduction in aggregate size was observed in the treatments exposed to light and the effect was most marked in the presence of 50 µg/ml of Rose Bengal (Table 3.33). When the uptake of Rose Bengal by the aggregated cells was monitored spectrophotometrically it was found to be most significant at 50 µg/ml of Rose Bengal (Table 3.34). Images of the biomass observed with epifluorescence microscopy showed the attachment of the Rose Bengal to the aggregates (Figure 3.24).

Table 3.32 – Growth of aggregated cells of *P. putida* CP1 following photodynamic inactivation with Rose Bengal (0-100 µg/ml) in minimal medium.

	Dose (J/m^2)	**0.00**	**1.98**	**5.86**	**11.72**	**NA**
Experimental conditions	**Time (min) / [µg/ml]**	**0**	**60**	**180**	**360**	**24 hours dark repair**
Light	**0**	+	+	+	+	+
	50	+	+	+	+	+
	100	+	+	+	+	+
Dark	**0**	+	+	+	+	+
	50	+	+	+	+	+
	100	+	+	+	+	+

Growth (+).

Table 3.33 – Size of aggregates in μm^2 of *P. putida* CP1 following photodynamic inactivation with Rose Bengal (0-100 µg/ml) in minimal medium.

	Dose (J/m^2)	0.00	1.98	5.86	11.72
Experimental conditions	Time (min) / [µg/ml]	0	60	180	360
Light	0	$3.04(\pm2.63)x10^4$	$4.27(\pm9.31)x10^4$	$9.44(\pm1.47)x10^3$	$1.03(\pm5.05)x10^3$
	50	$1.16(\pm2.38)x10^6$	$5.66(\pm5.16)x10^5$	$6.14(\pm7.30)x10^5$	$8.84(\pm19.5)x10^5$
	100	$1.10(\pm0.85)x10^5$	$1.63(\pm2.60)x10^5$	$1.05\pm(1.55)x10^5$	$4.29(\pm4.33)x10^4$
Dark	0	$5.04(\pm3.32)x10^4$	$1.28(\pm3.05)x10^4$	$1.30(\pm1.37)x10^4$	$1.64(\pm3.37)x10^4$
	50	$8.12(\pm9.06)x10^5$	$1.27(\pm8.12)x10^5$	$3.73(\pm1.73)x10^5$	$1.01(\pm1.41)x10^4$
	100	$4.12(\pm7.58)x10^4$	$1.12(\pm0.81)x10^5$	$9.40(\pm110)x10^4$	$5.58(\pm7.13)x10^5$

Table 3.34 – Percentage of Rose Bengal uptake by the biomass of aggregated cells of *P. putida* CP1 following photodynamic inactivation in minimal medium.

	Dose (J/m^2)	0.00	1.98	5.86	11.72
Experimental conditions	Time (min) / [µg/ml]	0	60	180	360
Light	50	25.37±0.60	51.22±3.00	58.37±1.81	67.97±4.56
	100	4.81±0.57	15.97±10.08	13.45±0.50	13.29±2.52
Dark	50	35.12±1.43	56.56±4.25	51.50±0.21	58.96±5.24
	100	14.29±0.84	13.45±0.09	13.45±0.50	14.29±2.50

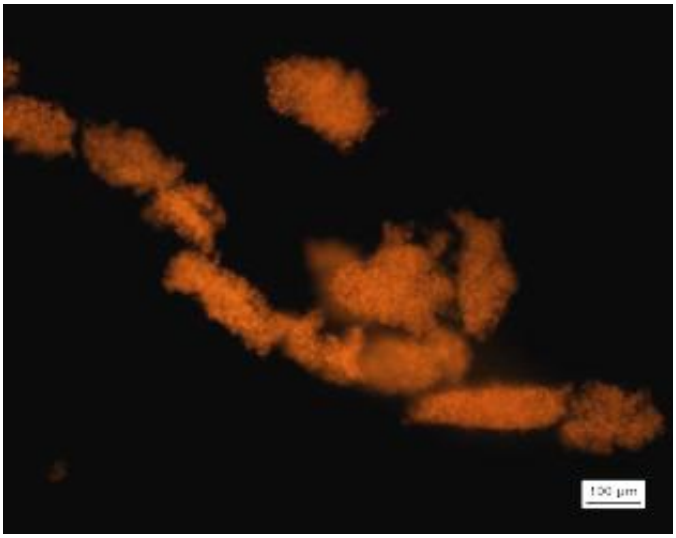

(a)

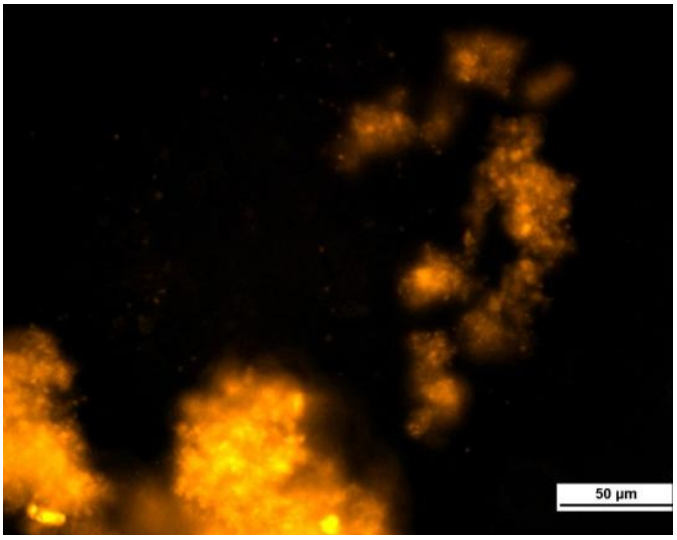

(b)

Figure 3.24 – Epifluorescence microscopy of aggregated cells of *P. putida* CP1 following photodynamic inactivation with Rose Bengal (50 µg/ml). At 10X at t=0 h (a) and at 40X at t=6 hours of incubation in the dark (b).

In Figure 3.25 the absorption of Rose Bengal in the supernatant over-time is given. The absorbance ratio of Rose Bengal present in the supernatant of aggregated cells treated by PDI showed no changes under light and dark exposure independent of the concentration tested (50 µg/ml or 100 µg/ml). The analysis of absorbance ratio (Figure 3.26), calculated with Equation 4, indicated that the Rose Bengal was predominant removed by aggregated cells as a biosorptive processes.

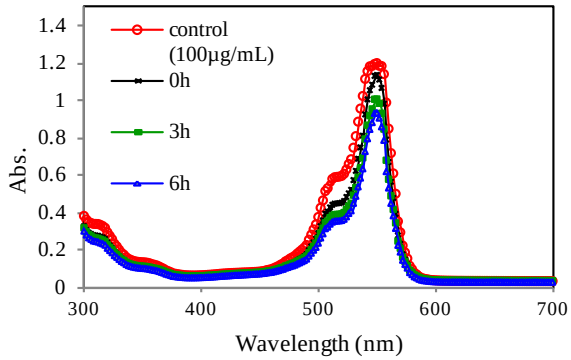

Figure 3.25 – Absorption spectrum of supernatant of aggregated cells and Rose Bengal (50 µg/ml) upon 6 hours of photodynamic inactivation treatment.

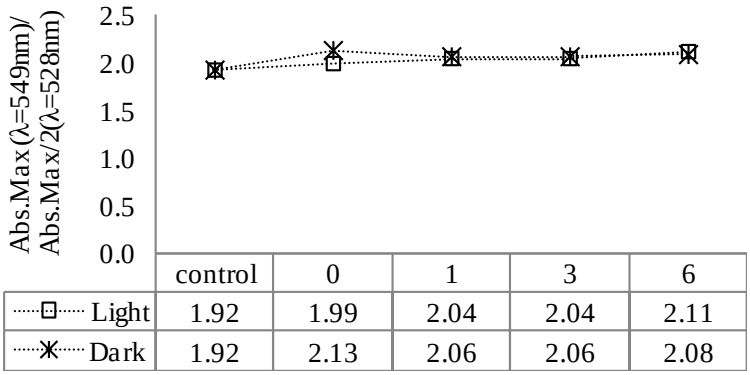

	control	0	1	3	6
Light	1.92	1.99	2.04	2.04	2.11
Dark	1.92	2.13	2.06	2.06	2.08

Figure 3.26 – Absorption ratio of Rose Bengal (50 µg/ml) in the supernatant of aggregated cells upon 6 hours of photodynamic inactivation treatment.

4 Main Findings

4 Main findings

UV-C disinfection

- Phosphate Buffered Saline, ¼ Strength Ringers solution, Milli-Q water and minimal medium were suitable aqueous media for UV-C disinfection studies. Tap water was not a suitable medium as it did not allow bacterial survival and therefore it could not be used as an aqueous medium in the UV disinfection studies.

- The time for total inactivation of 10^6cell/ml of planktonic forms of *E. coli* and *P. putida* CP1 was less than 10 seconds using UV-C (7.3 mJ/cm^2).

- Rates of inactivation of 10^6cell/ml free-swimming bacteria in the UV-C studies in PBS, Ringers and Milli-Q water were between ~1.01 cm^2/mJ and ~1.14 cm^2/mJ and were similar for *E. coli* and *P. putida* CP1.

- The inactivation rate of the 10^7cell/ml *P. putida* CP1 in Ringers was significantly lower (~0.87 cm^2/mJ).

- Dark repair (1-Log) was observed when 10^7cell/ml (*P. putida* CP1 in Ringers) following 20 seconds (14.6 mJ/cm^2) of UV-C disinfection and overnight incubation in the dark. Viability was partially lost (38%) after 20 seconds of treatment and recovered (up to 86%) following overnight incubation.

- Inactivation of free-swimming 10^6 and 10^7cell/ml of *P. putida* CP1 in minimal medium took, respectively, 10 and 60 seconds (7.3 - 43.8 mJ/cm^2). The rates of inactivation for both inoculum sizes were identical ~0.79 cm^2/mJ and they were significantly lower than in PBS, Ringers and Milli-Q.

- Dark repair in minimal medium (2-Log) was only observed with the inoculum size 10^7cell/ml, but not for 10^6cell/ml. Viability at the end of UV-C

disinfection of 10^7cell/ml in minimal medium was 47% with no recovery in the 24 hours dark repair sample.

- Aggregated cells 10^8cell/ml took 2 hours (5.256 mJ/cm^2) to be inactivated by UV-C disinfection. Dark repair was 2-Log. Viability was reduced but not totally lost following extensive UV-C exposure (6 hours) and, kept at the same level in the 24 hours dark repair sample. Aggregated cells presented inclusions. The initial size of aggregated cells (10^4 µm^2) was reduced by 1 order of magnitude following UV-C exposure. No detectable changes in the carbohydrate and protein fraction of EPS were observed following UV-C treatment.

UV-A/B disinfection

- The time for total inactivation of *E. coli* and *P. putida* CP1 (10^7cell/ml) in Phosphate Buffered Saline, ¼ Strength Ringers solution and Milli-Q water was between 15 and 60 minutes.

- Small-colony-variants occurred in all UV-A/B inactivation studies.

- The rates of disinfection varied between 0.15 min^{-1} and 0.25 min^{-1}. They were influenced by medium composition but not by microbial species.

- Dark repair, evaluated for *P. putida* CP1 in Ringers, was detected as 3-Log. Viability was partially lost (43%) after 120 minutes of UV-A/B and recovered (up to 49%) following overnight incubation.

- In minimal medium the time for total inactivation of 10^6 to 10^7cell/ml was between 30 and 60 minutes. There were no statistical differences between the rates of inactivation (0.14 min^{-1}) of both inoculum sizes.

- Dark repair, evaluated for *P. putida* CP1 (10^7cell/ml) in minimal medium was 3-Log. Viability was totally lost after 120 minutes of UV-A/B and it did not recover following overnight incubation.

- Time for total inactivation of aggregated cells in minimal medium was 4 hours. 1-Log dark repair was observed.

- Minor reduction of viability of aggregated cells was observed following 6 hours of treatment and in the 24 hours dark incubated sample.

- EPS of aggregated cells presented a ratio of carbohydrates and proteins as 4/1. The amounts of bound carbohydrates dramatically increased during UV-A/B exposure. No changes were observed in the other components of EPS.

- Propidium iodide detection increased during UV-A/B exposure indicating cell injury.

TiO_2 photocatalysis

- Phosphate Buffered Saline, ¼ Strength Ringers solution, Milli-Q water and Tap water were suitable to host photocatalytic studies.

- Total inactivation of *E. coli* and *P. putida* CP1 (10^7cell/ml) occurred only in Ringers solution following 90 and 60 minutes, respectively. In PBS, Milli-Q water and tap water the maximum inactivation was 5-Log which was achieved above 90 minutes for *E. coli* and 30 minutes for *P. putida* CP1.

- The rates of inactivation of free-swimming bacteria by photocatalytic disinfection were between ~0.025 min^{-1} and 0.231 min^{-1}. They were highly significantly different depending on aqueous media composition and microbial strain. Inactivation occurred more rapidly in Ringers, followed by Milli-Q, Tap water and lastly by PBS.

- Dark repair, evaluated in *P. putida* CP1 and in Ringers solution showed that the organism did not recover culturability after 24 hours of overnight incubation in the dark.

- Viability decreased, evaluated for *P. putida* CP1 in Ringers solution, showed that only 3% of cells were viable following 120 minutes of treatment and they were not viable in the overnight 24 hours dark incubated sample.

- In the presence of 1 g/l and in minimal medium, free-swimming *P. putida* CP1 did not experience culturability decay. The medium was then considered as suitable to host photocatalytic studies of both free-swimming and aggregated cells. Minimal medium exerted a highly significant influence in the rates of inactivation of *P. putida* CP1.

- The maximum inactivation of 10^7cell/ml of *P. putida* CP1 by photocatalysis in minimal medium was 5-Log reduction following 60 minutes of treatment. A residual 2-Log cell number value was found up to 120 minutes of treatment and in the overnight dark incubated sample.

- Viability of free-swimming cells of *P. putida* CP1 treated by photocatalytic treatment decreased to 23% at the end of treatment and recovery was not observed in the 24 hours dark incubated sample.

- Photocatalysis of aggregated cells of *P. putida* CP1 showed a maximum reduction of culturability of 5-Log after 6 hours of treatment. Growth after 24 hours of overnight incubation in the dark was observed.

- Viability of aggregated cells at time 0 was reduced considerably from 77% down to 45% following 3 hours of photocatalytic treatment.

- Although disruption of the aggregated cells was observed by phase-contrast microscopy, the fragmentation was not quantified as nanoparticles hampered sizing.

- An association of the aggregated cells and the TiO_2 nanoparticles and photocatalyst was observed by both phase-contrast and epifluorescence microscopy.

- Inclusions were present in the aggregates and there were evidence of their destruction following photocatalysis.

Photodynamic inactivation

- Rose Bengal at 10 µg/ml enhanced kill of free-swimming bacteria at 45 minutes with light, while kill in the dark took 60 minutes.

- In the dark, 50 µg/ml of Rose Bengal was the most toxic concentration tested.

- No survival after overnight incubation occurred at any concentrations with light and at 50 and 100 µg/ml in the dark.

- Free-swimming *P. putida* CP1 aggregated at 120 minutes under both light and dark conditions in all concentrations tested, except in both light and dark conditions with 10 µg/ml.

- In PBS, PDI of free-swimming bacteria with 10 µg/ml of Rose Bengal showed no kill occurred in any conditions tested including the overnight sample. Aggregation was noted at 60 minutes in the dark with no sensitiser.

- In distilled water and with 10 µg/ml of Rose Bengal, the bacterium survived poorly after 15 minutes. In the absence of the sensitiser the organism survived well up to 60 minutes. Aggregation occurred in the absence of RB after 15 minutes of light exposure. Growth overnight was only detected in the absence of RB.

- Photodynamic inactivation was not achieved with free-swimming *P. putida* CP1 and 10, 50 or 100 µg/ml Rose Bengal in minimal medium.

- PDI of aggregated cells did not take place in minimal medium with either 50 or 100 µg/ml. No kill in the dark took place.

- Fragmentation of aggregates occurred under light exposure alone, but not in the dark. Considerable disruption of aggregates occurred with 50 µg/ml of Rose Bengal under light exposure but not in the dark.

- Changes in the size of aggregates with 100 µg/ml of Rose Bengal did not occur under light exposure, but size increased considerably in the dark.

- Aggregated cells presented a high affinity for Rose Bengal. Decay of remaining colour was higher under light exposure when in comparison to dark exposure.

- Rose Bengal was found to be a highly potent EPS marker which allowed visualization of EPS in both aggregated cells and free-swimming cells present in solution.

5 Discussion

5 Discussion

The suitability of aqueous media for ultraviolet disinfection of *E. coli* (DSMZ 498) and *P. putida* CP1 bacteria was investigated. To do this, five aqueous media (Milli-Q water, ¼ Strength Ringers solution, Phosphate Buffered Saline, tap water and minimal medium) were used. This variety of aqueous matrices aimed to offer a range of conditions to elucidate whether the medium composition interfered with the survival of bacteria in the dark and with light treatments. All media were found to be suitable except tap water. The use of buffers as aqueous environments is recommended in photodisinfection studies of bacteria. They act to prevent loss of culturability of bacteria during UV treatment. UV disinfection studies have been reported using sodium phosphate buffer 0.01 M (Zimmer and Slawson, 2002), quarter strength Ringers solution (Chan and Killick, 1995), phosphate buffer saline (Lakretz *et al.*, 2010; Pinggui *et al.*, 2009) and sterile buffered water (Chang *et al.*, 1985).

In Tap water, the culturability of both *E. coli* and *P. putida* CP1 free-swimming cells decreased following inoculation. Tap water is chlorinated in Ireland. According to the Environmental Protection Agency in Ireland, all drinking water delivered to final consumers ought to be chlorinated with a dose of 15 mg/min/l of chlorine (Environmental Protection Agency, 2011). The loss of culturability of the bacteria is attributed to the residual chlorine. A similar reduction in culturability of *E. coli* O157:H7 was found by Zhao and Matthews (2000) when they tested the susceptibility of the organism suspended in PBS with various concentrations of free-chlorine (50-200 ppm or mg/l).

Ireland *et al.*, (1993) have suggested that tap water is not suitable for use in photocatalytic studies if it is not previously dechlorinated. Instead of dechlorinating the tap water, it was of the interest in the present work to use it *in natura*. In a hypothetical condition, where one of the photodisinfection treatments hereby proposed was applied as a "point-of-use" treatment to chlorinated tap water, dechlorination of tap water was unlikely to occur. Therefore, it was relevant to

evaluate the synergetic effects of this medium with the photodisinfection treatments proposed.

Minimal medium used in this work has offered an appropriate environment to produce aggregated cells of *P. putida* CP1 in the presence of fructose. Moreover, it may also have played a role of a 'simulated real water matrix'. The diverse mineral content of this medium includes phosphates, potassium, magnesium, sulphate and iron, amongst others. These components of minimal medium are in ppm fractions which may find similarities with the groundwater composition in Ireland (Environmental Protection Agency, 2006). In this way, minimal medium application as a possible simulated water matrix to test new photodisinfection treatments was of great interest. Furthermore, the use of simulated water matrices has been supported by previous studies (Mamane-Gravetz and Linden, 2006; Mamane-Gravetz and Linden, 2005).

Representation of the inactivation of microorganisms is normally presented in terms of total number of inactivated cells per volume (Rengifo-Herrera *et al.*, 2008; Gumy *et al.*, 2006) , logarithm of the number of cells (Hara-Kudo *et al.*, 2006) , survival ratio in absolute value or percentage (Maness *et al.*, 1999) and log of the survival ratio (Lakretz *et al.*, 2010; Min *et al.*, 2005). As it is necessary to compare the performance of different systems, the total number of cells plotted by either time or dose is a useful way to display to what extent the initial inoculum was inactivated by the treatment. One should note for either expression of percentage or log reduction units, the extent of cells removal is not evident, as the real inoculum size variation is hidden by the log or percentage units' expression. Therefore, expression of cells number is defended as the clearest way to demonstrate and compare various photodisinfection treatments efficiencies (Mccullagh *et al.*, 2007). In this work both the number of cells and logarithm survival fraction, following UV treatments and photocatalytic disinfection, were presented.

Assessment of bacterial survival following ultraviolet disinfection studies is traditionally performed by the evaluation of culturability (Bohrerova and Linden, 2006b; Zimmer and Slawson, 2002). The method is widely used and standardised,

little biological material (sample) is needed for the analysis, and in the case of the pour-plate technique long incubation is possible without colony merging (Josset *et al.*, 2008). The plate count technique is a prevailing tool used to isolate microorganisms, obtaining them in pure cultures, classifying and identifying them and enumerating viable cells. The method is based on the assumption that a microbial cell is allowed to grow on a solid medium and form one single colony. The capacity of a cell to grow and form a colony depends basically upon the ability of the growing medium to satisfy the growth requirements of the cell, the length of incubation time, and whether every single cells besides being viable is also capable to grown and form a colony (Hattori, 1988). In the present work, three variants of the plate count method were used: the drop-plate (or Miles-Misra), the spread-plate and the pour-plate technique.

In UV-C studies, the pour-plate was largely employed whereas in UV-A/B and photocatalytic treatments the drop-plate was the most used method. This choice was in agreement with previous studies from Barbosa *et al.*, (1995) which verified the reliability of drop-plate (Miles-Misra) in comparison to pour-plate and spread-plate to count *E. coli* and *Beijerinckia derxii*. The drop-plate was adequate for counting *E. coli*; however the method was not adequate to quantify cluster-forming *B. derxii* (Barbosa *et al.*, 1995). The drop-plate method is also not recommended for counting microorganisms with swarming type of motility, such as *Proteus mirabilis, P. vulgaris,* and *Vibrio parahaemolyticus* (Herigstad *et al.*, 2001). During the study of UV-C disinfection of aggregated cells, the drop-plate method was not used to quantify the survival of aggregated *P. putida* CP1. The reason was that clusters of the bacteria would grow and fully cover the surface of the drop, therefore not allowing for a more accurate estimation of the remaining number of colonies.

Nevertheless, the drop-plate technique offers attractive advantages over spread or pour-plate techniques. For instance, less time is required to dispense drops than that required to spread plates, easier count of distinct groups of colonies in the drops (as opposed to counting contiguous numerous colonies), higher accuracy of the distribution of colonies in a small area of a drop when in comparison to larger areas

of a plate and material saving as less plates are required for the plating (Herigstad *et al.*, 2001).

Although the plate count method is widely used in the evaluation of disinfection studies, the method presents drawbacks too. The plate count method is an indirect observation of the metabolism of individual bacteria; therefore the unit used remains as the cfu/ml (colony-forming unit). In this way, cfu/ml is only an estimation of the number of total organisms. It includes only those bacterial cells which are capable to grow and form colonies. The disadvantage of this method, when used to assess efficiency of disinfection, is that it underestimates the presence of 'viable but nonculturable' (VBNC) bacterial cells. VBNC cells which were injured during disinfection treatment and are not able to grow may remain viable and infective. Other disadvantages of plate counts include merging of colonies, operator-dependent count and deadline reading results (Josset *et al.*, 2008).

Alternative approaches include direct observation methods such as epifluorescence microscopy and flow-cytometry. The counts of cells in this case occur directly and rapid results are obtained in a semi-automated or fully-automated manner (Josset *et al.*, 2008). A fluorochrome pair which is often used with epifluorescence microscopy is the LIVE/DEAD® Bacterial Viability Kit (*Bac*Light™). This kit evaluates the membrane integrity of bacterial cells with two stains, SYTO 9 and propidium iodide. The kit acts in a selective way in which the live cells are stained green (SYTO 9) but those that have injured membranes are stained red (propidium iodide). As damaged membranes are often associated with viability, cells with damaged membranes are stained red and are considered dead. Intermediate states of staining are possible and they are classified as "unknown" by the kit's manufacture's manual (http://probes.invitrogen.com/media/pis/mp07007.pdf).

The LIVE/DEAD® Bacterial Viability Kit (*Bac*Light™) added useful information during the investigation of the status of the membrane of cells following incubation in aqueous media, photodisinfection treatment or during evaluation of dark repair. The method has been recommended as an additional tool to the plate count in the investigations of the effect of UV-C and UV-A disinfection and photocatalysis on *E.*

coli cells (Pigeot-Rémy *et al.*, 2012). In the case of the survival of *P. putida* CP1 subsequent to the incubation in Tap water, the cells were no longer culturable and the Live/Dead method showed their membrane was greatly damaged. The fact that UV-C did not completely affect membrane integrity of *P. putida* CP1 photolysed in Ringers is likely to be the reason why not all the cells were stained red at the end of 14.7 mJ/cm^2 of treatment. It has been demonstrated elsewhere that although UV-C radiation rapidly disrupts DNA integrity, cell membranes are less affected (Suehiro *et al.*, 2003). They showed by using dielectrophoretic impendence measurements, that *E. coli* K12 cells, treated by 25 mJ/cm^2 of UV-C had lost culturability although they presented intact cell membranes.

Loss of viability of *P. putida* CP1 in minimal medium was caused by a prolonged UV-C exposure compared to exposure in Ringers. The organism lost membrane integrity after 10 minutes as determined by the detection of a population of orange and red cells. The orange emission is a feature of a mixture of green and red emissions and indicates membrane damage (Josset *et al.*, 2008). Part of these damaged cells showed dark repair overnight. An important drawback of the Live/Dead method used with epifluorescence microscopy is the occurrence of unknown states. Berney *et al.*, (2007) highlighted that "unknown" states hampers routine evaluation of microbiological quality of water.

The findings of the present work suggest that the Live/Dead method is not sufficient to be used as a single tool in the evaluation of damage caused to bacterial cells by UV-C disinfection. The extent of damage of membrane was observed to be relatively dependent on the dose and the medium composition. Another drawback of the method is that it became unreliable depending of the number of fields observed for a single experiment and the number of samples counted, disadvantage also noted by Josset *et al.*, (2008).

P. putida CP1 demonstrated dark repair. Induction of dark repair of *P. aeruginosa* has been noted by detection of the expression of the rec*A* gene system. This took place after exposing of the microorganisms to UV-C fluence higher than 40 mJ/cm^2, which is the standard recommended for drinking water disinfection (Jungfer *et al.*,

2007). Although the authors did not discuss the recovery of culturability in their study with *P. aeruginosa*, they warn of the possibility of activation of repair systems in pathogenic bacteria species with relevance for drinking waters. If *P. putida* CP1 had similar mechanisms of repair to that of *P. aeruginosa* it is possible that, at the comparatively lower UV dose applied to the organism, dark repair was also able to arise.

Dark repair by *P. putida* CP1 was particularly evident in minimal medium. Minimal medium was a turbid medium with high UV absorptivity which could account for the protection of cells from UV-C. Even by increasing the UV-C dose delivered to minimal medium and free-swimming *P. putida* CP1, as was carried out for the inoculum 10^7cell/ml, dark repair was still observed. Jungfer *et al.*, (2007) noted that injured bacteria may regenerate in water distribution systems particularly when they are aided by shading effects such as particles, aggregation or a mechanism of protection in biofilms They showed that the respiratory activity of biofilm bacteria in a water distribution system was greater following UV-C disinfection (40 mJ/cm^2) but not when chlorine dioxide was applied. They also suggested that UV disinfection should be applied with high standards to surface waters which are highly contaminated and turbid as is often the case in developing countries.

The influence of inoculum size on UV disinfection has been demonstrated by Abshire and Dunton (1981). They studied the inactivation of various inoculum sizes of *Pseudomonas aeruginosa* 10^6, $10^{7,}$ 10^8 cell/ml in saline solution and found that a 6-Log inactivation was achieved by UV-C doses of 18, 21 and 31.5 mJ/cm^2, respectively. In this study, significant statistical differences in the inactivation rates caused by the inoculum size were observed in Ringers though not in minimal medium indicating the importance of the aqueous medium in determining responses to photodisinfection.

Both *E. coli* and *P. putida* CP1 showed a 6-Log inactivation with UV doses in the order 5 – 8 mJ/cm^2. This was in keeping with other reports in the literature where UV doses to inactivate 10^6cell/ml of planktonic *E. coli* by monochromatic UV-C radiation were established between 1 and 15 mJ/cm^2 (Hijnen *et al.*, 2006). Chang *et*

al., (1985) demonstrated 5 to 6-Log inactivation of *E. coli* (ATTCC 11229) in sterile buffered water after 11 mJ/cm^2. Butler, Lund and Carlson (1987) demonstrated complete inactivation of an environmental *E. coli* isolate (10^7cell/ml) after a delivered UV-dose of 7 mJ/cm^2 and Zimmer and Slawson (2002) which showed a 5-Log inactivation *E. coli* (ATT 11229) after 10 mJ/cm^2. The response of *E. coli* and *P. putida* CP1 to UV-C treatment was similar. This similarity in response was also reported by Wu, Clevenger and Deng (2005) who showed that inactivation of 10^9cell/ml *P. putida* by UV-C, in low nutrient conditions at 14.7 mJ/cm^2, was ~5.1-Log while the same dose caused a 5.8-Log inactivation of *E. coli*.

Despite the similarity between the UV-C dose needed to inactivate *E. coli* and that reported in the literature, the inactivation rates obtained in this study were higher than reported. Values of inactivation rate found in this present work were between 1.1-1.3 cm^2/mJ; while in the review of Hijnen *et al.*, (2006) inactivation rates obtained during UV-C disinfection of various strains of *E. coli* were calculated as 0.506±0.049 cm^2/mJ with r^2=0.71 (r-squared values). This difference can be attributed to the methodology used in the measurement of the UV-C fluence-rate.

The inactivation curve of *P. putida* CP1 10^7cell/ml photolysed in minimal medium acquired a tailing aspect at higher fluence. Mamane-Gravetz and Linden (2004) pointed out that tailing is often associated with clumping of the organisms which prevents inactivation at higher fluences or to a variation in the sensitivity to UV by members of the population. Minimal medium has a variety of inorganic compounds (calcium chloride, magnesium chloride and iron sulphate). Iron and manganese, for instance, interfere in the UV transmittance of water (Bitton, 1994), whereas salts of calcium, iron and magnesium were found to form fouling in quartz/glass sleeves of photochemical reactors (Guerrero-Beltran and Barbosa-Cánovas, 2004; Blatchley III, 1997).

The presence of particles such as goethite (α-FeOOH) also significantly affected UV disinfection of *E. coli* as demonstrated by Youxian, Clevenger and Deng (2005). At the lowest concentration (~0.2 to 2.0 µm) of goethite particles the inactivation curve presented tailing at higher fluence <10 mJ/cm^2. Tailing during UV inactivation in

turbid waters was also observed by Cantwell and Hofmann *et al.*, (2008). The authors demonstrated that during inactivation of *E. coli* in unfiltered river water after an initial 2.5-Log inactivation (99.7%) tailing occurred. Resistance of the surviving part of the population, which was 20% superior, was related to protection by aggregation of organisms to each other or to particles (Templeton *et al.*, 2008).

P. putida CP1 is an interesting environmental isolate which has been studied in the laboratory for a number of years. The organism is non-pathogenic making it easy to handle avoiding any concerns associated with working with pathogens as outlined by (Lewandowski and Beyenal, 2007). The bacterium aggregates when grown under certain environmental conditions and so is a useful model organism for studying the response of aggregated cells to photodisinfection. Aggregated cells tend to be more resistant to environmental stress than their planktonic counterparts however few studies have been conducted on the response of aggregated cells to photodisinfection.

The estimation of the number of cells in aggregated *P. putida* CP1 was initially carried out by performing sonication, serial dilution and the pour plate method. The result obtained was similar to that of previous studies (Fakhruddin and Quilty, 2007). As a method of dispersion of aggregated cells, prior to cell counts, sonication presented drawbacks. The first is that after sonication, smaller aggregates were still present which could interfere with cell number determinations. Secondly, prolonged sonication time to improve dispersion of aggregates could lead to inactivation of some of the cells. Salhani and Uelker-Deffur (1998) warned that if sonication was utilized during quantitative determination of bacterial numbers in larger aggregates a compromise has to be made between incomplete disaggregation and destruction of single bacteria. Therefore, it was decided that sonication would not be used in this study. The size and number of the aggregates changed substantially during the UV-C treatment. This caused further problems in the enumeration of cells during treatment. Bohrerova and Linden (2006b) observed a highly variable number of cfu/ml during the UV-C treatment (0 and 60 mJ/cm^2) of aggregated cells of *Mycobacterium terrae* filtered through 100-, 41- and 20 µm Nylon filters.

The inactivation curve of aggregated cells during UV-C disinfection presented two regions. The first was characterized by a log-linear response with a k_1 value of 0.0048 cm^2/mJ. The second region, above 1314 mJ/cm^2, was characterized with a tailing response with a k_2 value of 0.0006 cm^2/mJ. The slower rate of disinfection of aggregated cells of *P. putida* CP1, when compared to free-swimming organisms, is in agreement with a recent report which found a superior chlorine resistance of detached biofilm clusters and biofilms when compared to planktonic cells (Behnke *et al.*, 2011). The tailing observed in the inactivation curve is expected as it is a phenomenon in which clumped organisms are protected from radiation. For instance in a study from Mamane-Gravetz and Linden (2004) tailing attributed to clumping was observed in inactivation of *Bacillus subtilis* (ATTC 663) spores at fluence higher than 60 mJ/cm^2. Tailing during UV-C response of aggregated cells is likely to be related with another factor, the size of the aggregates. As an example, Farnood (2005) showed that during UV-C disinfection by increasing the size of wastewater flocs the inactivation rate decreased. The correlation of that report with the present work is that at higher UV-C doses the remaining cells were most probably enclosed in more internal areas of larger aggregates.

From the culturability data, it can be interfered that aggregated cells were not impenetrable to UV-C as all cells lost culturability at the end of exposure. In total an estimated UV-C dose of 5256 mJ/cm^2 produced in 120 minutes by a 15 W low-pressure mercury lamp was sufficient to inactivate aggregated cells of *P. putida* CP1 ($6x10^8$cell/ml). Similar resistance to UV-C doses were found in biofilm bacteria attached to urinary catheters by Bak *et al.*, (2010). In that work a collimated beam device coupled with one 6 W low-pressure mercury bulb emitting in the UV-C line was used. In that study, the bulb was placed at 9 cm of distance from the surface of the catheters which received a fluence-rate of 400 $\mu W/cm^2$. In the present study the distance between the quartz immersion well, which separated the 15 W low-pressure mercury lamp from the bacterial suspension, and the outside wall of the annular reactor was 10 cm. The fluence-rate measured at that distance was 730 $\mu W/cm^2$. In this way, considering the centimetre difference between the 9 cm distance measured by Back *et al.*, (2010) and the 10 cm measured in the present work, the reactor setup hereby used presented roughly the double irradiance power. In this way, the

inactivation of aggregated cells by UV-C was relatively more difficult than that of the biofilm reported by Bak *et al.*, (2010) since both situations had a similar bacterial load of ~10^8cell/ml.

Viability of aggregates did not change significantly during UV-C exposure. This result may be explained by a number of different factors. The first is that rupturing of aggregates could have caused release of viable internalised cells or chunks of cells. That in turn could have accounted for an increase in the detection of live cells, even though UV-C was continuously inactivating other externally located cells. In this way, although cells were being inactivated, new "released cells" were increasing the live signal. Another factor which could have contributed to inconclusive results of live and dead stains and epifluorescent microscopy is the intrinsic limitations of the method. Epifluorescence microscopy analysis of aggregated cells registered the overall/averaged signal of live and dead emissions. The fact that aggregated cells had countless layers of cells, and that aggregates of various size were present, and that these cells were stained and emitted fluorescent signal simultaneously would account for very variable dead and live signal. This way, epifluorescent emission did not allow for an accurate quantitative monitoring of the percentage of live and dead cells.

Even under prolonged UV-C exposure aggregated cells remained viable. *P. putida* CP1 aggregated cells, which lost their culturability during the course of UV-C disinfection experiments, retained their viability. This might be also explained by an acquired increase in resistance to UV exposure. For instance, UV-adapted cells of *Bacillus subtilis* strain MW01 were shown to have increased UV-C resistance in all vegetative stages of growth and sporulation in relation to the control strain DE69 (Wassmann *et al.*, 2011).

The distribution of the live and dead populations within the aggregate was not clearly identified by the epifluorescence microscopy method employed. In previous research, Chen, *et al.*, (2007) demonstrated that the distribution of live and dead cells in aerobic granules changed with the size of the aggregates. For instance, aggregates of diameter <1000 µm presented fair amounts of dead and live cells throughout their structures. In opposition to this, greater aggregates presented more dead cells at the

core of their structure and both live and dead cells at the periphery. In the present study, there was no evidence that a standard distribution of live and dead cells occurred. For a more in depth study of the distribution of live and dead cells in aggregated cells of *P. putida* CP1, further studies would be required.

Information which was taken from the epifluorescent analysis is that part of the population remained viable after the treatment and overnight incubation. The usefulness of the epifluorescence method has previously been demonstrated for the analysis of viable and non-viable cells of bacterial in biofilm attachment to percutaneous implants (Oka *et al.*, 2008). In that study it appeared that only a few layers of cells were formed. Therefore, the visualization of single live and dead cells was feasible. But in the case of three-dimensional and more in depth structures, such as aggregated cells, the signal may be obscured by the successive layers of cells. Therefore, other microscopic methods may provide more detailed information. That way, in order to monitor the extent of UV-C damage caused to different depth sectors of the aggregates, confocal microscopy would be a more adequate method.

The aggregated cells were embedded in a matrix of extracellular polymeric substances or EPS. The matrix allows cells to be highly protected from UV, chlorine and other potential point-of use disinfectants. The importance of this resistance of aggregated cells is that, even if UV treatment is applied to a water supply, cells embedded in EPS, could remain alive in the water. Aggregation of *P. putida* CP1 was a factor which decreased UV-C disinfection efficiency in comparison to free-swimming cells of the organism. This result corroborates the findings of previous works in this field which stated that aggregation impairs disinfection (Bichai *et al.*, 2011; Bohrerova and Linden, 2006a).

Likewise biofilms, cells in aggregates are communities united by and embedded in an EPS matrix. The difference then is that aggregated cells are free-floating in the medium whereas biofilms are actually attached to a surface. Another essential difference is that in the environment biofilms are formed of multispecies. Moreover, there are differences regarding aging, layers and cell communication which is expected to be more complex in biofilms. However, from a biomechanical perspective, leaving aside ecological interactions, in both cases inner cells are more

protected from environmental stressors. Ultimately, aggregated cells and biofilm cells have an overall higher chance of survival when compared to free-swimming counterparts.

In this study, UV-C disinfection was found to cause disruption of aggregated cells. Disruption was not observed when the aggregated cells were stirred in the dark, which indicated that the aggregated bacterium presented some level of resistance to shearing forces. Heterogeneity was a feature of size distribution of intact aggregated cells of *P. putida* CP1 that was grown overnight in fructose and minimal medium. Phase-contrast microscopy showed average aggregate sizes of ~33,000 μm^2 (3.3 mm^2) with dimensions of ~700 x 300 µm (length x width). The size of the aggregates was very variable which was also observed by Stoodley *et al.*, (2001) when studying detached clumps of biofilm. As mentioned earlier the aggregated cells of *P. putida* CP1 were more difficult to inactivate than free-swimming bacteria. One of the reasons that confer higher resistance on aggregated forms of microbial species is the size of the aggregate (Behnke *et al.*, 2011).

During the first hour of UV-C treatment aggregate size was greatly reduced as was culturability. During the second hour, the average size remained unaltered and culturability decreased only slowly. The meaning of this finding is that during the first hour, single free-swimming cells among the aggregates, together with cells at the surface of the aggregates were inactivated by UV-C. The remaining cells, which were still culturable in the second hour, were probably the ones which were located in the depth of the aggregates. They were protected by many layers of external cells, by EPS and by minimum medium salts. That is the reason why they took longer to be inactivated. It is clear as well, that these cells were likely to be located inside aggregates of greater size ($>10^4$ μm^2) which were gradually disrupted by UV-C action during the first hours of treatment. As it has been observed from the data, in the second hour of treatment the average size of aggregates present was of smaller dimensions. Therefore the UV-C prolonged exposure during the second hour was enough to cross the smaller aggregates ($>10^3$ μm^2) reaching in depth protected cells.

During UV-C disinfection, both the free-swimming cells and the aggregated cells may have benefitted from the presence of cell debris from other photolysed cells. That debris could act as a carbon source and a physical barrier to UV. Regrowth or support of microbial growth by free-swimming cells following UV-C disinfection was observed by Tang, Dziallas and Grossart (2011). The authors treated freshwater zooplankton and bacteria applying UV dose of ~1.0 $x10^4$ mJ/cm^2. In that work, dark repair was evaluated after 2 or 3 days and there was a positive correlation between free-swimming recovery and presence of zooplankton. Bacterial recovery was significant in the presence of zooplankton and the authors attributed that to protection by aggregation and use of debris of the zooplankton as carbon source to aid in recover after UV treatment.

As mentioned before, the size of the aggregates of *P. putida* CP1 in this study was in the range ~700 x 300 µm (length x width). This is much smaller than aerobic granules of SBR (sludge-blanket reactor) where the diameter was found to be between 0.3-5.0 mm (Toh *et al.*, 2003). However, much larger than wastewater flocs which ranged between 45 to 150 µm (filtered fractions) (Farnood, 2005) and aggregates of single species, such *Mycobacterium terrae*, which ranged up to approximately ~100 µm (filtered fractions) (Bohrerova and Linden, 2006b).

The aggregates were found to harbour inclusions of approximately 50 µm of diameter. These structures which were more evident during UV-C treatment were also disrupted following the treatment. *P. putida* CP1 aggregates when grown on fructose but not on glucose. The formation of the inclusions is thought to be associated with fructose metabolism and substrate induced stress. The inclusions were not stained by the fluorochromes used during epifluorescence analysis. Calcofluor-white targeted β-polysaccharides, while FITC stained proteins (Chen *et al.*, 2007). This finding, while preliminary, suggests that carbohydrate and protein were not major components of these structures.

Quantification of both free and bound EPS fractions of aggregated cells was carried out during UV-C disinfection. The findings revealed that the EPS was composed mainly of protein followed by carbohydrates. That is expected from EPS

composition of microbial aggregates (Sheng *et al.*, 2010). However, EPS is known to vary immensely according to various features, such as microorganism species, shearing forces, nutrient and temperature conditions (Flemming and Wingender, 2010), analytical methods, growth conditions, bioreactor (Sheng *et al.*, 2010) and extraction methods (Eboigbodin and Biggs, 2008). The amount of total carbohydrate (7.62 mg/g) and proteins (10.65 mg/g) present in aggregated cells of *P. putida* CP1 were consistent with other research, which found overall summed amounts of carbohydrates and proteins similar to those of the present research (Scott *et al.*, 2005).

Biochemical analysis of EPS components showed no detectable changes in the carbohydrate and protein fractions following UV-C treatment. However, rupturing of the aggregates is an indication that UV-C caused structural changes of the EPS. In their paper, Espeland and Wetzel (2001) discussed denaturation of enzymes in biofilms upon absorption of UV-A and UV-B wavelengths. To support this finding they mentioned that according to Voet and Voet (1995) energy required to denaturate proteins is ~0.4 kJ/mol, whereas hydrogen bonds are broken by energy of about 20 kJ/mol (Voet and Voet, 1995). In addition, wavelengths between 300-700 nm have energy of 150-400 kJ/mol (Schwarzenbach, Gschwend and Imboden, 2002). Therefore, it is rational that UV-C photons, with shorter wavelengths and higher energies, may cause both protein denaturation and hydrogen bonds breaking. UV-C disinfection is efficiently absorbed by organic compounds with unsaturated bonds and which are composed of conjugated bonds. When a UV-C photon hits an electron of the conjugated bond, it is excited to a higher energy level (Cutler and Zimmerman, 2011). The destabilization of the electron-pair may distress the whole molecular structure and, therefore, cause conformational changes (Jagger, 1967).

The rupture of the EPS matrix of aggregated cells of *P. putida* CP1 supports previous research in the area which links absorption of UV radiation and EPS destruction. For instance, Lakretz, Ron and Mamane (2011) have shown that treatment of biofilms of *Pseudomonas aeruginosa* with UV/H_2O_2 prevented further colonization and disorganised the biofilm structure.

Another component of the EPS matrix which has an important structural role is extracellular DNA or eDNA (Flemming and Wingender, 2010). Data available from research conducted in this laboratory has found the presence of eDNA (extracellular) in aggregated cells of *P. putida* CP1, however, in lesser amounts than the protein and carbohydrate fractions. One possible further explanation for the disruption of aggregated cells of *P. putida* CP1 upon UV-C exposure is the alteration of the molecule of eDNA, and therefore their functions.

As distinct from UV-C disinfection, which showed quick inactivation rates in the order of seconds, the time taken to inactivate bacterial cells by UV-A/B disinfection was longer and took in the order of several minutes. These findings are supported by other studies which confirm that in fact UV-C has a superior bactericidal action (Pigeot-Rémy *et al.*, 2012) to UV-A and UV-B alone. As demonstrated by its emission spectrum, the medium-pressure mercury lamp used in the present work, to irradiate bacterial suspensions, produced multiple wavelengths in the UV-B, UV-A and the visible area. As the bulb was immersed in a Pyrex glass well, to allow cooling, wavelengths emitted bellow 300 nm, if any, were blocked. Therefore, even if UV-C germicidal radiation was produced by the medium-pressure bulb, it did not photolysed bacteria.

Under UV-A/B exposure damage to microbial cells was less likely to be caused by DNA photon absorption. Rather, cell membranes and proteins, which are targets of UV-A/B radiation, were more likely to be affected. That would be one of the reasons why the rates of disinfection of UV-A/B treatment were found to be different from what was reported in the UV-C section. Another significant point is the power and intensity of the lamps. Even though the power (400 W) and the intensity of UV-A/B lamp was greatly superior to the power and intensity of UV-C lamp (15 W-0.730 mW/cm^2), the most harmful effect-related to quicker loss of culturability was observed when the bacteria were exposed to UV-C germicidal wavelength. The medium-pressure mercury lamps required more electrical energy to be driven than the low-pressure UV-C lamps. But although UV-A/B lamp produced more intensity, and therefore more photons of energy, it was less efficient than the UV-C reactor to inactivate free-swimming cells. That difference is attributed to the energy of UV-C.

Direct exposure to UV-A may cause damage to bacteria by delaying growth and inducing cell membrane damage (Byrne *et al.*, 2011). Direct damage caused by exposure of bacteria to UV-A/B has been proposed as an effect of reactive oxygen species (ROS). Such species are generated from dissolved oxygen in water reacting in photochemical pathways with photosensitised intracellular molecules, and/or naturally occurring dissolved organic matter which can absorb between 320-400 nm (Byrne *et al.*, 2011). Sinha and Harder (2002) explains that UV-A causes photosensitising reactions with DNA sub-products and subsequently secondary damage to DNA by generation of reactive oxygen species and singlet oxygen. Furthermore, direct damage of enzymes by UV-A and UV-B has been reported by Espeland and Wetzel (2001).

When the inactivation rates of *E. coli* and *P. putida* CP1 by UV-A/B disinfection were compared, the response between the organisms was similar. Nevertheless, aqueous media caused high significant levels of differences between the inactivation rates by UV-A/B. Aqueous media composition has been shown to exert an influence on the response of bacteria to UV-A disinfection (Fernández and Pizarro, 1999) and solar disinfection (Rincón and Pulgarin, 2007). For instance, the protective effect of saline NaCl and/or $MgSO_4$ salts has been demonstrated during UV-A disinfection of *Pseudomonas aeruginosa* by Fernández and Pizarro (1999). Their study showed that at low concentrations these salts could protect bacteria from osmotic stress and were more resistant to UV-A than bacteria incubated in aqueous media without salts. In parallel to that, in the present study, inactivation of free-swimming bacteria took place at lower rates in PBS. One possible explanation for the lower rate of the response in PBS is that the presence of phosphates contributed to osmotic balance and that in turn delayed the disruptive effect of UV-A and UV-B wavelengths.

Phosphate ions are capable of UV absorption and therefore act as sunblock to bacteria. In addition, their presence has shown to decrease photocatalytic disinfection efficiency (Rincón and Pulgarin, 2004b). The reason has been related to the supportive effect these ions had in bacterial growth and by serving as a source of nutrient (Sathasivan *et al.*, 1997). In a comparison with Ringers solution, also a

buffered environment, the same protective effect was not provided to cells. The results presented with Ringers and PBS are in agreement with Rincón and Pulgarin (2007) who showed that *E. coli* incubated in phosphate buffered saline demonstrated a slightly higher resistance to action of solar disinfection (which includes UV-A region), than when challenged in buffer KCl/NaCl solution or in Milli-Q water. In this later medium, the UV-A solar disinfection had the quickest inactivating effect. The authors did not particularly mention that KCl/NaCl were involved with photosensitised reactions, but they noted that other ionic material could react with light and oxygen to form reactive oxygen species and that could improve disinfection rates (Rincón and Pulgarin, 2007). In this present work, it seems that synergistic effects of PBS ions were more protective to cells than in Ringers solution. Photochemical reactions between the ions present in Ringers could have enhanced generation of ROS and contributed to a higher rate of inactivation in this medium.

In this work, SCVs were observed after UV-A/B exposure of both free-swimming *E. coli* and *P. putida* CP1 which is in agreement with findings of previous studies (Pigeot-Rémy *et al.*, 2012; Robertson *et al.*, 2005). Robertson, Robertson and Lawton (2005) who demonstrated the formation of SCVs in *E. coli* and *P. aeruginosa* following UV-A exposure, but not when TiO_2 was added to the microbial suspension, confirm the findings of the present work. Pigeot-Rémy *et al.*, (2012) have also noted the same observation.

Dark repair took place when *P. putida* CP1 was challenged in Ringers solution by UV-A/B treatment. The inoculum size applied to the aqueous media ($\sim 10^7$=10,000,000cell/ml) could have afforded protection by shielding part of the cells from receiving a sufficient UV-A/B dose required to achieve complete inactivation. That is in agreement with the results of viability studies which showed that at the end of 120 minutes of exposure part of the cells still had their membrane integrity preserved. Furthermore, *P. putida* CP1 may possess a mechanism for dark-repair similar to that observed in *P. putida* laboratory strain 2IDINH and *Pseudomonas* sp. strain MF8 which demonstrated dark repair following UV-B inactivation (Zenoff *et al.*, 2006).

UV-A/B response was delayed in minimal medium when in comparison to the response in relatively more transparent Ringers solution, PBS and Milli-Q water. The presence of minerals is likely to have played a major role in such delayed response. Presence of mineral particles has influenced UV penetration in water (Mamane-Gravetz *et al.*, 2006). Depending on the composition, concentration, light properties and size, particles may be potentially antagonistic to UV disinfection of microorganisms (Youxian *et al.*, 2005). Besides shielding the suspended microorganisms, the attachment of free-swimming cells to minimal medium particles cannot be ruled out as an extra mechanism of protection. In phase-microscopy analysis, while Milli-Q, Ringers and PBS rarely presented particulate matter, minimal medium showed the presence of a heavy reticulated net of minerals which could have helped the bacteria to protect against UV exposure.

Robertson and Lawton (2005) found that in 120 minutes the inactivation of *E. coli* by UV-A+TiO_2 photocatalysis was 4-Log, whereas the inactivation by UV-A alone ($\lambda >$ 330 nm) was higher, 5-Log. Likewise, in that study the inactivation of *P. aeruginosa* was 4-Log by photocatalysis and 6-Log by UV-A/B. As observed in the present work for similar inoculum size of bacteria, the action of UV alone in that study was superior to the action of photocatalytic treatment. The rates of disinfection in the present work were superior most probably because of the extension of the wavelength lamp emission in the UV-B region.

In this work, after 120 minutes of UV-A/B exposure, 40% of *P. putida* CP1 cells were not viable in Ringers, while at this time viability of this organism had been completely lost in minimal medium. The difference between the two levels of inactivation in Ringers and in minimal medium may be related to the diverse ionic composition of the aqueous environment. For example, as explained before, minimal medium could have caused extra-damage because its ions could have allowed, in the presence of oxygen, the production of ROS (reactive oxygen species) (Rincón and Pulgarin, 2007), while the same phenomenon did not take place in Ringers. They also suggested that Fe present in aqueous media acted as a photosensitiser.

The inactivation curve of aggregated cells during UV-A/B disinfection presented two regions. The first characterized by a log-linear response with value of k_1= 0.3194 min^{-1}. The second region characterized as a tailing of k_2= 0.0036 min^{-1}. The dual pattern of response to disinfection was similar to that observed for UV-C. Depending on factors related to the sensitivity of the organism tested, the response-curve may not totally fit a log-linear correlation. Inactivation of microorganisms however does not always follow a log-linear of first-order of kinetics relationship and deviations of the Chick-Watson kinetics model may occur (Hijnen *et al.*, 2006; Mamane-Gravetz and Linden, 2005; Min *et al.*, 2005; Haas, 2002). For instance, a delayed response to disinfection occurs at low UV fluence (dose), causing a 'shoulder' effect; whereas a tailing is observed when no further inactivation occurs at higher doses (Mamane-Gravetz and Linden, 2005).

As evidenced by phase-contrast microscopy, heterogeneicity was a feature of the distribution of aggregated cells of *P. putida* CP1. In a study conducted by Kollu and Örmeci (2012) flocculation resulted in a scattered UV dose response of *E. coli*. The reason was that the presence of particles and flocculation made the system very heterogeneous. Likewise, in the present study, the presence of particles (such as in minimal medium) and flocs (such as aggregates of *P. putida* CP1) makes the liquor of aggregated cells a very heterogeneous system which would have accounted for the scattering, that is variable counts of colonies, in the UV response. Another factor which makes a flocculated microbial system highly heterogeneous is the mixing during UV disinfection, which could allow flocculation and defloculation and in turn random protection from UV by embedded microbes (Kollu and Örmeci, 2012).

Like in UV-C, during UV-A/B studies aggregated cells of *P. putida* CP1 presented part of the population as dead cells. However most of the cells were viable. By analysis of epifluorescence microscopy of aggregated cells a pattern of distribution in viable and non-viable cells was not observed. Monier and Lindown (2003) noticed the aggregates of *Pseudomonas syringae* formed on bean leaves did not follow any particular pattern. They found that non-viable cells were sometimes located on the surface of aggregates, or forming microcolonies-type structure within an aggregated and localized either on the edges or in the centre of the aggregates. They

hypothesised that successive episodes of stress, dead and re-growth of survival cells at the surface of the aggregates could cause such pattern of dead micro-colonies distribution. On the other hand, aggregated cells of *P. putida* CP1 were not allowed to grow for more than 24 hours. In this way this organisational pattern distribution of dead cells, perhaps, was not allowed to form, therefore suggesting that they could have assumed rather a random distribution within the aggregates.
As culturability results showed no survival of colonies was found after 4 hours of UV-A/B exposure. That means that following UV-A/B studies all the cells embedded in aggregates received a dose of radiation sufficient to inhibit their survival. With the help of Live/Dead analysis, it has been observed that viable cells remained after UV-A/B treatment after 6 hours and in the overnight dark repair sample. The regrowth overnight then was expected to occur.

In UV-A/B studies aggregated cells of *P. putida* CP1 presented a size of 1 order of magnitude smaller than in UV-C studies. Another intricate difference between aggregated cells produced for UV-A/B inactivation studies is that they presented a high amount of bound carbohydrate. To explain the reason for smaller aggregated cells produced during UV-A/B studies: two hypothesis were raised: the first was that the smaller size of aggregated cells in UV-A/B studies was a results of random process of the production of aggregated cells of *P. putida* CP1, and therefore this system has intrinsic variability. The second was that the higher amount of bound-EPS produced could actually have altered the aggregation of the aggregated cells of *P. putida* CP1. Although neither of these hypotheses has been examined for their impact on the size of aggregated cells, it was of interest in this study to highlight the occurrence of variability of the size of the aggregated cells between photodisinfection runs. As *P. putida* CP1 is suggested as a model to test photodisinfection studies, the variability of the aggregates produced is a factor that should be taken into account when protocols with *P. putida* CP1 aggregated cells are reproduced.

Hydrophobic particles are thermodynamically unstable and aggregate irreversibly over time (Boardman and Kelley, 2002). The presence of a high carbohydrate-acidic fraction and humic acids in the EPS of river water flocs was responsible for a more

negative overall charge of the flocs. That in turn caused lower hydrophobicity and as a consequence it did not favour aggregation (Droppo *et al.*, 2009). In this way, the presence of a high quantity of carbohydrates in bound-EPS may partially address the smaller size of aggregated cells of *P. putida* CP1 produced for UV-A/B studies. Contrary to what was observed in aggregated cells of *P. putida* CP1, in other biological systems in which EPS have a major participation, such as environmental biofilms, the carbohydrate fraction present was only a minor component (Flemming, 2009).

Following UV-A/B exposure, the number of smaller aggregates increased. As in UV-C studies, inclusions bodies of aggregated cells were also present during UV-A/B disinfection. Those were not noted to be disrupted as previously observed in UV-C studies. The presence of inclusions could have afforded to block part of the UV-A/B wavelengths to reach more internal located cells within the aggregates. They could have offered an extra protection to these cells and their composition, formation and function are suggested to be determined by future research. The multistaining pattern of aggregated cells during UV-A/B disinfection shifted from light blue-green colour (of FITC and Calcofluor-white), indicating carbohydrate and protein detection, to more red/pinky emissions (of propidium iodide). The increased detection of propidium iodide in UV-A/B treated aggregates indicated that membrane injury in aggregates had increased during UV treatment.

The values of pH, dry-weight and fructose consumption during UV-A/B studies were regular over time. No changes in the pH indicated that the H^+ concentration over time was constant. Therefore, hydrolysis, disinfection or biodegradation of the biomass generating new acidic compounds was not readily detected. Despite that, minimal medium was buffered and even if changes in the proton concentration occurred they did not occur to a highly significant level.

In the dark, the free-swimming *E. coli* (DSMZ 498) and *P. putida* CP1 survived well in all the aqueous media, including tap water, when present with TiO_2. Survival of *E. coli* in Ringers and TiO_2 was also found by previous research (Tim Cushnie *et al.*, 2009; Rincón and Pulgarin, 2007). Interestingly those studies also observed survival

of the organism in Milli-Q and TiO_2 (Tim Cushnie *et al.*, 2009; Rincón and Pulgarin, 2007). Interestingly, the bacteria did not die-off when incubated in autoclaved tap water and in the presence of TiO_2 photocatalyst. This finding was also observed in a previous work by Rincón and Pulgarin (2004b). In that study the authors explain that anions can interact with the TiO_2 surface at different levels according to their composition. In the case of tap water it is possible that chlorine residuals were quenched by TiO_2 explaining the inactivity of the killing effect of tap water previously observed in the absence of the catalyst.

The response of free-swimming bacteria to photocatalytic treatment with 1 g/l of TiO_2 was dependent upon aqueous media composition. This is in agreement with previous research (Tim Cushnie *et al.*, 2009; Rincón and Pulgarin, 2007; Mccullagh *et al.*, 2007; Gogniat *et al.*, 2006; Rincón and Pulgarin, 2004b). The fastest inactivation was observed for both organisms in Ringers which is an isotonic environment. It has been suggested that in an isotonic medium bacteria are protected against osmotic stress. Therefore they are more resistant against oxidant attack, and a larger number of reactive oxygen species are required to attack cells (Dunlop *et al.*, 2002). For this reason, in Ringers a delay in the initial rate of disinfection was expected to occur. Nevertheless, sodium chloride present in Ringers enhances interaction between the bacterial cell wall and the photocatalyst TiO_2, which in turn enhances rate of photocatalytic disinfection (Gogniat *et al.*, 2006). The reason is that the bacteria closer to the sites of $^{\bullet}OH$ and other radicals generated during the photocatalytic process will be more effectively damaged (Gogniat *et al.*, 2006). This interaction between the bacterial cell and the catalyst enhanced the rates of disinfection in relation to other media, not only in Ringers solution, but also in saline (0.9% NaCl) as demonstrated by previous work (Tim Cushnie *et al.*, 2009). There is also a probability of hypochlorite generation from the oxidation of Cl^-, which could have enhanced the inactivation effect in Ringers (Tim Cushnie *et al.*, 2009).

Conversely, PBS is an aqueous medium which did not facilitate photocatalytic disinfection. As explained before, in UV-A/B disinfection, this effect is partially due to the supportive effect of phosphate ions on bacterial growth (Sathasivan *et al.*, 1997) , and to the capacity of UV absorption by phosphates (Rincón and Pulgarin,

2004b). More importantly however is the antagonistic effect of phosphate ions to the attachment of bacteria to TiO_2 nanoparticles (Gogniat *et al.*, 2006). The reason for that has been postulated by Rincón and Pulgarin (2004b); as the phosphates associate with the catalyst surface, a negative layer is formed around the nanoparticles so that the catalyst repulses bacteria. Furthermore, the phosphates hamper disinfection efficiency of photocatalysis because they can act as a scavenger of $^{\bullet}OH$ radicals (Rincón and Pulgarin, 2004b). Milli-Q water did not enhance the rates of disinfection as was observed in Ringers but it also did not hamper the inactivation as was the case in PBS.

When TiO_2 was added to the tap water a decrease in the photocatalytic efficiency, compared to the inactivation in Ringers and Milli-Q water, was observed. It is possible that chlorine anions were adsorbed onto TiO_2 nanoparticles therefore decreasing the sites available for binding the bacteria and therefore by decreasing photocatalytic activity (Rincón and Pulgarin, 2004b).

Minimal medium had a more complex composition of minerals than PBS. The rate of photocatalytic disinfection in minimal medium was superior to the rate in phosphate buffered saline. As explained earlier, phosphates protect the microbial cell by acting like shields for UV. Moreover these ions support cell growth and in turn enhance endurance to photocatalytic treatment. Besides, in minimal medium, ROS generation may play a significant role.

UV photocatalysed suspensions of bacteria took longer than 24 hours to grow in agar plates. This slow growth of colonies in the presence of TiO_2 needs to be considered when calculating survival (Tim Cushnie *et al.*, 2009). Furthermore, the emergence of small-colony-variants was not observed in photocatalytic studies. (Robertson *et al.*, 2005) It has been also suggested that the addition of the catalyst could prevent selection of a resistant mutant phenotype (Robertson *et al.*, 2005).

Initial investigations in this study tested the efficiency of photocatalytic inactivation with various concentrations of TiO_2 (0.2-2.0 g/l). When below 1 g/l of TiO_2 (e.g. 0.2 and 0.5 g/l) or above (e.g. 1.5 g/l or 2.0 g/l) were investigated, kill was not as

efficient as with 1 g/l TiO_2. Thus, 1 g/l was chosen as the most suitable concentration to induce the maximum rate of photocatalytic inactivation with the UV reactor used in this work.

The concentration of TiO_2 is positively correlated with bactericidal activity up to 1g/l (Maness *et al.*, 1999). Cho *et al.*, (2004) demonstrated that *E. coli* inactivation efficiency was dependent upon the concentration of TiO_2 but also that it did not occur in a proportional matter. This author explained that at 1 g/l the efficiency was double that at 0.1 g/l, whereas no improvement of the photo-activity was found with 2.0 g/l of TiO_2. By increasing the concentration of TiO_2 more surface sites are available, but the amount of light penetration into the microbial suspension also decreases through increased light scattering by the nanoparticles, which in turns affects bactericidal efficiency (Cho *et al.*, 2004; Maness *et al.*, 1999; Bekbölet, 1997).

Although photocatalysis was able to inactivate bacteria in water, the addition of the catalyst, did not improve the disinfection rates previously obtained with UV-A/B treatment. In agreement with this finding, Herrera-Melian *et al.*, (2000) demonstrated that the rates of UV disinfection and solar disinfection were not improved by the addition of TiO_2.

The medium-pressure lamp used in the present work produced UV-A/B which is capable to photo-excite TiO_2 and to generate $^{\bullet}OH$ radicals. Nevertheless, the action of UV-A/B disinfection alone was previously shown to cause inactivation of bacteria. Routinely, in photocatalysis studies instead of medium-pressure lamps, lamps with low power usage, lower irradiance emission and which emit majorly in the UV-A wavelengths are used (Cho *et al.*, 2004; Maness *et al.*, 1999; Bekbölet, 1997). Therefore, comparatively to the medium-pressure used in the present work the lamps used in these other studies do not have the same inactivation efficiency. In this way, although 1 g/l of TiO_2 was added to the microbial suspension to induce photocatalytic inactivation, the high UV-A/B emission of the medium-pressure lamp alone was found to have superior inactivation efficiency.

The inactivation curves of UV-A/B treatment and photocatalysis were divergent suggesting that the mechanisms of kill were not the same. Above a certain time of treatment (e.g. >30 minutes for *P. putida* and >90 minutes for *E. coli*), the inactivation curves of bacteria in Ringers, Tap water, Milli-Q and Minimal medium, presented tailing. Gumy (2006) proposed that after 60 minutes of photocatalytic treatment the inactivation of *E. coli* formed intermediate products. Then, as the reaction progresses, the concentration of such intermediates increase and this saturates the reaction leading to a lack of further inactivation or a "tailing" response.

Delay in the initial inactivation by the photocatalytic process (shoulder) was observed in inactivation curves of free-swimming *E. coli* in tap water and Milli-Q water. The shoulder is a phenomenon dependent upon medium composition and organism response. It has been observed as part of the response of bacteria to photocatalytic process Cho *et al.*, (2004). The shoulder was not as evident in inactivation curves of *P. putida* CP1 in these media, but it did occur with *P. putida* CP1 in minimal medium.

In Tap water the shoulder occurred possibly as a result of the competition between organic matter and ions present in the water and the bacteria for photoactive sites on the TiO_2 surface. Prior exposure of bacteria to hypoosmotic stress in Milli-Q water could have started up an adaptive stress response. That has been observed in a number of bacteria as a response to previous exposure to mild cytotoxic stressors, such as oxidative stress. The consequence of this exposure is the enhancement of bacterial resistance to further exposure to other types of stress which is accompanied by the induction of several proteins (Crawford and Davies, 1994). Whether Milli-Q water caused an adaptive stress response in bacteria, that could have contributed to delay the damage caused by $^{\bullet}OH$ radicals; therefore explaining the shoulder curve type. Nonetheless, prolonged incubation in hypotonic medium, such as distilled water and Milli-Q, may cause efflux of salts such as sodium and magnesium weakening the cell wall. As a consequence cell death may occur (Morbach and Krämer, 2002; Blake *et al.*, 1999). Therefore, following prolonged incubation in Milli-Q water, bacteria were expected to be more vulnerable to photocatalytic

treatment. The shoulder in minimal medium could have occurred as a consequence of shielding and scavenging by $^{\bullet}OH$ by the ions.

E. coli has been extensively used as a model organism in photocatalytic disinfection (Nadtochenko *et al.*, 2005; Huang *et al.*, 2000; Maness *et al.*, 1999; Ireland *et al.*, 1993). That is the reason why the organism was chosen to be challenged in this research. Besides, it was also of interest to determine the response of aggregated cells of *P. putida* CP1. Furthermore, it was also of interest to determine the response of these free-swimming organisms to photocatalytic treatment in minimal medium as that was the medium utilized to grow aggregated cells. Both studies with *P. putida* CP1 and minimal medium were not found in the literature of photocatalytic disinfection.

Loss of viability of *P. putida* CP1 in Ringers following photocatalytic treatment was higher than following UV-A/B alone. That is an indication that the mechanisms which took place with the addition of TiO_2 were much more harmful to the cells. Another supportive evidence of the further damage caused by photocatalysis was confirmed by absence of dark repair. The same level of viability loss was not observed when photocatalysis took place in minimal medium. That could be related to the scavenging of $^{\bullet}OH$ radicals by ions, such as phosphate (Rincón and Pulgarin, 2004b), and the shielding effects of this medium could also have played a role.

The culturability of aggregated cells was only partially lost after 6 hours of photocatalytic treatment. As explained before, scavenging of $^{\bullet}OH$ radicals by phosphates and anion absorption onto the TiO_2 surface were factors which could have delayed inactivation in minimal medium. As well as those, the competition between sub-products generated by the photocatalytic destruction of aggregated cells and viable bacterial cells could cause decay in inactivation rate. Besides, in the case of aggregated cells the number of cells in the aggregates (10^8cell/ml) and the presence of EPS (extracellular polymeric substances) may have contributed to decay in photocatalytic efficiency.

Electrostatic attraction between the bacterial cell and TiO_2 nanoparticles are favoured by neutral pH as, between pH 3 and 9, bacteria are negatively charged, whereas up to pH 7 TiO_2 is positively charged (Gumy *et al.*, 2006). It was expected that in minimal medium the neutral pH favoured the interactions between the bacterial cells and the nanoparticles. By extension, it is hypothesised that the association between the positively charged TiO_2 catalyst and, negatively charged EPS (Sponza, 2003) was also favoured in minimal medium, as evidenced by phase-contrast and epifluorescence microscopy.

Even though aggregates and nanoparticles were found in close association, the presence of EPS and shielding provided by TiO_2 nanoparticles did not allow for ROS attack. That could explain the poor inactivation of aggregates by photocatalytic process in the conditions studies by this work. Hessler *et al.*, (2012) investigated the protective role of extracellular polymeric substances (EPS) in planktonic cells against ROS. Their study demonstrated that capsular EPS enhanced the attachment of TiO_2 nanoparticles of planktonic *P. aeruginosa*. They argued, however, that the presence of EPS delayed attack and damage caused by ROS, by acting as a physical isolation barrier between cells and radicals.

Contrary to what has been found with planktonic cells of *P. aeruginosa* by Hessler *et al.*, (2012), the EPS surrounding planktonic cells of *E. coli* demonstrated no influence of microbial inactivation by $^{\bullet}OH$ radicals formed from photolysis of nitrates (Gong *et al.*, 2012). In that study, the smaller amounts of EPS have been accounted for the absence of protection to planktonic cells of *E. coli* (Gong *et al.*, 2012).

Although the aggregated cells were not inactivated by the photocatalytic process as effectively as by UV treatment, their rupture following photocatalysis was observed. Fragmentation of aggregated cells could have been caused either by UV-A/B absorption or as a result of ROS attack. Liu *et al.*, (2007) demonstrated that photocatalysis with 0.1 g/l of TiO_2 degraded less carbohydrates and proteins of bacteria when EPS was present. That is evidence that the EPS is highly influential on the rate of photocatalytic degradation of bacteria. That author argued that the

competition between EPS and bacterial cells for ROS was offered as an explanation for the delayed inactivation of cells.

When the aggregated cells of *P. putida* CP1 were sonicated to allow counting, the dispersed cells had a coccoid shape. This change in the phenotype has been associated with nutritional stress (Fakhruddin and Quilty, 2007; Fakhruddin and Quilty, 2006). It is possible that compared to free-swimming cells of *P. putida* CP1 used in this study, the cells in aggregates which had a coccoid form would have a lower cellular volume and therefore less cellular surface would be exposed to the attack of reactive oxygen species of photocatalytic process. The lower rate of photocatalytic inactivation of aggregated cells could also be related with resistance of this phenotype to oxidative stress damage as it has been demonstrated by attached bacteria (Gage *et al.*, 2005).

Viability loss of aggregated cells following photocatalytic treatment was the highest among the photodisinfection treatments (UV-C, UV-A/B and UV-A/B+TiO_2). As nanoparticles were in close proximity with the aggregates, it is possible that even when the efficiency of inactivation was lower than UV-C and UV-A/B, the action of $^{\bullet}OH$ radicals and other ROS caused a more definitive damage to cell membranes. As pointed out by previous research, the attachment of bacteria to nanoparticles facilitates cell membrane damage (Hessler *et al.*, 2012; Gogniat *et al.*, 2006). The photocatalytic process promotes the decay of microorganism by destroying first the polysaccharides and proteins at the cell wall (Kiwi and Nadtochenko, 2005), then followed by the destruction of the cell membrane. As the bacterial cell membrane is damaged during the photocatalytic process, free-TiO_2 particles may gain access to the intracellular compartments and cause further damage (Hessler *et al.*, 2012; Huang *et al.*, 2000). Lastly, adsorption onto the TiO_2 surface and degradation of fructose during photocatalytic process, is likely to explain the lower values of fructose detected during photocatalytic treatment compared with other treatments.

Rose Bengal (RB) is a xanthene compound with three aromatic rings arranged linearly and an oxygen atom in the centre of the ring. It produces in the presence of oxygen and under visible light excitation 80% of singlet oxygen and 20% of anion

superoxide (Perussi, 2007). The molecule of Rose Bengal has a fourth halogenated ring with I and Cl atoms altogether with the COO^- groups which confers its negative charge. Rose Bengal was chosen for the photodynamic inactivation of *P. putida* CP1. Previous investigations in the laboratory showed that while the biomass of aggregated *P. putida* CP1 bound easily to Rose Bengal, a lower evidence of attachment was observed with methylene blue. Based on the premise that a photosensitiser needs to locate itself in the vicinity of the microbial cell to promote inactivation (Hamblin *et al.*, 2002) , Rose Bengal was chosen in the photodynamic inactivation investigations of both free-swimming and aggregated cells of *P. putida* CP1.

Rose Bengal was able to promote total inactivation of 10^6cell/ml of free-swimming *P. putida* CP1 in Ringers solution after a dose of 1.46 J/cm^2 applied in 45 minutes. Similarly, Demidova and Hamblin (2005) showed a ~4.5-Log reduction of *E. coli* (10^7cell/ml) following a dose of 8 J/cm^2 with 35 µM (~35.71 µg/ml) of Rose Bengal. In another work, *E. coli* (10^5cell/ml) was completely inactivated in the presence of 2 mg/l of Rose Bengal following 45 minutes of exposure by a solar simulator with a fluence-rate of 950 W/m^2 (Rengifo-Herrera *et al.*, 2007). One difference between the present study, where an LED device was used, and the investigation from Rengifo-Herrera *et al.*, (2007) is that the solar simulator produced an additional disinfectant effect provided by 4% of photons in the UV-A/B and 0.5% of photons in the UV-C region.

Rose Bengal demonstrated higher efficiency compared to methylene blue in the photodynamic inactivation of Gram-negative bacteria (Melo *et al.*, 2011) and faecal coliforms (Jemli *et al.*, 2002). In this later study, they found no change in the PDI efficiency by increasing concentrations of Rose Bengal from 10 and up to 50 µg/ml. This finding from Jemli *et al.*, (2002) also supports the present work which did not show any improvement of inactivation rates by increasing the sensitiser above 10 µg/ml. In a study from Melo *et al.*, (2011), the photodynamic inactivation was more strictly dependent upon the visible light dose applied than the concentration. An efficiency of 5-Log inactivation of *P. aeruginosa* and 4-Log of *E. coli* arouse when 10 µg/ml of Rose Bengal received a dose of 12 J/m^2. The authors attributed the

difference in the activity of Rose Bengal and methylene blue as a result of the higher quantum yield of the former, which could have accounted for a higher singlet oxygen production (Melo *et al.*, 2011). The effective concentration of homogeneous phase Rose Bengal used to inactivate bacteria was set as 10 µMolar, which is also below the cytotoxic limit (Shrestha and Kishen, 2012).

A limiting factor in the photodynamic inactivation of the organisms was the low fluence-rate produced by the LED device (0.580 mW/cm^2). The fluence-rate generated by a laser light produced higher fluence-rates varying from 50-400 mW/cm^2 (Demidova and Hamblin, 2005) to 526 mW/cm^2 (Rossoni *et al.*, 2010). As a consequence, a shorter exposure time taken for PDI to kill bacteria has been reported by previous works (Rossoni *et al.*, 2010; Demidova and Hamblin, 2005). In a study by Rossoni *et al.*, (2010) 180 seconds were needed to photosensitise Rose Bengal (50 µg/ml) and to cause a 4-Log inactivation of Enterobacteriaceae strains. That is a much lower irradiation time than the 45 minutes required to kill 10^6cell/ml of *P. putida* CP1 in Ringers.

Another difference between the present study and others, such as Rossoni *et al.*, (2010) and Demidova and Hamblin (2005), is that the toxicity of Rose Bengal manifested as a result of the long exposure time required to achieve kill with light. If, however, the fluence-rate was greater, the rate of singlet oxygen produced per unit of time ought to have been higher. As a consequence kill would have been achieved more rapidly, potentially before a cytotoxic effect provoked cell death.

When *P. putida* CP1 was challenged by PDI with Rose Bengal in Ringers, kill was only observed at the lower concentration of the sensitiser. It could be that at high concentration (50-100 µg/ml) of Rose Bengal the molecules of this sensitiser were self-aggregating and becoming more negative. Thus by electrostatic repulsion they were impeded to bind or penetrate the negative cell wall. Shielding from light caused by a high concentration of Rose Bengal could also have been an issue to the photodynamic efficiency in these conditions. Besides, by increasing the concentration of sensitiser more molecules of Rose Bengal are available and they may compete with bacteria for singlet oxygen. At a lower load of sensitiser (10

µg/ml) however, these factors would have been less influential to the PDI effect observed.

A lengthy time (>45 minutes) was required to inactivate free-swimming cells of *P. putida* CP1 in Ringers. In addition, no survival was observed in the overnight sample or in the dark control, that indicating that the sensitiser had a toxic effect on cells during prolonged incubation. Rose Bengal properties that inhibit bacterial growth are well known. For example, the sensitiser is used as an additive in malt extract agar acting as a selective aid in the isolation of Fungi as it inhibits the growth of bacteria (Gentry *et al.*, 2009; Ottow, 1972). In photodynamic studies, the toxicity of Rose Bengal depends on the incubation time, the type of bacteria and the conditions of the experiment. Demidova and Hamblin (2005) showed no toxicity in the dark for *E. coli* (35 µM) or *Staphylococcus aureus* (0.35 µM) (Demidova and Hamblin, 2005). Rossoni *et al.* (2010) showed that for a 50 µg/ml Rose Bengal presented some level of toxicity to *Enterobacteriaceae* species. In another investigation, the dark toxic effect of Rose Bengal in PDT of the oral pathogen Gram-positive *Streptococcus mutans* were showed at concentrations >2.5 µMolar (Paulino *et al.*, 2005).

Studies of PDI in distilled water and PBS with Rose Bengal at 10 µg/ml showed different effects on bacterial survival with and without light when in comparison to Ringers. The organism was very susceptible to the presence of Rose Bengal in distilled water with and without light, and it was not affected by the sensitiser when in PBS. In the investigations of Demidova and Hamblin (2005), for example, the aqueous media was phosphate buffered saline. As previously mentioned, phosphate medium has been shown to delay the attachment of *E. coli* to TiO_2 while in NaCl/KCl it enhanced its attachment (Gogniat *et al.*, 2006). As in photocatalytic inactivation, it is possible that the aqueous medium also exerts functions of enhancement of inactivation or cell protection. This could address the superior disinfection of *P. putida* CP1 with Rose Bengal in Ringers solution compared to the results achieved in PBS. As previously mentioned, PBS has confirmed aspects of protection and enhancement of organism resilience and growth under photodisinfection conditions (Rincón and Pulgarin, 2007; Rincón and Pulgarin, 2004b).

An aggregative behaviour of free-swimming *P. putida* CP1 was observed when stirring with PBS in the dark, and immediately after being incubated with light alone in distilled water. Interestingly, in that last case, was the only condition in which the organism survived well after overnight incubation. That observation establishes a link between organism survival and aggregation. In addition to that, in Ringers, an aggregative behaviour of *P. putida* CP1 was observed with both light and dark conditions at 0, 50 and 100 µg/ml of Rose Bengal. The lower sensitiser concentration, 10 µg/ml, did not cause aggregation of *P. putida* CP1 in Ringers. Aggregation was not observed in minimal medium, neither in the presence nor absence of sensitiser. As the balance of mineral content in minimal medium was diverse from the contents in Ringers, this could explain the aggregation previously observed.

Microbial aggregation is triggered by environmental conditions such as predation, substrate gradient, slow growth, and chemical or physical stress (Bossier and Verstraete, 1996). Stirring and light irradiation of the cells are classified as types of physical stress, whereas the presence of Rose Bengal is categorised as chemical stress type. *Pseudomonads* species, including *P. putida*, are known to produce intracellular pigments, such as pyoverdines (Meyer, 2000). This type of molecule could act as a photosensitiser and provoke a photodynamic effect in the intracellular environment. In this way, aggregation under light may have occurred potentially as an attempt to decrease the irradiation achieving inner located cells. However, there were cases in which under light exposure *P. putida* CP1 did not aggregate. In this way, a clear link between the effect of light, medium, sensitiser and stirring to cause aggregation was not established; yet they may have acted synergistically resulting in the triggering of the aggregation of free-swimming cells.

Photosensitisers used in photodynamic inactivation follow a general rule applied to Gram-staining of bacteria. While they are relatively more easily retained by Gram-positive cells, which stain with crystal violet, it is more difficult for them to be retained by Gram-negative bacteria (Perussi, 2007). The reason for the affinity between bacteria and the photosensitiser is in the differences between their cell wall.

The outer surface of the cell wall membrane of Gram-negative cells is negatively charged by phosphates and carboxylic acids present in the LPS (Jori and Coppellotti, 2007). In Gram-positive bacteria the cell wall is a protective layer of 20-80 μm which is separated from the cell membrane by the periplasmatic space (Jori and Coppellotti, 2007; Cabeen and Jacobs-Wagner, 2005). The size exclusion limit of Gram-positive bacteria cell walls is about 50,000 to 70,000 Da. Therefore, they are relatively more permeable to antimicrobials than Gram-negative bacteria (Lambert, 2002), which on the other hand, have a size exclusion limit of about 600-700 Da (Nikaido, 1994). Teichoic acids help to give to the surface of Gram-positive bacteria a negative charge and may play an important role in the passage of ions through the wall (Bauman, 2007).

The overall charge of the wall in Gram-positive bacteria is the reason why most of the antibacterial agents are positively charged with bivalent cations (Weidenmaier and Peschel, 2008). In this way it is expected that the permeability of the Gram-negative *P. putida* CP1 to Rose Bengal would not be high. Besides, it has been suggested that the uptake of anionic photosensitiser Rose Bengal is mediated by a combination of electrostatic interactions and by protein transporters (George *et al.*, 2009). It is believed that Rose Bengal does not bind well to planktonic cells in the case of Gram-negative cells, such as *Pseudomonads* and *E. coli*. The negatively charged dye diffuses through superficial sites of the cell membrane but it does not gain deeper penetration. Furthermore, the quantity of Rose Bengal to gain access to the Gram-negative is not sufficient to drive PDI. On the contrary, during photodynamic inactivation, RB mediates the generation of ROS and singlet oxygen in the extracellular environment. In the case of Gram-positive cells, Rose Bengal gains access slowly, yet higher than that of Gram-negative, to the inner of the cells by a diffusion-controlled process. Superior activity of Rose Bengal towards Gram-positive cells is partially attributed to this and to the fact that Gram-negative cells may have carotenoids which protect them from irradiation (Demidova and Hamblin, 2005).

During the irradiation of Rose Bengal with a 525 nm LED device throughout the photodynamic studies, bleaching of Rose Bengal was observed. An intense pink

colour observed in the initial suspension, was gradually replaced by weakened colour intensity. Photobleaching or aggregation of the sensitiser may affect the production of ROS and singlet oxygen (Moreira *et al.*, 2012).

During the epifluorescence microscopic analysis of aggregated cells interaction with Rose Bengal attached to the biomass showed changes in its predominant colour emission; initially a red colour, followed by a more green /yellowish faded shade. This change either indicated modification of the conformation of the molecule by the light or by interaction with the EPS. Jemli *et al.*, (2002) has reported that upon solar irradiation Rose Bengal photobleaches and that reduced photodynamic inactivation. Besides, upon illumination Rose Bengal undergoes photochemical changes in its molecules and the sub-products formed do not absorb the same amount of light nor do they have the same photosensitizing properties (Rengifo-Herrera *et al.*, 2007). This is another reason why prolonged incubation would not favour the photodynamic effect but rather cytotoxic effects of the sensitisers.

The ability of singlet oxygen to promote microbial inactivation is partially dependent upon the electrostatic interactions between the surface charge of microbial cell membranes and charges of the sensitiser. When aggregated cells surrounded by EPS matrix were studied, the interactions taking place between the biomass and the sensitiser are much more complex than those between Rose Bengal and the planktonic cells. When the sensitiser is in suspension, it has to bond to the EPS matrix, to being closer to target microbial cells. The matrix is not only a physical barrier to the close proximity of the sensitiser to the cells, it also could have acted as a barrier to the wavelengths which excite the dye and promote singlet oxygen generation. These are greatly influential matters in explaining the reason why aggregated cells of *P. putida* CP1 were more difficult to inactivate by PDI than free-swimming counterparts. In addition to this, during the inactivation of aggregated cells Rose Bengal, which is an anionic dye, may have aggregated at the surface of the suspended biofilm. As a consequence it does not penetrate the negatively charged EPS (Shrestha and Kishen, 2012; Y. Guo *et al.*, 2010).

A high attachment of Rose Bengal onto the biomass occurred. This led to colour removal. There was no evidence of biodegradation of the sensitiser remaining in the supernatant as revealed by the steadiness in the values of absorption ratio. Therefore it also signifies that the dye was removed by the biomass predominantly by a process of biosorption (Vitor and Corso, 2008). As opposed to this, Rose Bengal molecules which were retained onto the biomass of the aggregates, could have suffered alterations such as enzymatic attack, i.e. biodegradation. In this context, many species of *Pseudomonads* have been used to decolorize by biodegradation organic dyes (Chengalroyen and Dabbs, 2012). Such biodegradative interactions would afford to cause changes in the structure of the photosensitiser, and therefore preclude the photodynamic effect. In this way, the only evidence of changes in the chemical structure of the Rose Bengal attached from the biomass of *P. putida* CP1 was observed from the epifluorescence analysis.

As Rose Bengal is an anionic molecule, it is not expected to highly interact with cell membranes and wall. Moreover, it is also a highly electrophilic molecule which may have interacted with H^+ in the EPS (hydrogen bonding). Furthermore, other types of Van der Waals forces could have been present between the dye and EPS, such as dipole-dipole and London (between electron clouds). As Flemming (2009) explains, these types of weak physicochemical interactions keep the EPS together; their gross overall force can even exceed covalent bonds. Moreover, the presence of cation bridging (Flemming, 2009) in the EPS, promoted by divalent cations such as Ca^{2+}, could also attract the negative Rose Bengal molecule. Therefore, the Rose Bengal charge could have restrained interaction with the cell walls, but the possibility of other types of interaction are likely to explain the affinity between Rose Bengal and the EPS of aggregated cells of *Pseudomonas putida* CP1. For this reason, Rose Bengal was found to be an excellent marker of EPS of these organisms.

There was evidence of destruction of EPS during photodynamic inactivation with 50 µg/ml. The average size of aggregated cells decreased 2-3 orders of magnitude when compared to stirring in the dark. A lower effect of photolysis by LED green light was also observed as the aggregates decreased in size under light exposure. It was not

unexpected that the irradiation by green light could have caused photosensitisation reactions of the biomolecules in the EPS matrix or in the cells.

The evidence of destruction of EPS in the presence of light and 50 µg/ml of Rose Bengal, however strongly suggests that the Rose Bengal was able to cause severe damage to the matrix structure. According to Mantareva *et al.*, (2011) the destruction of biofilm EPS matrix by singlet oxygen may occur by attack of carbohydrates by singlet oxygen. The fragmentation of the aggregated cells following PDI treatment may have occurred as part as singlet oxygen attack on the carbohydrate portion of the EPS matrix (Wainwright *et al.*, 2002). Evidence of destruction of EPS in biofilms following PDI process has been addressed as important by Wainwright and Crossley (2004), as no other antimicrobial therapy is able to effective destroy the matrix. Wainwright *et al.*, (2002) showed the destruction of EPS matrix of *Pseudomonas aeruginosa* biofilms (10^6cell/ml), reaching an approximate 3-4 Log reduction of the bacterial infestation. In this study the authors also highlighted the importance of a photodisinfection process to destroy the EPS.

An absence of destruction of aggregated cells with photodynamic inactivation with 100 µg/ml of RB may have occurred by an enhancement of clumping of aggregated cells as facilitated by the sensitiser. In addition and as mentioned previously, the high concentration of sensitiser might have hampered the PDI effect by hindering light penetration. That was not considered as a problem during the experimental trials, as the sensitiser was highly incorporated by the biomass of aggregated cells. Nonetheless, the sensitiser associated with the biomass may also have acted as a light shield.

Although fragmentation of the EPS matrix was noted during PDI treatment, no evidence of inactivation was found. This, however, was considered as a limitation of the method of microbiological evaluation, which was the presence and absence of growth by turbidity. Therefore, more research needs to be undertaken before a more conclusive association between loss of cell viability and the fragmentation of PDI is established.

In the case of a sensitiser used for water disinfection, it is undesirable that the sensitiser is retained by microbial cells or is in suspension. In the first case, it may be metabolized to more toxic by-products, and in the second it will require further removal. In this way, sensitisers such as Rose Bengal, which has a killing action more dependent upon extracellular generation of ROS and Singlet oxygen and does not need to be tightly bound to the cells, are an advantage for water disinfection purposes.

An attempt to immobilise a porphyrin (tetraphenyl-porphyrin) in a solid carrier PVDF (Polyvinylidene-fluoride) was prepared by using dichloromethane (DMA) (DATA NOT SHOWN). Equal amounts (10 ml) of the stock solutions (P4VP/TPP 1:1 vol/vol) were mixed and stirred thoroughly for 30 minutes or until the polymer and TPP sensitiser were completely dissolved. Then the sensitiser loaded polymeric films were cast on the bottom of Petri dishes. The Petri dishes were used as a photodynamic inactivation reactor of *P. putida* CP1 in Ringers and with the LED device at emitting at 525 nm to excite the porphyrin. No inactivation took place even at prolonged incubation (>12 hours). The microscopic analysis showed the sensitiser was well immersed in the polymer domains. In order to achieve significant results, the material ought perhaps to be more transparent than what has been produced, which was quite opaque. Moreover other classes of sensitisers with a higher singlet oxygen yield could be used to optimize the results achieved thus far. Other experimental conditions such as the initial number of cells, irradiation conditions and stirring must also be taken into account by future investigations. A similar attempt was made with Rose Bengal and methylene blue covalently bound in a polystyrene polymeric film cast on Petri dish. The polymer presented a porous structure which was used to achieve from 1.5 to 3-Log inactivation of 10^4 cell/ml (Nakonechny *et al.*, 2012).

In the case of the application of photosensitisation in clinical usage, it is desirable that the sensitiser is absorbed by the microbial cell so that the photodynamic effect can take place intracellularly (Shrestha and Kishen, 2012; Mantareva *et al.*, 2011). In the case of photodynamic inactivation for attenuation of microbial contamination of water, the presence of the sensitiser in solution is not strictly necessary. Therefore,

the use of sensitiser which can be retained by the microbial cells is not the main point when a PDI method is being applied for such purpose.

As demonstrated by previous work, Rose Bengal immobilised in solid carriers was capable of attenuating levels of Gram-negative and Gram-positive bacteria in water (Dahl *et al.*, 1989; Bezman *et al.*, 1978). Instead, other parameters have more relevance in the field, such as encountering molecules which preserve high singlet oxygen yields even after being immobilised. Modifications of the sensitiser molecule or its combination with compounds such as chitosan, which makes the cell wall permeable, have been shown to improve PDI inactivation by immobilised sensitisers (Shrestha and Kishen, 2012).

Three photodisinfection technologies were studied for the inactivation of free-swimming and aggregated Gram-negative bacterial cells. Superiority of UV-C over UV-A/B was demonstrated. The addition of TiO_2 nanoparticles caused diverse damage to that observed by UV radiation alone, in addition dark repair was inhibited when the catalyst was used. This in combination of avoidance of selection of resistant phenotypes (Pigeot-Rémy *et al.*, 2012) is a crucial advantage of the photocatalytic method over UV. Moreover, from the energetic perspective, an attempt to inactivate model bacterial with visible light was carried out with considerable success. However, optimization of the method is necessary to achieve a higher level of destruction of the aggregated cells.

Aggregated cells of *P. putida* CP1 were studied for the first time as a model organism in the comparison of the effect of the three diverse photodisinfection techniques (UV disinfection, TiO_2 photocatalysis and Photodynamic Inactivation.

The main objective of this thesis was to demonstrate how the aggregates behaved when challenged by photodisinfection and this has been showed and compared with the outputs of their free-swimming counterparts. The undoubted importance of *E. coli* has helped in the choice of this organism as the other model bacterium used in the thesis. Interestingly, the organism responded similarly to *P. putida* CP1, the second bacterial model, to the photodisinfection technologies investigated. As

formerly explained in the introduction section, Gram-negative bacteria species play a major role in the contamination of waters. They also play a major role causing infections, with highlight to the aforesaid importance of *Pseudomonads*. In this premise resides their importance as models for the development of water photodisinfectants.

6 Conclusions

6 Conclusions

- The composition of the aqueous medium influenced the response of bacterial cells to photodisinfection. The presence of chlorine in tap water made this an unsuitable medium for UV-C and UV-A/B studies while the presence of minerals in an aqueous medium significantly reduced the effect of photodisinfection.

- UV-C was the most effective radiation for photodisinfection. It was more effective than UV-A/B, UV-A/B in combination with 1g/l of TiO_2 (titanium dioxide) and photodynamic inactivation using Rose Bengal.

- The Gram-negative bacteria, *E. coli* (DSMZ 498) and *Pseudomonas putida* CP1, were similarly affected by UV-C and UV-A/B treatment.

- Photodisinfection of aggregated bacterial cells was successfully demonstrated using UV-C and UV-A/B although the rate of disinfection was slower than that for planktonic cells.

- Dark repair was observed for both planktonic and aggregated cells using UV disinfection. This was attributed to the presence of extracellular polymeric substances (EPS) in the case of the aggregated cells and to the short disinfecting times used in the case of the planktonic cells.

- The use of a nonculturable approach, such as the LIVE/DEAD® Bacterial Viability Kit (*Bac*Light™), together with a culturable approach, such as the plate count, was important to determine more accurately the response of the cells to photodisinfection than using a culturable approach only.

7 Bibliography

7 Bibliography

1. APHA., AWWA and WPCF. (1998). *Standard methods for the examination of water and wastewater*. 20th ed. Washington, D.C., USA: American Public Health Association, American Water Works Association and Water Pollution Control Federation.

2. Abshire, R.L. and Dunton, H. (1981). Resistance of selected strains of Pseudomonas aeruginosa to low-intensity ultraviolet radiation. *Applied and Environmental Microbiology,* **41**(6), 1419-1423.

3. Aidan, A., Mehrvar, M., Ibrahim, T.H. and Nenov, V. (2007). Particulates and bacteria removal by ceramic microfiltration, UV photolysis, and their combination. *Journal of Environmental Science and Health, Part A: Toxic/Hazardous Substances and Environmental Engineering,* **42**(7), 895-901.

4. Alhede, M., Kragh, K.N., Qvortrup, K., Allesen-Holm, M., van Gennip, M., Christensen, L.D. *et al.* (2011). Phenotypes of Non-Attached Pseudomonas aeruginosa aggregates resemble surface attached biofilm. *PLoS ONE,* **6**(11), e27943.

5. Almeida, A., Faustino, M.A.F., Tomé, A.C. and Neves, M.G.P.M.S. (2011). Porphyrins as Antimicrobial Photosensitizing Agents *IN:* Hamblin, M.R. and Jori, G. (eds.) *Photodynamic inactivation of microbial pathogens.* Cambridge: Royal Society of Chemistry, pp.83-160.

6. Alrousan, D.M.A., Dunlop, P.S.M., McMurray, T.A. and Byrne, J.A. (2009). Photocatalytic inactivation of E. coli in surface water using immobilised nanoparticle TiO_2 films. *Water Research,* **43**(1), 47-54.

7. Aquionics. (2008). Disinfecting wastewater: Productive UV disinfection for wastewater. *Filtration & Separation,* **45**(10), 24-25.

8. Armbruster, C.R., Forster, T.S., Donlan, R.M., O'Connell, H.A., Shams, A.M. and Williams, M.M. (2012). A biofilm model developed to investigate survival and disinfection of Mycobacterium mucogenicum in potable water. *Biofouling,* **28**(10), 1129-1139.

9. BBC-UK. (2012). Pseudomonas bacteria found at Ulster Hospital. *BBC news Northern Ireland*, 29 January. Available from: http://www.bbc.co.uk/news/uk-northern-ireland-16779722 [Accessed 10 February 2012].

10. Bak, J., Ladefoged, S.D., Tvede, M., Begovic, T. and Gregersen, A. (2009). Dose requirements for UVC disinfection of catheter biofilms. *Biofouling*, **25**(4), 289-296.

11. Bak, J., Ladefoged, S.D., Tvede, M., Begovic, T. and Gregersen, A. (2010). Disinfection of Pseudomonas aeruginosa biofilm contaminated tube lumens with ultraviolet C light emitting diodes. *Biofouling*, **26**(1), 31-38.

12. Barbosa, H.R., Rodrigues, M.F.A., Campos, C.C., Chaves, M.E., Nunes, I., Juliano, Y. *et al.* (1995). Counting of viable cluster-forming and non cluster-forming bacteria: A comparison between the drop and the spread methods. *Journal of Microbiological Methods*, **22**(1), 39-50.

13. Bauman, R.W. (2007). *Microbiology with Diseases by Taxonomy*. 2nd ed. Pearson International Edition.

14. Behnke, S., Parker, A.E., Woodall, D. and Camper, A.K. (2011). Comparing the chlorine disinfection of detached biofilm clusters with those of sessile biofilms and planktonic cells in single-and dual-species cultures. *Applied and Environmental Microbiology*, **77**(20), 7176-7184.

15. Bekbölet, M. (1997). Photocatalytic bactericidal activity of TiO_2 in aqueous suspensions of E. coli. *Water Science and Technology*, **35**(11–12), 95-100.

16. Benabbou, A.K., Derriche, Z., Felix, C., Lejeune, P. and Guillard, C. (2007). Photocatalytic inactivation of Escherichia coli: effect of concentration of TiO_2 and microorganism, nature, and intensity of UV irradiation. *Applied Catalysis B: Environmental*, **76**(3-4), 257-263.

17. Bergey, D.H. and Holt, J.G. (1994). *Bergey's manual of determinative bacteriology*. 9th ed. Baltimore: Williams & Wilkins.

18. Berney, M., Hammes, F., Bosshard, F., Weilenmann, H.U. and Egli, T. (2007). Assessment and nterpretation of bacterial viability by using the LIVE/DEAD BacLight kit in combination with flow cytometry. *Applied and Environmental Microbiology,* **73**(10), 3283-3290.

19. Bezman, S., Burtis, P., Izod, T. and Thayer, M. (1978). Photodynamic inactivation of E. coli by rose bengal immobilized on polystyrene beads. *Photochemistry and Photobiology,* **28**(3), 325-329.

20. Bhatkhande, D.S., Pangarkar, V.G. and Beenackers, A.A.C.M. (2002). Photocatalytic degradation for environmental applications-a review. *Journal of Chemical Technology & Biotechnology,* **77**(1)

21. Bichai, F., Leveille, S. and Barbeau, B. (2011). Comparison of the role of attachment, aggregation and internalisation of microorganisms in UVC and UVA (solar) disinfection. *Water Science Technology*, **63**(9), 1823-1831.

22. Bichai, F., Inmaculada Polo-Lopez, M. and Fernandez Ibanez, P. (2012). Solar disinfection of wastewater to reduce contamination of lettuce crops by Escherichia coli in reclaimed water irrigation. *Water Research*, **46**(18), 6040-6050.

23. Bitton, G. (1994). *Wastewater microbiology*. 3th ed. New York: Wiley-Liss.

24. Blake, D., Maness, P., Huang, Z., Wolfrum, E., Huang, J. and Jacoby, W. (1999). Application of the photocatalytic chemistry of titanium dioxide to disinfection and the killing of cancer cells. *Separation and Purification Methods,* **28**(1), 1-50.

25. Blanco, J., Malato, S., Fernández-Ibañez, P., Alarcón, D., Gernjak, W. and Maldonado, M.I. (2009). Review of feasible solar energy applications to water processes. *Renewable and Sustainable Energy Reviews,* **13**(6-7), 1437-1445.

26. Blanco-Galvez, J., Fernández-Ibáñez, P. and Malato-Rodríguez, S. (2007). Solar photocatalytic detoxification and disinfection of water: recent overview. *Journal of Solar Energy Engineering,* **129**, 4.

27. Blatchley III, E.R., Shen, C., Naunovic, Z., Lin, L.S., Lyn, D.A., Robinson, J.P. *et al.* (2006). Dyed microspheres for quantification of UV dose distributions: Photochemical reactor characterization by Lagrangian actinometry. *Journal of Environmental Engineering,* **132**(11), 1390-1403.

28. Blatchley III, E.R. (1997). Numerical modelling of UV intensity: application to collimated-beam reactors and continuous-flow systems. *Water Research,* **31**(9), 2205-2218.

29. Blossey, E.C., Neckers, D.C., Thayer, A.L. and Schaap, A.P. (1973). Polymer-based sensitizers for photooxidations. *Journal of the American Chemical Society,* **95**(17), 5820-5822.

30. Boardman, G.D. and Kelley, M.B. (2002). Removal of organisms by flocculation/sedimentation *IN:* Lingireddy, S. (ed.) *Control of microorganisms in drinking water.* Reston, VA: ASCE: American Society of Civil Engineers, pp.81-92.

31. Bohrerova, Z. and Linden, K.G. (2006a). Assessment of DNA damage and repair in Mycobacterium terrae after exposure to UV irradiation. *Journal of Applied Microbiology,* **101**(5), 995-1001.

32. Bohrerova, Z. and Linden, K.G. (2007). Standardizing photoreactivation: Comparison of DNA photorepair rate in Escherichia coli using four different fluorescent lamps. *Water Research*, **41**(12), 2832-2838.

33. Bohrerova, Z. and Linden, K.G. (2006b). Ultraviolet and Chlorine Disinfection of Mycobacterium in Wastewater: Effect of Aggregation. *Water Environment Research,* **78**(6), 565-571.

34. Bolton, J.R. (2000). Calculation of ultraviolet fluence rate distributions in an annular reactor: significance of refraction and reflection. *Water Research,* **34**(13), 3315-3324.

35. Bolton, J.R., Bircher, K.B., Tumas, W. and Tolman, C.A. (2001). Figures-of-merit for the technical development and application of advanced oxidation

technologies for both electric- and solar- drive systems. *Pure Applied Chemistry*, **73**(4), 627-637.

36. Bolton, J.R. and Linden, K.G. (2003). Standardization of methods for fluence (UV Dose) determination in bench-scale UV experiments. *Journal of Environmental Engineering*, **129**(3), 209-215.

37. Bonnett, R. (1995). Photosensitizers of the porphyrin and phthalocyanine series for photodynamic therapy. *Chemical Society Reviews*, **24**(1), 19-33.

38. Bonnett, R., Krysteva, M.A., Lalov, I.G. and Artarsky, S.V. (2006). Water disinfection using photosensitizers immobilized on chitosan. *Water Research*, **40**(6), 1269-1275.

39. Bossier, P. and Verstraete, W. (1996). Triggers for microbial aggregation in activated sludge? *Applied Microbiology and Biotechnology*, **45**(1), 1-6.

40. Boulos, L., Prévost, M., Barbeau, B., Coallier, J. and Desjardins, R. (1999). LIVE/DEAD® BacLight™: application of a new rapid staining method for direct enumeration of viable and total bacteria in drinking water. *Journal of Microbiological Methods*, **37**(1), 77-86.

41. Bradford, M.M. (1976). A rapid and sensitive method for the quantitation of microgram quantities of protein utilizing the principle of protein-dye binding. *Analytical Biochemistry*, **72**(1–2), 248-254.

42. Braunstein, J.L., Loge, F.J., Tchobanoglous, G. and Darby, J.L. (1996). Ultraviolet disinfection of filtered activated sludge effluent for reuse applications. *Water Environment Research*, **68**(2), 152-161.

43. Bridier, A., Briandet, R., Thomas, V. and Dubois-Brissonnet, F. (2011). Resistance of bacterial biofilms to disinfectants: a review. *Biofouling*, **27**(9), 1017-1032.

44. Burdman, S., Jurkevitch, E., Schwartsburd, B., Hampel, M. and Okon, Y. (1998). Aggregation in Azospirillum brasilense: effects of chemical and physical factors and involvement of extracellular components. *Microbiology-Uk*, **144**(7), 1989-1999.

45. Burdman, S., Jurkevitch, E., Soria-Diaz, M.E., Serrano, A.M.G. and Okon, Y. (2000). Extracellular polysaccharide composition of Azospirillum brasilense and its relation with cell aggregation. *FEMS Microbiology Letters*, **189**(2), 259-264.

46. Burguete, M.I., Galindo, F., Gavara, R., Luis, S.V., Moreno, M., Thomas, P. *et al.* (2009). Singlet oxygen generation using a porous monolithic polymer supported photosensitizer: potential application to the photodynamic destruction of melanoma cells. *Photochemical & Photobiological Sciences*, **8**(1), 37-44.

47. Butler, R., Lund, V. and Carlson, D. (1987). Susceptibility of Campylobacter jejuni and Yersinia enterocolitica to UV radiation. *Applied and Environmental Microbiology*, **53**(2), 375-378.

48. Byrne, J.A., Fernandez-Ibañez, P.A., Dunlop, P.S.M., Alrousan, D. and Hamilton, J.W.J. (2011). Photocatalytic enhancement for solar disinfection of water: a review. *International Journal of Photoenergy*, **2011**, 1-12.

49. Cabeen, M.T. and Jacobs-Wagner, C. (2005). Bacterial cell shape. *Nature Reviews Microbiology*, **3**(8), 601-610.

50. Calin, M.A. and Parasca, S. (2009). Light sources for photodynamic inactivation of bacteria. *Lasers in Medical Science*, **24**(3), 453-460.

51. Calleja, G.B. (1984). *Microbial Aggregation*. Florida: C R C Press LLC.

52. Cantwell, R.E. and Hofmann, R. (2008). Inactivation of indigenous coliform bacteria in unfiltered surface water by ultraviolet light. *Water Research*, **42**(10), 2729-2735.

53. Chan, Y.Y. and Killick, E.G. (1995). The effect of salinity, light and temperature in a disposal environment on the recovery of E.coli following exposure to ultraviolet radiation. *Water Research*, **29**(5), 1373-1377.

54. Chang, J.C.H., Ossoff, S.F., Lobe, D.C., Dorfman, M.H., Dumais, C.M., Qualls, R.G. *et al.* (1985). UV inactivation of pathogenic and indicator microorganisms. *Applied and Environmental Microbiology,* **49**(6), 1361-1365.

55. Chen, M.Y., Lee, D.J., Tay, J.H. and Show, K.Y. (2007). Staining of extracellular polymeric substances and cells in bioaggregates. *Applied Microbiology and Biotechnology,* **75**(2), 467-474.

56. Chengalroyen, M. and Dabbs, E. (2012). The microbial degradation of azo dyes: minireview. *World Journal of Microbiology and Biotechnology,* 1-11.

57. Cho, M., Chung, H., Choi, W. and Yoon, J. (2004). Linear correlation between inactivation of E. coli and OH radical concentration in TiO_2 photocatalytic disinfection. *Water Research,* **38**(4), 1069-1077.

58. Choi, Y. and Choi, Y. (2010). The effects of UV disinfection on drinking water quality in distribution systems. *Water Research,* **44**(1), 115-122.

59. Chong, M.N., Jin, B., Chow, C.W.K. and Saint, C. (2010). Recent developments in photocatalytic water treatment technology: A review. *Water Research,* **44**(10), 2997-3027.

60. Collins, C.H. and Lyne, P.M. (1976). *Microbiological Methods.* Boston, MA: Butterworths.

61. Cooper, A.T. and Goswami, D.Y. (2002). Evaluation of methylene blue and rose bengal for dye sensitized solar water treatment. *Journal of Solar Energy Engineering,* **124**, 305-310.

62. Costerton, J.W., Geesey, G. and Cheng, K.J. (1978). How bacteria stick. *Scientific American,* **238**(1), 86-95.

63. Costerton, J.W., Stewart, P.S. and Greenberg, E.P. (1999). Bacterial Biofilms: A Common Cause of Persistent Infections. *Science,* **284**(5418), 1318-1322.

64. Costerton, J.W. (2007). *The biofilm primer.* Berlin; New York: Springer.

65. Cotton, C. and Passantino, L. (2005). Regulations in the United States: requirements and guidance for ultraviolet disinfection of drinking water. *Journal of Environmental Engineering and Science*, **4**(S1), S57-S63.

66. Crawford, D.R. and Davies, K. (1994). Adaptive response and oxidative stress. *Environmental Health Perspectives*, **102**(Suppl 10), 25-28.

67. Cripps, C., Bumpus, J.A. and Aust, S.D. (1990). Biodegradation of azo and heterocyclic dyes by Phanerochaete chrysosporium. *Applied and Environmental Microbiology*, **56**(4), 1114.

68. Cutler, T.D. and Zimmerman, J.J. (2011). Ultraviolet irradiation and the mechanisms underlying its inactivation of infectious agents. *Animal Health Research Reviews*, **12**(01), 15-23.

69. Dahl, T.A., Midden, W.R. and Hartman, P.E. (1989). Comparison of killing of gram-negative and gram-positive bacteria by pure singlet oxygen. *Journal of Bacteriology*, **171**(4), 2188-2194.

70. Dalrymple, O.K., Stefanakos, E., Trotz, M.A. and Goswami, D.Y. (2010). A review of the mechanisms and modeling of photocatalytic disinfection. *Applied Catalysis B: Environmental*, **98**(1-2), 27-38.

71. Demidova, T.N. and Hamblin, M.R. (2005). Effect of cell-photosensitizer binding and cell density on microbial photoinactivation. *Antimicrobial Agents and Chemotherapy*, **49**(6), 2329-2335.

72. Derosa, M.C. and Crutchley, R.J. (2002). Photosensitized singlet oxygen and its applications. *Coordination Chemistry Reviews*, **233-234**, 351-371.

73. Dolmans, D.E.J.G.J., Fukumura, D. and Jain, R.K. (2003). Photodynamic therapy for cancer. *Nature Reviews Cancer*, **3**(5), 380-387.

74. Donlan, R.M. (2002). Biofilms: microbial life on surfaces. *Emerging Infectious Diseases*, **8**(9), 881-890.

75. Downes, A. and Blunt, T.P. (1877). Researches on the effect of light upon bacteria and other organisms. *Proceedings of the Royal Society of London,* **26,** 488-500.

76. Droppo, I.G., Liss, S.N., Williams, D., Nelson, T., Jaskot, C. and Trapp, B. (2009). Dynamic existence of waterborne pathogens within river sediment compartments. Implications for water quality regulatory affairs. *Environmental Science & Technology,* **43**(6), 1737-1743.

77. DuBois, M., Gilles, K.A., Hamilton, J.K., Rebers, P.A. and Smith, F. (1956). Colorimetric method for determination of sugars and related substances. *Analytical Chemistry,* **28**(3), 350-356.

78. Dunlop, P.S.M., Byrne, J.A., Manga, N. and Eggins, B.R. (2002). The photocatalytic removal of bacterial pollutants from drinking water. *Journal of Photochemistry and Photobiology A: Chemistry*, **148**(1-3), 355-363.

79. Eboigbodin, K.E. and Biggs, C.A. (2008). Characterization of the extracellular polymeric substances produced by Escherichia coli using infrared spectroscopic, proteomic, and aggregation studies. *Biomacromolecules,* **9**(2), 686-695.

80. Environmental Protection Agency (2009). *EPA Drinking Water Advice Note N0.4. Disinfection By-Products in Drinking Water (Version 1).* Wexford: EPA.

81. Environmental Protection Agency (2006). *Groundwater Quality in Ireland.* Water quality in Ireland 2004-2006. Wexford: EPA.

82. Environmental Protection Agency (2011). *The provision and quality of drinking water in in Ireland. A report for the year 2010.* Wexford: EPA.

83. Environmental Protection Agency. (1998). *Water treatment manuals: disinfection*. Wexford: EPA.

84. Ergaieg, K. and Seux, R. (2009). A comparative study of the photoinactivation of bacteria by meso-substituted cationic porphyrin, rose Bengal and methylene blue. *Desalination,* **246**(1-3), 353-362.

85. Espeland, E. and Wetzel, R. (2001). Complexation, stabilization, and UV photolysis of extracellular and surface-bound glucosidase and alkaline phosphatase: implications for biofilm microbiota. *Microbial Ecology,* **42**(4), 572-585.

86. FDA. (2006). *The "bad bug book".* 2nd ed. US Food and Drug Adminstration.

87. Fakhruddin, A.N.M. and Quilty, B. (2005). The influence of glucose and fructose on the degradation of 2-chlorophenol by Pseudomonas putida CP1. *World Journal of Microbiology and Biotechnology,* **21**(8), 1541-1548.

88. Fakhruddin, A.N.M. and Quilty, B. (2007). Measurement of the growth of a floc forming bacterium Pseudomonas putida CP1. *Biodegradation,* **18**(2), 189-197.

89. Fakhruddin, A.N.M. and Quilty, B. (2006). The response of Pseudomonas putida CP1 cells to nutritional, chemical and environmental stresses. *World Journal of Microbiology and Biotechnology,* **22**(5), 507-514.

90. Farnood, R.R. (2005). Flocs and Ultraviolet Disinfection *IN:* Droppo, I.G., Leppard, G.G., Liss, S.N. and Milligan, T.G. (eds.) *Flocculation in natural and engineered environmental systems.* New York: CRC Press, pp.385-396.

91. Farrell, A. and Quilty, B. (2002a). Substrate-dependent autoaggregation of Pseudomonas putida CP1 during the degradation of mono-chlorophenols and phenol. *Journal of Industrial Microbiology and Biotechnology,* **28**(6), 316-324.

92. Farrell, A. and Quilty, B. (2002b). The enhancement of 2-chlorophenol degradation by a mixed microbial community when augmented with Pseudomonas putida CP1. *Water Research,* **36**(10), 2443-2450.

93. Fernández, R.O. and Pizarro, R.A. (1999). Pseudomonas aeruginosa UV-A-induced lethal effect: influence of salts, nutritional stress and pyocyanine. *Journal of Photochemistry and Photobiology B: Biology,* **50**(1), 59-65.

94. Field, A.P. (2005). *Discovering statistics using SPSS: (and sex, drugs and rock 'n' roll).* 2nd ed. London; Thousand Oaks, CA: Sage.

95. Flemming, H.C. and Wingender, J. (2010). The biofilm matrix. *Nature Reviews Microbiology,* **8**(9), 623-633.

96. Flemming, H.C., Neu, T.R. and Wozniak, D.J. (2007). The EPS matrix: the "house of biofilm cells". *Journal of Bacteriology,* **189**(22), 7945-7947.

97. Flemming, H.C. (2009). *Why microorganisms live in biofilms and the problem of biofouling.* Berlin Heidelberg: Springer.

98. Friedman, B.A., Dugan, P.R., Pfister, R.M. and Remsen, C.C. (1969). Structure of exocellular polymers and their relationship to bacterial flocculation. *Journal of Bacteriology,* **98**(3), 1328-1334.

99. Fujishima, A., Rao, T.N. and Tryk, D.A. (2000). Titanium dioxide photocatalysis. *Journal of Photochemistry and Photobiology C: Photochemistry Reviews,* **1**(1), 1-21.

100. Gadgil, A. (1998). Drinking water in developing countries. *Annual Review of Energy and the Environment,* **23**(1), 253-286.

101. Gage, J., Roberts, T. and Duffy, J. (2005). Susceptibility of Pseudomonas aeruginosa biofilm to UV-A illumination over photocatalytic and non-photocatalytic surfaces. *Biofilms,* **2**(3), 155-163.

102. Gamage, J. and Zhang, Z. (2010). Applications of photocatalytic disinfection. *International Journal of Photoenergy,* **2010**, 1-11.

103. Gentry, T., Maier, M.R., Pepper, I.L. and Gerba, C.P. (2009). *Environmental Microbiology.* Amsterdam; Boston: Elsevier/Academic Press Inc.

104. George, S., Hamblin, M.R. and Kishen, A. (2009). Uptake pathways of anionic and cationic photosensitizers into bacteria. *Photochemical Photobiology Science,* **8**(6), 788-795.

105. Gleeson, C. and Gray, N.F. (1997). *The coliform index and waterborne disease : problems of microbial drinking water assessment.* 1st ed. New York: E & Fn Spon.

106. Glenn, J.K. and Gold, M.H. (1983). Decolorization of several Polymeric Dyes by the Lignin-Degrading Basidiomycete Phanerochaete-Chrysosporium. *Applied and Environmental Microbiology,* **45**(6), 1741-1747.

107. Gogniat, G., Thyssen, M., Denis, M., Pulgarin, C. and Dukan, S. (2006). The bactericidal effect of TiO_2 photocatalysis involves adsorption onto catalyst and the loss of membrane integrity. *FEMS Microbiology Letters,* **258**(1), 18-24.

108. Gong, A.S., Lanzl, C.A., Cwiertny, D.M. and Walker, S.L. (2012). Lack of influence of extracellular polymeric substances (EPS) level on hydroxyl radical mediated disinfection of Escherichia coli. *Environmental Science & Technology,* **46**(1), 241-249.

109. Goodsell, D.S. (2001). The molecular perspective: ultraviolet light and pyrimidine dimers. *The Oncologist,* **6**(3), 298-299.

110. Goulding, C., Gillen, C. and Bolton, E. (1988). Biodegradation of substituted benzenes. *Journal of Applied Microbiology,* **65**(1), 1-5.

111. Gray, N.F. (2005). *Water technology: an introduction for environmental scientists and engineers.* 2nd ed. Oxford: Elsevier Butterworth-Heinemann.

112. Grum, F.C. and Becherer, R. (1979). *Optical radiation measurements*. New York: Academic Press.

113. Guerrero-Beltran, J.A. and Barbosa-Cánovas, G.V. (2004). Advantages and limitations on processing foods by UV light. *Food Science and Technology International,* **10**(3), 137-147.

114. Guillard, C., Bui, T., Felix, C., Moules, V., Lina, B. and Lejeune, P. (2008). Microbiological disinfection of water and air by photocatalysis. *Comptes Rendus Chimie,* **11**(1-2), 107-113.

115. Gumy, D., Morais, C., Bowen, P., Pulgarin, C., Giraldo, S., Hajdu, R. *et al.* (2006). Catalytic activity of commercial of TiO_2 powders for the abatement of the

bacteria (E. coli) under solar simulated light: Influence of the isoelectric point. *Applied Catalysis B: Environmental,* **63**(1-2), 76-84.

116. Guo, Y., Rogelj, S. and Zhang, P. (2010). Rose Bengal-decorated silica nanoparticles as photosensitizers for inactivation of gram-positive bacteria. *Nanotechnology*, **21**(6), 065102-7.

117. Guo, M., Hu, H., Bolton, J.R. and El-Din, M.G. (2009). Comparison of low- and medium-pressure ultraviolet lamps: Photoreactivation of Escherichia coli and total coliforms in secondary effluents of municipal wastewater treatment plants. *Water Research,* **43**(3), 815-821.

118. Haas, C.H. (2002). General Kinetics of Disinfection Processes *IN:* Lingireddy, S. (ed.) *Control of Microorganisms in Drinking Water*. ASCE, pp.183-188.

119. Hamblin, M.R., O'Donnell, D.A., Murthy, N., Rajagopalan, K., Michaud, N., Sherwood, M.E. *et al.* (2002). Polycationic photosensitizer conjugates: effects of chain length and Gram classification on the photodynamic inactivation of bacteria. *Journal of Antimicrobial Chemotherapy,* **49**(6), 941-951.

120. Hara-Kudo, Y., Segawa, Y. and Kimura, K. (2006). Sanitation of seawater effluent from seaweed processing plants using a photo-catalytic TiO_2 oxidation. *Chemosphere,* **62**(1), 149-154.

121. Hashmi, J.T., Hamblin, M.R., Hamblin, M.R., Sharma, S.K., Kharkwal, G.B., Jori, G. *et al.* (2011). *Photodynamic Inactivation of Microbial Pathogens: Medical and Environmental Applications*. The Royal Society of Chemistry.

122. Hattori, T. (1988). *The viable count: quantitative and environmental aspects*. Madison, Wiscosin: Science Tech Inc.

123. Henriques, I.D.S. and Love, N.G. (2007). The role of extracellular polymeric substances in the toxicity response of activated sludge bacteria to chemical toxins. *Water Research,* **41**(18), 4177-4185.

124. Herigstad, B., Hamilton, M. and Heersink, J. (2001). How to optimize the drop plate method for enumerating bacteria. *Journal of Microbiological Methods,* **44**(2), 121-129.

125. Herrera Melian, J., Doña Rodríguez, J., Viera Suarez, A., Tello Rendon, E., Valdes do Campo, C., Arana, J. *et al.* (2000). The photocatalytic disinfection of urban waste waters. *Chemosphere,* **41**(3), 323-327.

126. Hessler, C.M., Wu, M.Y., Xue, Z., Choi, H. and Seo, Y. (2012). The influence of capsular extracellular polymeric substances on the interaction between TiO_2 nanoparticles and planktonic bacteria. *Water Research,* **46**(15), 4687-4696.

127. Hijnen, W.A.M. and Medema, G.J. (2010). *Elimination of micro-organisms by drinking water treatment processes: a review.* London: IWA Publishing.

128. Hijnen, W.A.M., Beerendonk, E.F. and Medema, G.J. (2006). Inactivation credit of UV radiation for viruses, bacteria and protozoan (oo)cysts in water: A review. *Water Research,* **40**(1), 3-22.

129. Hofmann, R., Andrews, B. and Lachmaniuk, P. (2004). Guidelines for ultraviolet disinfection of drinking water: Considerations for Ontario. *Journal of Toxicology and Environmental Health, Part A,* **67**(20), 1805-1812.

130. Hrudey, S.E., Payment, P., Huck, P.M., Gillham, R.W. and Hrudey, E.J. (2003). A fatal waterborne disease epidemic in Walkerton, Ontario: comparison with other waterborne outbreaks in the developed world. *Water Science & Technology,* **47**(3), 7-14.

131. Huang, Z., Maness, P., Blake, D.M., Wolfrum, E.J., Smolinski, S.L. and Jacoby, W.A. (2000). Bactericidal mode of titanium dioxide photocatalysis. *Journal of Photochemistry and Photobiology A: Chemistry,* **130**(2-3), 163-170.

132. Ireland, J.C., Klostermann, P., Rice, E.W. and Clark, R.M. (1993). Inactivation of Escherichia coli by titanium dioxide photocatalytic oxidation. *Applied and Environmental Microbiology,* **59**(5), 1668-1670.

133. Jagger, J. (1967). *Introduction to research in ultraviolet photobiology*. Prentice-Hall New Jersey.

134. Jemli, M., Alouini, Z., Sabbahi, S. and Gueddari, M. (2002). Destruction of fecal bacteria in wastewater by three photosensitizers. *Jounal of Environmental Monitoring*, **4**(4), 511-516.

135. Jori, G. and Coppellotti, O. (2007). Inactivation of pathogenic microorganisms by photodynamic techniques: mechanistic aspects and perspective applications. *Anti-Infective Agents in Medicinal Chemistry (Formerly Current Medicinal Chemistry-Anti-Infective Agents)*, **6**(2), 119-131.

136. Josefsen, L.B. and Boyle, R.W. (2008). Photodynamic therapy and the development of metal-based photosensitisers. *Metal-Based Drugs*, **2008**, 276109-24.

137. Josset, S., Keller, N., Lett, M., Ledoux, M.J. and Keller, V. (2008). Numeration methods for targeting photoactive materials in the UV-A photocatalytic removal of microorganisms. *Chemical Society Reviews*, **39**(27), 744-755.

138. Jungfer, C., Schwartz, T. and Obst, U. (2007). UV-induced dark repair mechanisms in bacteria associated with drinking water. *Water Research*, **41**(1), 188-196.

139. Kay, D., Fricker, C. and Royal Society of Chemistry. (1997). *Coliforms and E. coli: problem or solution?* Cambridge: Royal Society of Chemistry.

140. Kiil, K., Binnewies, T.T., Willenbrock, H., Hansen, S.K., Yang, L., Jelsbak, L. et al. (2008). Comparative genomics of Pseudomonas *IN:* Rehm, B. (ed.) *Pseudomonas. Model organism, pathogen, cell factory*. Weinheim: Wiley VCH, pp.1-24.

141. Kim, S.Y., Kwon, O.J. and Park, J. (2001). Inactivation of catalase and superoxide dismutase by singlet oxygen derived from photoactivated dye. *Biochimie*, **83**(5), 437-444.

142. Kiwi, J. and Nadtochenko, V. (2005). Evidence for the mechanism of photocatalytic degradation of the bacterial wall membrane at the TiO_2 interface by ATR-FTIR and laser kinetic spectroscopy. *Langmuir,* **21**(10), 4631-4641.

143. Kollu, K. and Örmeci, B. (2012). Effect of particles and bioflocculation on ultraviolet disinfection of Escherichia coli. *Water Research,* **46**(3), 750-60.

144. Kowalski, W. (2009). *Ultraviolet Germicidal Irradiation Handbook.UVGI for Air and Surface Disinfection*. 1st ed. Springer.

145. Krasnovsky Jr, A. (1998). Singlet molecular oxygen in photobiochemical systems: IR phosphorescence studies. *Membrane & Cell Biology,* **12**(5), 665-690.

146. Kuznetsova, N.A., Yuzhakova, O.A., Strakhovskaya, M.G., Shumarina, A.O., Kozlov, A.S., Krasnovsky, A.A. *et al.* (2011). New heterogeneous photosensitizers with phthalocyanine molecules covalently linked to aminopropyl silica gel. *Journal of Porphyrins and Phthalocyanines,* **15**(7), 718-726.

147. Kuznetsova, N.A., Makarov, D.A., Kaliya, O.L. and Vorozhtsov, G.N. (2007). Photosensitized oxidation by dioxygen as the base for drinking water disinfection. *Journal of Hazardous Materials,* **146**(3), 487-491.

148. Labas, M.D., Brandi, R.J., Zalazar, C.S. and Cassano, A.E. (2009). Water disinfection with UVC radiation and H2O2. A comparative study. *Photochemical & Photobiological Sciences,* **8**(5), 670-676.

149. Lakretz, A., Ron, E.Z. and Mamane-Gravetz, H. (2010). Biofouling control in water by various UVC wavelengths and doses. *Biofouling,* **26**(3), 257-267.

150. Lakretz, A., Ron, E.Z. and Mamane-Gravetz, H. (2011). Biofilm control in water by a UV-based advanced oxidation process. *Biofouling*, **27**(3), 295-307.

151. Lambert, P. (2002). Cellular impermeability and uptake of biocides and antibiotics in Gram-positive bacteria and mycobacteria. *Journal of Applied Microbiology,* **92**(s1), 46S-54S.

152. LeChevallier, M.W., Babcock, T.M. and Lee, R.G. (1987). Examination and characterization of distribution system biofilms. *Applied and Environmental Microbiology,* **53**(12), 2714-2724.

153. Lengeler, J.W., Drews, G. and Schlegel, H.G. (1999). *Biology of the prokaryotes*. Stuttgart: Blackwell Science.

154. Lewandowski, Z. and Beyenal, H. (2007). *Fundamentals of biofilm research*. CRC Press.

155. Li, Q., Mahendra, S., Lyon, D.Y., Brunet, L., Liga, M.V., Li, D. *et al.* (2008). Antimicrobial nanomaterials for water disinfection and microbial control: Potential applications and implications. *Water Research,* **42**(18), 4591-4602.

156. Liao, B.Q., Allen, D.G., Droppo, I.G., Leppard, G.G. and Liss, S.N. (2001). Surface properties of sludge and their role in bioflocculation and settleability. *Water Research,* **35**(2), 339-350.

157. Lingireddy, S. (ed.) (2002). *Control of microorganisms in drinking water*. Reston VA: ASCE: American Society of Civil Engineers.

158. Liu, Y., Li, J., Qiu, X. and Burda, C. (2007). Bactericidal activity of nitrogen-doped metal oxide nanocatalysts and the influence of bacterial extracellular polymeric substances (EPS). *Journal of Photochemistry and Photobiology A: Chemistry,* **190**(1), 94-100.

159. Logan, B.E. and Hunt, J.R. (1987). Advantages to microbes of growth in permeable aggregates in marine systems. *Limnology and Oceanography,* **32**(5), 1034-1048.

160. Lonnen, J., Kilvington, S., Kehoe, S.C., Al-Touati, F. and McGuigan, K.G. (2005). Solar and photocatalytic disinfection of protozoan, fungal and bacterial microbes in drinking water. *Water Research,* **39**(5), 877-883.

161. Lu, Z., Zhou, L., Zhang, Z., Shi, W., Xie, Z., Xie, H. *et al.* (2003). Cell damage induced by photocatalysis of TiO_2 thin films. *Langmuir,* **19**(21), 8765-8768.

162. Magaraggia, M., Coppellotti, O., Fabris, C., Guidolin, L. and Jori, G. (2011). Inactivation of Microbial Pathogens by Photosensitized Process: Environmental Applications *IN:* Hamblin, M.R. and Jori, G. (eds.) *Photodynamic inactivation of microbial pathogens*. Cambridge: Royal Society of Chemistry, pp.405-423.

163. Maisch, T. (2007). Anti-microbial photodynamic therapy: useful in the future? *Lasers in Medical Science*, **22**(2), 83-91.

164. Malato, S., Fernández-Ibáñez, P., Maldonado, M.I., Blanco, J. and Gernjak, W. (2009). Decontamination and disinfection of water by solar photocatalysis: Recent overview and trends. *Catalysis Today*, **147**(1), 1-59.

165. Malato, S., Blanco, J., Alarcón, D.C., Maldonado, M.I., Fernández-Ibáñez, P. and Gernjak, W. (2007). Photocatalytic decontamination and disinfection of water with solar collectors. *Catalysis Today*, **122**(1-2), 137-149.

166. Mamane-Gravetz, H. and Linden, K.G. (2005). Relationship between physiochemical properties, aggregation and u.v. inactivation of isolated indigenous spores in water. *Journal of Applied Microbiology*, **98**(2), 351-363.

167. Mamane-Gravetz, H. and Linden, K.G. (2004). UV disinfection of indigenous aerobic spores: implications for UV reactor validation in unfiltered waters. *Water Research*, **38**(12), 2898-2906.

168. Mamane-Gravetz, H., Ducoste, J.J. and Linden, K.G. (2006). Effect of particles on ultraviolet light penetration in natural and engineered systems. *Applied Optics*, **45**(8), 1844-1856.

169. Mamane-Gravetz, H. and Linden, K.G. (2006). Impact of Particle Aggregated Microbes on UV Disinfection. I: Evaluation of Spore–Clay Aggregates and Suspended Spores. *Journal of Environmental Engineering*, **132**(6), 596-606.

170. Maness, P.C., Smolinski, S., Blake, D.M., Huang, Z., Wolfrum, E.J. and Jacoby, W.A. (1999). Bactericidal activity of photocatalytic TiO_2 reaction: Toward an understanding of its killing mechanism. *Applied and Environmental Microbiology*, **65**(9), 4094-4098.

171. Manjón, F., Villen, L., García-Fresnadillo, D. and Orellana, G. (2007). On the factors influencing the performance of solar reactors for water disinfection with photosensitized singlet oxygen. *Environmental Science & Technology,* **42**(1), 301-307.

172. Mantareva, V., Kussovski, V., Angelov, I., Wöhrle, D., Dimitrov, R., Popova, E. *et al.* (2011). Non-aggregated Ga (III)-phthalocyanines in the photodynamic inactivation of planktonic and biofilm cultures of pathogenic microorganisms. *Photochemical Photobiological Sciences,* **10**(1), 91-102.

173. Masschelein, W. and Rice, R.G. (2002). *Ultraviolet light in water and wastewater sanitation*. Boca Raton, FL: Lewis Publishers.

174. Matsunaga, T., Tomoda, R., Nakajima, T. and Wake, H. (1985). Photoelectrochemical sterilization of microbial cells by semiconductor powders. *FEMS Microbiology Letters,* **29**(1-2), 211-214.

175. McCullagh, C., Skillen, N., Adams, M. and Robertson, P.K.J. (2011). Photocatalytic reactors for environmental remediation: a review. *Journal of Chemical Technology and Biotechnology,* **86**(8), 1002-1017.

176. McNaught, A.D. and Wilkinson, A. (1997). *Compendium of Chemical Terminology.* 2nd ed. Oxford, UK: Blackwell Science.

177. Mccullagh, C., Robertson, J.M.C., Bahnemann, D.W. and Robertson, P.K.J. (2007). The application of TiO 2 photocatalysis for disinfection of water contaminated with pathogenic micro-organisms: a review. *Research on Chemical Intermediates,* **33**(3), 359-375.

178. Melo, W.C.M.A., Castro, L.F., Dal'Mas, R.M. and Perussi, J.R. (2011). Effectiveness of photodynamic therapy on Gram-negative bacteria. *Science Against Microbial Pathogens: Communicating Current Research and Technological Advances,* 662-667.

179. Meltzer, T.H. (1997). *Pharmaceutical water systems.* Littleton, Colo.: Tall Oaks.

180. Meyer, J.M. (2000). Pyoverdines: pigments, siderophores and potential taxonomic markers of fluorescent Pseudomonas species. *Archives of Microbiology*, **174**(3), 135-142.

181. Miller, G.L. (1959). Use of Dinitrosalicylic Acid Reagent for Determination of Reducing Sugar. *Analytical Chemistry*, **31**(3), 426-428.

182. Mills, A., Davies, R.H. and Worsley, D. (1993). Water purification by semiconductor photocatalysis. *Chemical Society Reviews*, **22**(6), 417-425.

183. Min, C., Hyenmi, C., Wonyong, C. and Jeyong, Y. (2005). Different inactivation Behaviors of MS-2 phage and Escherichia coli in TiO_2 photocatalytic disinfection. *Applied and Environmental Microbiology*, **71**(1), 270-275.

184. Monier, J.M. and Lindow, S. (2003). Differential survival of solitary and aggregated bacterial cells promotes aggregate formation on leaf surfaces. *Proceedings of the National Academy of Sciences*, **100**(26), 15977-15982.

185. Morbach, S. and Krämer, R. (2002). Body shaping under water stress: osmosensing and osmoregulation of solute transport in bacteria. *Chembiochem: A European Journal of Chemical Biology*, **3**(5), 384-397.

186. Moreira, L.M., Lyon, J.P., Romani, A.P., Severino, D., Rodrigues, M.R. and de Oliveira, H.P.M. (2012). Phenotiazinium dyes as photosensitizers (PS) in photodynamic therapy (PDT): spectroscopic properties and photochemical mechanisms *IN:* Farrukh, M.A. (ed.) *Advanced Aspects of Spectroscopy*. 1st ed. INTECH, pp.n/a-n/a.

187. Murthy, P.S. and Venkatesan, R. (2009). Industrial Biofilms and their Control *IN:* Anonymous*Marine and Industrial Biofouling*. Berlin: Springer, pp.65-101.

188. Nadtochenko, V.A., Rincón, A.G., Stanca, S.E. and Kiwi, J. (2005). Dynamics of E. coli membrane cell peroxidation during TiO_2 photocatalysis studied by ATR-FTIR spectroscopy and AFM microscopy. *Journal of Photochemistry and Photobiology A: Chemistry*, **169**(2), 131-137.

189. Nakonechny, F., Pinkus, A., Hai, S., Yehosha, O., Nitzan, Y. and Nisnevitch, M. (2012). Eradication of Gram-positive and Gram-negative bacteria by photosensitizers immobilized in polystyrene. *Photochemistry and Photobiology,* n/a-n/a.

190. Navntoft, C., Ubomba-Jaswa, E., McGuigan, K.G. and Fernández-Ibáñez, P. (2008). Effectiveness of solar disinfection using batch reactors with non-imaging aluminium reflectors under real conditions: Natural well-water and solar light. *Journal of Photochemistry and Photobiology B: Biology,* **93**(3), 155-161.

191. Nic, M., Jirat, J. and Kosata, B. (2010). *Compendium of Chemical Terminology* [Online]. Available from: http://goldbook.iupac.org/FT07376.html [Accessed 27 April 2010].

192. Nichols, W.W., Evans, M.J., Slack, M.P.E. and Walmsley, H.L. (1989). The penetration of antibiotic into aggregates of mucoid and non-mucoid Pseudomonas aeruginosa. *Journal of General Microbiology,* **135**(Part 5), 1291-1303.

193. Nikaido, H. (1994). Prevention of Drug Access to Bacterial Targets - Permeability Barriers and Active Efflux. *Science,* **264**(5157), 382-388.

194. Ohta, N. and Robertson, A.R. (2005). *Colorimetry: fundamentals and applications*. Chichester, West Sussex, England ; Hoboken, NJ, USA: J. Wiley.

195. Oka, Y., Kim, W.C., Yoshida, T., Hirashima, T., Mouri, H., Urade, H. *et al.* (2008). Efficacy of titanium dioxide photocatalyst for inhibition of bacterial colonization on percutaneous implants. *Journal of Biomedical Materials Research Part B: Applied Biomaterials,* **86**(2), 530-540.

196. Oleinick, N.L. (2010). *Basic Photosensitization.*[Online]. Available from: http://photobiology.info/Oleinick.html [Accessed 10 May 2010].

197. Oleinick, N.L. and Evans, H.H. (1998). The photobiology of photodynamic therapy: cellular targets and mechanisms. *Radiation Research,* **150**(5), 146-156.

198. Oliveira, A., Almeida, A., Carvalho, C., Tomé, J., Faustino, M., Neves, M. *et al.* (2009). Porphyrin derivatives as photosensitizers for the inactivation of Bacillus cereus endospores. *Journal of Applied Microbiology,* **106**(6), 1986-1995.

199. Oppenländer, T. (2003). *Photochemical purification of water and air*. Weinheim: Wiley-VCH.

200. Ottow, J.C.G. (1972). Rose Bengal as a Selective Aid in the Isolation of Fungi and Actinomycetes from Natural Sources. *Mycologia,* **64**(2), pp. 304-315.

201. Panzarini, E., Inguscio, V. and Dini, L. (2011). Timing the multiple cell death pathways initiated by Rose Bengal acetate photodynamic therapy. *Cell Death & Disease,* **2**(6), 1-11.

202. Paulino, T.P., Ribeiro, K.F., Thedei Jr., G., Tedesco, A.C. and Ciancaglini, P. (2005). Use of hand held photopolymerizer to photoinactivate Streptococcus mutans. *Archives of Oral Biology,* **50**(3), 353-359.

203. Perussi, J.R. (2007). Inativação fotodinâmica de microrganismos. *Química Nova,* **30**(4), 988-994.

204. Phillips, R. (1983). *Sources and applications of ultraviolet radiation*. London ; New York: Academic Press.

205. Phoenix, D.A. and Harris, F. (2003). Phenothiazinium-based photosensitizers: antibacterials of the future? *Trends in Molecular Medicine,* **9**(7), 283-285.

206. Phoenix, D.A., Sayed, Z., Hussain, S., Harris, F. and Wainwright, M. (2003). The phototoxicity of phenothiazinium derivatives against Escherichia coli and Staphylococcus aureus. *FEMS Immunology & Medical Microbiology,* **39**(1), 17-22.

207. Pigeot-Rémy, S., Simonet, F., Atlan, D., Lazzaroni, J. and Guillard, C. (2012). Bactericidal efficiency and mode of action: A comparative study of photochemistry and photocatalysis. *Water Research,* **46**(10), 3208-3218.

208. Pinggui, W., Rongcai, X., Imlay, J.A. and Jian, K.S. (2009). Visible-light-induced photocatalytic inactivation of bacteria by composite photocatalysts of

palladium oxide and nitrogen-doped titanium oxide. *Applied Catalysis B: Environmental,* **88**(3-4), 576-581.

209. Pipes, W.O. (1982). *Bacterial indicators of pollution.* Boca Raton, Fla: CRC Press.

210. Polo-López, M.I., Fernández-Ibáñez, P., Ubomba-Jaswa, E., Navntoft, C., García-Fernández, I., Dunlop, P.S.M. *et al.* (2011). Elimination of water pathogens with solar radiation using an automated sequential batch CPC reactor. *Journal of Hazardous Materials,* **196**(0), 16-21.

211. Pozzo, R.L., Baltanas, M.A. and Cassano, A.E. (1997). Supported titanium oxide as photocatalyst in water decontamination: State of the art. *Catalysis Today,* **39**(3), 219-231.

212. Qualls, R.G., Flynn, M.P. and Johnson, J.D. (1983). The role of suspended particles in ultraviolet disinfection. *Journal (Water Pollution Control Federation),* **55**(10), pp. 1280-1285.

213. Raulio, M., Pore, V., Areva, S., Ritala, M., Leskela, M., Lindén, M. *et al.* (2006). Destruction of Deinococcus geothermalis biofilm by photocatalytic ALD and sol-gel TiO_2 surfaces. *Journal of Industrial Microbiology & Biotechnology,* **33**(4), 261-268.

214. Rehm, B. (2008). *Pseudomonas:model organism, pathogen, cell factory.* Weinheim; Chichester: Wiley-VCH.

215. Rengifo-Herrera, J.A., Mielczarski, E., Mielczarski, J., Castillo, N.C., Kiwi, J. and Pulgarin, C. (2008). Escherichia coli inactivation by N, S co-doped commercial TiO_2 powders under UV and visible light. *Applied Catalysis B: Environmental,* **84**(3-4), 448-456.

216. Rengifo-Herrera, J.A., Sanabria, J., Machuca, F., Dierolf, C.F., Pulgarin, C. and Orellana, G. (2007). A comparison of solar photocatalytic inactivation of waterborne E-coli using tris (2,2 '-bipyridineftuthenium(II), rose bengal, and TiO_2. *Journal of Solar Energy Engineering-Transactions of the Asme,* **129**(1), 135-140.

217. Richardson, S.D., Thruston, A., Caughran, T., Chen, P., Collette, T., Schenck, K. *et al.* (2000). Identification of new drinking water disinfection by-products from ozone, chlorine dioxide, chloramine, and chlorine. *Water, Air, & Soil Pollution,* **123**(1), 95-102.

218. Riedewald, F. and Sexton, A.W. (2007). Biofilms-Surwiwal and Growth of Bacteria in Compendial High Purity Water Systems. *Pharmaceutical Engineering,* **27**(NUMB 1), 42-53.

219. Rincón, A.G. and Pulgarin, C. (2007). Solar photolytic and photocatalytic disinfection of water at llaboratory and field scale. Effect of the chemical composition of water and study of the postirradiation events. *Journal of Solar Energy Engineering,* **129**, 100-110.

220. Rincón, A.G. and Pulgarin, C. (2004a). Bactericidal action of illuminated TiO_2 on pure Escherichia coli and natural bacterial consortia: post-irradiation events in the dark and assessment of the effective disinfection time. *Applied Catalysis B: Environmental,* **49**(2), 99-112.

221. Rincón, A.G. and Pulgarin, C. (2004b). Effect of pH, inorganic ions, organic matter and H2O2 on E. coli K12 photocatalytic inactivation by TiO_2: Implications in solar water disinfection. *Applied Catalysis B: Environmental,* **51**(4), 283-302.

222. Rincón, A.G. and Pulgarin, C. (2004c). Field solar E. coli inactivation in the absence and presence of TiO_2: is UV solar dose an appropriate parameter for standardization of water solar disinfection? *Solar Energy*, **77**(5), 635-648.

223. Robertson, J., Robertson, P.K.J. and Lawton, A. (2005). A comparison of the effectiveness of TiO_2 photocatalysis and UVA photolysis for the destruction of three pathogenic micro-organisms. *Journal of Photochemistry and Photobiology A: Chemistry,* **175**(1), 51-56.

224. Rossoni, R.D., Junqueira, J.C., Santos, E.L.S., Costa, A.C.B. and Jorge, A.O.C. (2010). Comparison of the efficacy of Rose Bengal and erythrosin in photodynamic therapy against Enterobacteriaceae. *Lasers in Medical Science*, **25**(4), 581-586.

225. Sadowsky, M.J. and Whitman, R.L. (2011). *The fecal bacteria*. Washington, DC: ASM Press.

226. Saito, T., Iwase, T., Horie, J. and Morioka, T. (1992). Mode of photocatalytic bactericidal action of powdered semiconductor TiO_2 on mutans streptococci. *Journal of Photochemistry and Photobiology B: Biology*, **14**(4), 369-379.

227. Salhani, N. and Uelker-Deffur, A. (1998). Improved quantification of aggregated bacteria by combined enzymatic and mechanical treatment of flocs and biofilm from a rotating drum bioreactor. *Water Research*, **32**(4), 1287-1295.

228. Sanz, E.N., Salcedo Dávila, I., Andrade Balao, J.A. and Quiroga Alonso, J.M. (2007). Modelling of reactivation after UV disinfection: Effect of UV-C dose on subsequent photoreactivation and dark repair. *Water Research*, **41**(14), 3141-3151.

229. Sathasivan, A., Ohgaki, S., Yamamoto, K. and Kamiko, N. (1997). Role of inorganic phosphorus in controlling regrowth in water distribution system. *Water Science and Technology*, **35**(8), 37-44.

230. Schastak, S., Ziganshyna, S., Gitter, B., Wiedemann, P. and Claudepierre, T. (2010). Efficient Photodynamic Therapy against Gram-Positive and Gram-Negative Bacteria Using THPTS, a Cationic Photosensitizer Excited by Infrared Wavelength. *PloS One*, **5**(7), e11674.

231. Schleheck, D., Barraud, N., Klebensberger, J., Webb, J.S., McDougald, D., Rice, S.A. *et al.* (2009). Pseudomonas aeruginosa PAO1 preferentially grows as aggregates in liquid batch cultures and disperses upon starvation. *PLoS One*, **4**(5), e5513.

232. Schwarzenbach, R.P., Gschwend, P.M. and Imboden, D.M. (2002). *Environmental organic chemistry*. Wiley-Interscience.

233. Sciacca, F., Rengifo-Herrera, J.A., Wéthé, J. and Pulgarin, C. (2011). Solar disinfection of wild Salmonella sp. in natural water with a 18 L CPC photoreactor: Detrimental effect of non-sterile storage of treated water. *Solar Energy*, **85**(7), 1399-1408.

234. Scott, H.E., Liss, S.N., Farnood, R.R. and Allen, D.G. (2005). Ultraviolet disinfection of sequencing batch reactor effluent: A study of physicochemical properties of microbial floc and disinfection performance. *Journal of Environmental Engineering and Science,* **4**(S1), 65-74.

235. Seven, O., Dindar, B., Aydemir, S., Metin, D., Ozinel, M.A. and Icli, S. (2004). Solar photocatalytic disinfection of a group of bacteria and fungi aqueous suspensions with TiO_2, ZnO and Sahara desert dust. *Journal of Photochemistry and Photobiology A: Chemistry*, **165**(1-3), 103-107.

236. Shang, C., Cheung, L.M., Ho, C. and Zeng, M. (2009). Repression of photoreactivation and dark repair of coliform bacteria by TiO_2-modified UV-C disinfection. *Applied Catalysis B: Environmental*, **89**(3-4), 536-542.

237. Shannon, M.A., Bohn, P.W., Elimelech, M., Georgiadis, J.G., Mariñas, B.J. and Mayes, A.M. (2008). Science and technology for water purification in the coming decades. *Nature,* **452**(7185), 301-310.

238. Sheng, G.P., Yu, H.Q. and Li, X.Y. (2010). Extracellular polymeric substances (EPS) of microbial aggregates in biological wastewater treatment systems: A review. *Biotechnology Advances,* **28**(6), 882-894.

239. Shrestha, A. and Kishen, A. (2012). Polycationic Chitosan-Conjugated Photosensitizer for Antibacterial Photodynamic Therapy. *Photochemistry and Photobiology,* **88**(3), 577-583.

240. Sinha, R.P. and Hader, D. (2002). UV-induced DNA damage and repair: a review. *Photochemical & Photobiological Sciences,* **1**(4), 225-236.

241. Smith, R.C., Prézelin, B.B., Baker, K.S., Bidigare, R.R., Boucher, N.P., Coley, T. *et al.* (1992). Ozone depletion: ultraviolet radiation and phytoplankton biology in antarctic waters. *Science,* **255**(5047), pp. 952-959.

242. Sommer, R., Cabaj, A., Haider, T. and Hirschmann, G. (2005). UV Drinking Water Disinfection Requirements, Testing and Surveillance Exemplified by the Austrian National Standards M 5873-1 and M 5873-2. *IUVA NEWS,* **6**(4), 27-35.

243. Spectroscopy TV *Led measurements using an integrating sphere.*[Online]. Available from: http://www.spectroscopytv.com/led-measurement-using-an-integrating-sphere/ [Accessed 10 June 2010].

244. Sponza, D.T. (2003). Investigation of extracellular polymer substances (EPS) and physicochemical properties of different activated sludge flocs under steady-state conditions. *Enzyme and Microbial Technology,* **32**(3–4), 375-385.

245. Steinberger, R. and Holden, P. (2005). Extracellular DNA in single-and multiple-species unsaturated biofilms. *Applied and Environmental Microbiology,* **71**(9), 5404-5410.

246. Stewart, M.H. and Olson, B.H. (1996). Bacteria resistance to potable water disinfectants *IN:* Hurst, C.J. (ed.) *Modeling disease transmission and its prevention by disinfection*. 1st ed.Cambridge: Cambridge Universtiy Press, pp.140-143.

247. Stimson, A. (1974). *Photometry and radiometry for engineers Allen Stimson*. New York: Wiley.

248. Stoodley, P., Wilson, S., Hall-Stoodley, L., Boyle, J.D., Lappin-Scott, H.M. and Costerton, J.W. (2001). Growth and detachment of cell clusters from mature mixed-species biofilms. *Applied and Environmental Microbiology,* **67**(12), 5608-5613.

249. Stoodley, P., Sauer, K., Davies, D.G. and Costerton, J.W. (2002). Biofilms as complex differentiated communities. *Annual Review of Microbiology,* **56**(1), 187-209.

250. Street, C.N. and Gibbs, A. (2010). Eradication of the corrosion-causing bacterial strains Desulfovibrio vulgaris and Desulfovibrio desulfuricans in planktonic and biofilm form using photodisinfection. *Corrosion Science*, **52**(4), 1447-1452.

251. Suehiro, J., Hamada, R., Noutomi, D., Shutou, M. and Hara, M. (2003). Selective detection of viable bacteria using dielectrophoretic impedance measurement method. *Journal of Electrostatics,* **57**(2), 157-168.

252. Sun, D.D., Tay, J.H. and Tan, K.M. (2003). Photocatalytic degradation of E. coliform in water. *Water Research,* **37**(14), 3452-3462.

253. Sunada, K., Watanabe, T. and Hashimoto, K. (2003). Studies on photokilling of bacteria on TiO_2 thin film. *Journal of Photochemistry and Photobiology A: Chemistry,* **156**(1), 227-233.

254. Tang, K.W., Dziallas, C. and Grossart, H. (2011). Zooplankton and aggregates as refuge for aquatic bacteria: protection from UV, heat and ozone stresses used for water treatment. *Environmental Microbiology,* **13**(2), 378-390.

255. Templeton, M.R., Andrews, R.C. and Hofmann, R. (2008). Particle-Associated Viruses in Water: Impacts on Disinfection Processes. *Critical Reviews in Environmental Science and Technology,* **38**(3), 137-164.

256. Tim Cushnie, T.P., Robertson, P.K.J., Officer, S., Pollard, P.M., McCullagh, C. and Robertson, J.M.C. (2009). Variables to be considered when assessing the photocatalytic destruction of bacterial pathogens. *Chemosphere,* **74**(10), 1374-1378.

257. Toh, S., Tay, J., Moy, B., Ivanov, V. and Tay, S. (2003). Size-effect on the physical characteristics of the aerobic granule in a SBR. *Applied Microbiology and Biotechnology,* **60**(6), 687-695.

258. Turgeon, S., Rodriguez, M.J., Thériault, M. and Levallois, P. (2004). Perception of drinking water in the Quebec City region (Canada): the influence of water quality and consumer location in the distribution system. *Journal of Environmental Management,* **70**(4), 363-373.

259. U.S. Pharmacopeia (2000). <1231> Water for pharmaceutical Purposes/General information- Sanitization *IN:* Anonymous U.S. Pharmacopeia, pp.2160-2162.

260. USEPA (2006). *Ultraviolet disinfection guidance manual for the final long term 2 enhanced surface water treatment rule (EPA 815-R-06-007).* Washington: U.S. Environmental Protection Agency.

261. Vitor, V. and Corso, C.R. (2008). Decolorization of textile dye by Candida albicans isolated from industrial effluents. *Journal of Industrial Microbiology & Biotechnology,* **35**(11), 1353-1357.

262. Voet, D. and Voet, J.G. (1995). *Biochemistry*. Inc., Somerset.: John Wiley & Sons.

263. Wainwright, M., Brandt, S.D., Smith, A., Styles, A., Meegan, K. and Loughran, C. (2010). Phenothiazinium photosensitisers VII: Novel substituted asymmetric N-benzylphenothiaziniums as photoantimicrobial agents. *Journal of Photochemistry and Photobiology B: Biology,* **99**(2), 74-77.

264. Wainwright, M. (1998). Photodynamic antimicrobial chemotherapy (PACT). *Journal of Antimicrobial Chemotherapy,* **42**(1), 13-28.

265. Wainwright, M. and Crossley, K.B. (2004). Photosensitising agents—circumventing resistance and breaking down biofilms: a review. *International Biodeterioration & Biodegradation,* **53**(2), 119-126.

266. Wainwright, M., Phoenix, D.A., Nickson, P.B. and Morton, G. (2002). The use of new methylene blue in Pseudomonas aeruginosa biofilm destruction. *Biofouling,* **18**(4), 247-249.

267. Wainwright, M., Meegan, K. and Loughran, C. (2011). Phenothiazinium photosensitisers IX. Tetra- and pentacyclic derivatives as photoantimicrobial agents. *Dyes and Pigments,* **91**(1), 1-5.

268. Wassmann, M., Moeller, R., Reitz, G. and Rettberg, P. (2011). Growth phase-dependent UV-C resistance of*Bacillus subtilis*: data from a short-term evolution experiment. *Archives of Microbiology,* **193**(11), 823-832.

269. Watts, R.J., Kong, S., Orr, M.P., Miller, G.C. and Henry, B.E. (1995). Photocatalytic inactivation of coliform bacteria and viruses in secondary wastewater effluent. *Water Research,* **29**(1), 95-100.

270. Weidenmaier, C. and Peschel, A. (2008). Teichoic acids and related cell-wall glycopolymers in Gram-positive physiology and host interactions. *Nature Reviews Microbiology,* **6**(4), 276-287.

271. Wingender, J.W., Neu, T.R. and Flemming, H.-. (eds.) (1999). *Microbial Extracellular Polymeric Substances. Characterization, Structure and Function*. Germany: Springer.

272. Wolfe, R.L. (1990). Ultraviolet disinfection of potable water. *Environmental Science & Technology,* **24**(6), 768-773.

273. Wols, B.A., Hofman, J.A.M.H., Beerendonk, E.F., Uijttewaal, W.S.J. and van Dijk, J.C. (2011). A systematic approach for the design of UV reactors using computational fluid dynamics. *AIChE Journal,* **57**(1), 193-207.

274. Youxian, W., Clevenger, T. and Baolin, D. (2005). Impacts of goethite particles on UV disinfection of drinking water. *Applied and Environmental Microbiology,* **71**(7), 4140-4143.

275. Yu, L. and Joo-Hwa, T. (2002). The essential role of hydrodynamic shear force in the formation of biofilm and granular sludge. *Water Research,* **36**(7), 1653-1665.

276. Zenoff, V.F., Sineriz, F. and Farías, M. (2006). Diverse responses to UV-B radiation and repair mechanisms of bacteria isolated from high-altitude aquatic environments. *Applied and Environmental Microbiology,* **72**(12), 7857-7863.

277. Zhang, X., Du, A.J., Lee, P., Sun, D.D. and Leckie, J.O. (2008). TiO_2 nanowire membrane for concurrent filtration and photocatalytic oxidation of humic acid in water. *Journal of Membrane Science,* **313**(1–2), 44-51.

278. Zhao, L. and Matthews, K.R. (2000). Influence of starvation, temperature, and pH on culturability of Escherichia coli O157:H7. *Journal of Food Safety,* **20**(3), 193-206.

279. Zimmer, J.L. and Slawson, R.M. (2002). Potential repair of Escherichia coli DNA following exposure to UV radiation from both medium-and low-pressure UV

sources used in drinking water treatment. *Applied and Environmental Microbiology,* **68**(7), 3293-3299.

280. de Paula, L.F., Santos, R.O., Menezes, H.D., de Britto, J.R., Vieira Jr, J.B., Filhoc, P.P.G. *et al.* (2010). A comparative study of irradiation systems for photoinactivation of microorganisms. *J.Braz.Chem.Soc,* **21**(4), 694-700.

281. ÖNORM (2001). *ÖNORM M 5873-1: Plants for the disinfection of water using ultraviolet radiation: Requirements and testing. Part 1. Low-pressure mercury plants.* Vienna, Austria: Österreichisches Normungsinstitut.

282. ÖNORM (2003). *ÖNORM M 5873-2 Plants for the disinfection of water using ultraviolet radiation: Requirements and testing. Part 2. Medium pressure mercury lamp plants.* Vienna, Austria: Österreichisches Normungsinstitut.